DEPARTAMENTO DE CIÊNCIAS DA VIDA

FACULDADE DE CIÊNCIAS E TECNOLOGIA
UNIVERSIDADE DE COIMBRA

Biomarkers for monitoring anti-amyloid-ß therapies in preclinical studies and clinical trials for Alzheimer's disease

Dissertação apresentada à Universidade de Coimbra para cumprimento dos requisitos necessários à obtenção do grau de Mestre em Biologia Celular e Molecular, realizada sob a orientação científica da Doutora Bianca Van Broeck (Janssen Pharmaceutica) e supervisão do Professor Doutor Carlos Duarte (Universidade de Coimbra)

Ana Catarina Carapinha Cascalho

2015

The work presented in this thesis resulted from a partnership between the University of Coimbra and Janssen Pharmaceutica NV, Beerse I. All experimental activities were performed at Janssen Pharmaceutica NV, Beerse I, a Johnson & Johnson pharmaceutical research and development facility in Beerse, Belgium.

All data presented in this thesis is strictly confidential

Beerse, 2015

ACKNOWLEDGEMENTS

First of all I want to thank Dr. Bianca Van Broeck for accepting to be my supervisor during this project. Thank you for all the help, guidance, support, and for sharing your knowledge. I leave a better scientist thanks to you!

I want to thank Dr. Marc Mercken for accepting me in his research group and for all the shared knowledge and help throughout the development of the project.

I would also like to thank to all the members of the Alzheimer's research group for welcoming me into the team and for the helpful scientific discussions.

A special thank you to Greet Meulders, Bart Hermans, and Daan Van Glabbeek for all the support and readiness to help me during my work. And also to Marc Vandermeeren, thank you for your help and mostly for you great company in the lab!

To Professors Carlos Duarte and Emilia Duarte, I would like to thank you for the great first year and for your availability to help with any questions.

To the Janssen interns, thank you all for the great times, with a special thanks to Harvey and Joe for the great moments and for always making me laugh!

To André, Sara and Ana, thank you for everything, for being a great company, for the support and laughs, and for making me feel at home in this foreign country.

A special thank you to Alberto, for the friendship and companionship, for the endless coffees and beers, without you it would not have been the same!

À minha família (Rosa, Pipa, Zé, Avó e Paula) sem as quais nada disto seria possível! Um sincero obrigada por todo o apoio, por toda a ajuda e pelas infinitas conversas. Obrigada por estarem sempre lá para mim, e serem o meu porto seguro!

Ao David, pelo apoio e ajuda, pela paciência para me aturar, pela amizade incondicional, um sincero obrigada!

To all that are not mentioned but in some way helped to realize this project in the best way,

- Thank you!

RESUMO

A doença de Alzheimer (DA) é a forma mais comum de demência no mundo, afetando mais de 35 milhões de pessoas e sendo responsável por dois terços dos casos de demência. Infelizmente, os únicos tratamentos disponíveis até aos dias de hoje são sintomáticos.

Atualmente, a hipótese da cascata da amiloide, na qual o péptido beta-amiloide (Aß) tem o papel central no desenvolvimento da doença, é a mais aceite para explicar a patologia desta doença, sendo suportada por uma extensa lista de fatores genéticos, patológicos e farmacológicos. Este péptido pode ser truncado em ambas as extremidades, dando origem a uma variedade de fragmentos de diferentes tamanhos. Devido ao seu papel central na DA, o desenvolvimento de terapias que tenham como alvo este péptido são de elevado interesse.

Com a contínua procura por possíveis tratamentos, o desenvolvimento de ferramentas que consigam avaliar a segurança e eficiência de novos candidatos terapêuticos é crucial. Para este efeito, os biomarcadores no líquido cefalorraquidiano (LCR) têm-se tornado cada vez mais úteis. A maioria dos estudos que incorporaram medições de biomarcadores têm-se focado no péptido *full-length* ($Aß_{1-x}$). No entanto existe também a necessidade de estudar os péptidos truncados, os quais podem contribuir para a patologia.

Neste projeto monitorizámos os efeitos de fármacos experimentais (inibidores da BACE1, moduladores e inibidores da γ-secretase) em diferentes espécies da Aß ($Aß_{1-37/38/40/42}$, $Aß_{x-37/38/40/42}$, $Aß_{11-x}$). De forma a termos em consideração possíveis diferenças entre modelos e espécies, os níveis destes biomarcadores foram avaliados em amostras pré-clínicas e clínicas (sobrenadante celular, e LCR de cães beagles e humano). Adicionalmente, foi também avaliada a interferência da matriz nas medições de $Aß_{1-42}$, e como esta interferência influencia a capacidade diagnóstica do péptido isolado ou combinado com outos péptidos.

Os nossos resultados mostraram que o péptido $Aß_{11-x}$ – um produto da clivagem alternativa da BACE – é reduzido de uma forma semelhante aos péptidos $Aß_{1-x}$ após inibição da BACE. Comparação entre péptidos *full-length* ($Aß_{1-x}$) e N-truncados ($Aß_{x-37/38/40/42}$) após inibição da BACE em LCR humano mostrou que ambos eram reduzidos de forma semelhante. No entanto, comparação dos mesmos péptidos em sobrenadante celular demonstrou que os péptidos *full-length* estavam significativamente mais reduzidos que os N-truncados. Com base nos nossos resultados, sugerimos que esta diferença se deve aos diferentes ratios entre Aß *full-length*/ Aß N-truncado nestes modelos. Estes resultados salientam a necessidade de estudar diferentes fragmentos de Aß quando se avalia os efeitos de novos candidatos terapêuticos, e que os resultados devem ser validados em diferentes modelos.

Adicionalmente, os nossos resultados destacaram o aumento da capacidade diagnóstica quando se compara $Aß_{1-42}$ com outros péptidos, como $Aß_{1-37}$, $Aß_{1-38}$ ou $Aß_{1-40}$, em vez de usar $Aß_{1-42}$ isolado. Este resultado foi independente do tipo de amostra estudada (LCR simples ou LCR enriquecido por Cromatografia Liquida de Alta Eficiência (CLAE)).

No geral este projeto amplificou e cimentou os conhecimentos existentes sobre biomarcadores da amiloide e da forma como estes respondem a determinadas terapias. No futuro estes conhecimentos serão úteis para o desenvolvimento de novas terapias que modifiquem o curso da doença de Alzheimer.

Palavras-chave: Doença de Alzheimer, Biomarcadores de ß-amiloide, $Aß_{11-x}$, ß-amilóide N-truncado, terapias-modificadoras do curso da doença.

ABSTRACT

Alzheimer's disease (AD) is the most common form of dementia worldwide, affecting over 35 million people and accounting for two thirds of the dementia patients. Unfortunately, despite intensive research, only symptomatic treatments are currently available.

Substantial genetic, pathological and pharmacological evidence supports the amyloid cascade hypothesis, in which amyloid ß (Aß) takes the central role in initiating the disease. This peptide can be truncated at both ends, resulting in a variety of Aß species. Due to its central role in AD pathogenesis, disease-modifying strategies targeting the Aß peptide are of major interest.

With the growing search for possible AD treatments, the availability of proper tools to evaluate the safety and efficacy of the therapeutic candidates is crucial, and cerebrospinal fluid (CSF) biomarkers have become increasingly helpful in that task. The majority of published studies focus on full length Aß ($Aß_{1-x}$) species as the main CSF biomarkers for target engagement, but there is a need to additionally investigate treatment effects on N-truncated Aß species, which could also contribute to AD pathogenesis.

In this project, we monitored the effects of various classes of experimental drugs (BACE1 inhibitors, γ-secretase inhibitors and γ-secretase modulators) on different Aß species ($Aß_{1-37/38/40/42/x}$, $Aß_{X-37/38/40/42}$, $Aß_{11-x}$). Biomarker levels were measured after treatment in preclinical and clinical samples (cell culture supernatant and CSF of beagle dogs and human healthy volunteers) to assess possible variability across models and species. Additionally, we investigated the effect of matrix interference on $Aß_{1-42}$ measurements, and compared the diagnostic value of individual Aß peptides with peptide ratios.

Our results showed that $Aß_{11-x}$ levels – a product of alternative BACE1 cleavage – were reduced similarly to $Aß_{1-x}$ upon BACE inhibition. Comparison of full-length ($Aß_{1-x}$) and N-truncated ($Aß_{x-37/38/40/42}$) species reduction profiles after BACE inhibitor treatment revealed that in human CSF both species were similarly reduced. However, in human neuroblastoma cell supernatant N-truncated Aß forms were less reduced than full-length species. We suggest that this differential effect is a result of distinct full-length/N-truncated Aß ratios in the different models. These results highlight the need to study several Aß species when monitoring the effects of novel Aß-targeting experimental drugs, and that results should be validated across different models.

Additionally, our results emphasized the increased diagnostic value of the ratio of $Aß_{1-42}$ with other Aß peptides, such as $Aß_{1-37}$, $Aß_{1-38}$ or $Aß_{1-40}$, as compared to the use of $Aß_{1-42}$ by itself. This effect was independent of the sample type (crude CSF or HPLC-enriched CSF).

Overall this project provided some interesting insights into how several amyloid ß biomarkers respond to disease-modifying therapies, and such results will be useful for the future development of amyloid-targeted therapies.

Key-words: Alzheimer's disease, Amyloid Biomarkers, $Aß_{11-x}$, N-truncated Aß species, disease-modifying therapies

TABLE OF CONTENTS

ACRONYMS

Aβ – Amyloid-β protein
AICD – APP intracellular domain
AD – Alzheimer's disease
ADAM – A desintegrin and metalloproteinase
APH1– Anterior pharynx defective 1
APLP1 – Amyloid precursor-like protein 1
APLP2 – Amyloid precursor-like protein 2
ApoE – Apolipoprotein E
APP – Amyloid precursor protein
AUC – Area Under the Curve
BACE1 – β-site APP cleaving enzyme 1
BACE2 – β-site APP cleaving enzyme 2
BACEi – BACE inhibitor
BBB – Blood brain barrier
CAA – Cerebral amyloid angiopathy
CM – Cisterna Magna
CNS – Central nervous system
CSF – Cerebrospinal fluid
CTF – Carboxy-terminal fragment
CV – Coefficient of Variation
ECL - Electrochemiluminescence
ECM – Extracellular matrix
EGF – Epidermal growth factor
EGFR – Epidermal growth factor receptor
ELISA – Enzyme-linked Immunosorbent assay
ER – Endoplasmic reticulum
ERK1/2 – Extracellular-regulated kinase 1/2
FAD – Familial Alzheimer's disease
FDG – 18F-fluorodeoxyglucose
Fe65 – Amyloid-β precursor protein-binding family B member 1
FTDP-17 – Frontotemporal dementia and Parkinsonism linked to chromosome-17
GGA – Golgi-localized γ-ear-containing ARF-binding protein
GSI – γ- secretase inhibitor
GSM - γ- secretase modulator
HRPO – Horseradish Peroxidase
Ig – Immunoglobulin
JIP – C-jun-amino-terminal kinase-interacting protein
KPI – Kunitz protease inhibitor
LDLR – Low-density lipoprotein receptor
LLOQ – Lower limit of Quantification
LOAD – Late onset Alzheimer's disease
LRP – Low-density lipoprotein receptor-related protein
LTP – Long-term potentiation
LV – Lateral Ventricle
MAP – Microtubule associated protein
MCI – Mild cognitive impairment
MMP – Matrix metalloproteinases
MRI – Magnetic resonance imaging
mRNA – Messenger RNA
MSD – Meso Scale Discovery
NC – non-Alzheimer's Disease
NEP – Neprysilin
NFT – Neurofibrillary tangles
NMDA – N-methyl-D-aspartate
ON - Overnight
P-tau – Phosphorylated tau
PBS – Phosphate Buffered saline
PET – Positron emission tomography
PHF – Paired helical filaments
PIB – Pittsburgh compound B
PNS – Peripheral Nervous System
PSEN1 – Presenilin 1
PSEN2 – Presenilin 2
RAGE – Receptor for advanced glycation end products
RP-HPLC – reverse-phase high-performance liquid chromatography
RT – Room Temperature
sAPPα – Secreted APPα fragment
sAPPβ – Secreted APPβ fragment
SPECT – Single-photon emission computed tomography
T-tau – Total tau
TGN – Trans Golgi network

Chapter I. Introduction

1 ALZHEIMER'S DISEASE

Firstly described in 1906, Alzheimer's disease (AD), which owes its name to the German neurologist Alois Alzheimer, is nowadays the most common neurodegenerative disease in the world.[1,2] AD affects more than 35 million people worldwide and accounts for almost two thirds of the dementia cases.[3,4]

Like all dementias, AD is defined by the improper functioning and progressive loss of neurons resulting in consequences for the memory, cognition and behaviour of the individual.[5] In the brain, AD is characterized by the presence of extracellular amyloid plaques, where the amyloid-ß (Aß) peptide is the key component, and intracellular neurofibrillary tangles (NFTs), in which the main constituent is the hyperphosphorylated tau protein. [2,6]

Age is the most important risk factor for the development of AD, 99% of the patients develop a characteristically late onset AD (LOAD) (over 60 years old). The remaining 1% of the patients have been found to have transmission of AD as an autosomal dominant disease (familial AD or FAD), and have a characteristic early onset, usually between 30 and 60 years of age.[7] Disease prevalence approximately doubles every 5 years beyond age 65. By the age of 85 at least one in three people will develop AD.[2] With an aging population, the social and economic impact of the disease is predicted to increase exponentially in the future.[3,5]

The quality of life of those affected by AD is highly diminished, and in later stages of the disease the patients often lose the ability to perform basic functions like walking and swallowing, becoming almost completely caretaker-dependent.[5] The high impact of this disease on both individual lives and on the society creates the need for a better comprehension of the mechanisms underlying this disease. This would eventually lead to the development of more effective therapeutics, since at present, neither prevention or treatment of AD is possible.[8]

2 NEUROPATHOLOGY OF AD

The brain of the AD patient is characterized by a particular set of hallmarks. Structurally, there is a generalized cortical atrophy that usually is more accentuated in the hippocampus and the temporal lobe, with synaptic and neuronal loss of cholinergic and glutamatergic neurons.[9,10] Pathologically, the most important hallmarks are the NFT and amyloid plaques (*Figure 1*).[2,6,11,12]

Although the mechanisms by which plaques and NFT affect neuronal functioning are not completely understood, several affected functions have been identified. The extracellular amyloid plaques are thought to impair proper synaptic functioning, while the presence of NFTs would supress the transport of crucial molecules for neuronal survival. Amyloid deposits can also accumulate in blood vessels, which is described as cerebral amyloid angiopathy (CAA). Together, these two misfolded protein aggregates are thought to result in the characteristic neurodegeneration of AD.[5]

Additional neuropathological findings include granulovacuolar degeneration (enlarged lysosome-like structures within which there is a dot-like inclusion) and Hirano bodies (eosinophilic inclusions made of mainly α-actin and located in the cytoplasm of hippocampal neurons).[2]

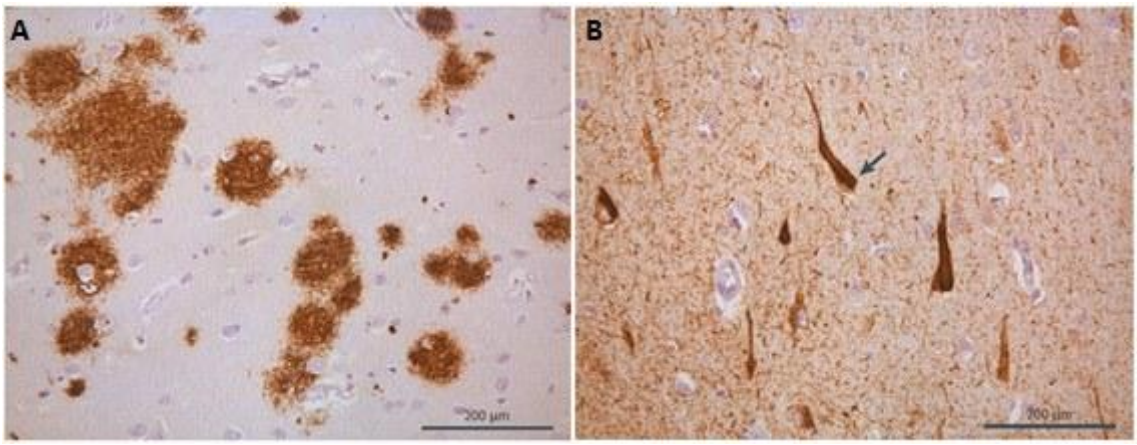

Figure 1 - Neuropathological hallmarks of AD. (a) Human cortical section from an AD patient showing amyloid plaques stained with an Aβ-specific antibody (b) Human cortical section from an AD patient showing NFT (arrow) stained with a phospho-tau-specific antibody. (Adapted from Aguzzi, A. & O'Connor, (2010)[12]).

2.1 NEUROFIBRILLARY TANGLES AND TAU

NFTs are intracytoplasmic neuronal inclusions (Figure 1b) that are composed mainly of paired helical filaments (PHFs) of hyperphosphorylated tau. The tau protein is a microtubule-associated protein (MAP) that is enriched in the neuronal axons.[2,13]

Tau is a MAP involved in regulating microtubule assembly, dynamic behaviour, spatial organization and stability.[14] Besides this function, tau has also been shown to regulate the axonal transport of several organelles like mitochondria.[15] Usually enriched in neuronal axons, tau can be found in the cytoplasm and in the nucleus, where it was shown to protect deoxyribonucleic acid (DNA) from heat stress-induced damage.[13]

Besides being one of the main pathological hallmarks of AD, tauopathy is also associated with other neurodegenerative diseases, including Pick's disease (PiD), corticobasal degeneration

(CBD), and progressive supranuclear palsy (PSP). Mutations in the tau gene have also been linked with frontotemporal dementia and Parkinsonism linked to chromosome-17 (FTDP-17), indicating that tau dysfunction is able to induce neuronal loss and clinical dementia in the absence of Aß deposition. No mutations have been found in the tau gene that are associated with FAD.[1,13,14] Although a SNP in the tau gene, MAPT, has been associated with a 10% increase risk for AD, through an increase in tau expression and greater brain atrophy of the entorhinal cortex and hippocampus.[16]

In tauopathies, tau usually displays a loss of affinity for microtubules and/or an increase in its susceptibility to aggregate. Phosphorylation appears to be the main event promoting tau detachment from microtubules, leading to its aggregation.[17]

Hyperphosphorylation of tau happens in two main regions: the proline-rich region, which will block tau binding to microtubules, and at tau's carboxyterminus.[13] Several protein kinases have been associated with tau's phosphorylation, like proline-directed kinases GSK-3ß, cyclin-dependent kinase 5 (CDK5), and extracellular-regulated kinase 1/2 (ERK1/2). Besides phosphorylation, the tau protein can undergo other post-translational modifications like ubiquitinylation, truncation, oxidation and glycosylation, which will facilitate the detachment from the microtubules. This event can be followed by the formation of misfolded tau aggregates, which will form the pretangles, which can evolve into ß-sheet containing structures – the PHFs – that will finally form the NFT intracytoplasmic inclusions.[13,15,18]

Tau-mediated toxicity is thought to arise from its dissociation from microtubules, and the aggregates by themselves. Tau's dissociation from microtubules can lead to the microtubule instability and to the impairment of vesicular transport, resulting eventually in synaptic dysfunction and cell death. The aggregates are thought to create a physical barrier in the neuron, blocking transport and intracellular communication leading to neuronal dysfunction and eventually death. Additionally, hyperphosphorylated tau seems to be able to sequester normal tau molecules and other microtubule-associated proteins into the aggregates.[13,15]

Similarly to Aß, recent evidence has suggested that the soluble oligomeric tau might be the most toxic species, while the NFT might be less toxic or even have a more protective role.[13,15,19]

In AD, tau pathology usually spreads through a typical pattern from the locus coeruleus into the entorhinal cortex (Braak stages I and II), towards the limbic system (dentate gyrus and hippocampus) (Braak stages III and IV) and then to more distant locations in the neocortex (Braak stages V and VI).[2,6,20]

Many studies have shown that there is a close correlation between tangle formation and AD progression, with the degree of dementia being positively related to the number of NFTs in the neocortex.[21,22] In addition, NFT presence appears to be necessary for Aß-mediated toxicity, indicating that it might be an interesting target, together with Aß, for AD therapies.[23,24]

2.2 AMYLOID PLAQUES

An amyloid plaque (or senile plaque (SP)) consists of a cluster of extracellular amyloid fibrils, with 8-10nm in diameter.[1]

Amyloid plaques (*Figure 1a*) are found extracellularly and are characterized by the high Aß peptide content. Depending on the morphology, they can be mainly subdivided into compact or dense core plaques (composed of packed amyloid fibrils) or diffuse plaques (Aß is found in an amorphous form instead of fibrils).[2,18,25]

Aß deposition can occur naturally with aging, meaning that one might have Aß deposits, usually from the diffuse type described above, without presenting clinical signs of dementia. On the other hand, all AD patients have Aß plaques in their brains. [2]

Plaque-mediated toxicity is thought to arise from Aß-toxic properties, which include a pro-oxidant effect, mitochondrial dysfunction, synaptic dysfunction, alteration of membrane permeability increasing intracellular calcium levels, interactions with some neurotransmitter receptors leading to excitotoxicity, among others which can be found described in (XX). Although these toxic effects have been associated with Aß, for most of them the mechanisms by which Aß causes them is still unclear.[26]

Plaques appear first in the basal temporal neocortex, and then progress to the entorhinal and hippocampal regions until the pathology spreads throughout the neocortex. This progression might be explained by Aß anterograde transport and synaptic exchange mechanisms from the regions where Aß aggregation starts, into the regions receiving their axonal inputs. [20]

The mechanism by which Aß starts accumulating and forming amyloid plaques is not clear, although several studies have suggested that this accumulation results from the formation of fibrillization centres, from which deposition would quickly progress to form the plaques.[27]

Interestingly, it was found that Aß deposits could promote the formation of NFT, which in turn would highly potentiate the toxic effect of the deposits.[28] However, the NFTs were not able to do the same, i.e. NFTs by themselves cannot promote Aß deposition, suggesting that sequentially

Aß deposition would be primordial to NFT formation.[13,29] Nevertheless, in the AD brain both of these hallmarks, Aß plaques and NFTs, are crucial elements of the pathology.[1]

3 DIAGNOSIS

The clinical diagnosis of AD is not an easy task, due to the overlap of symptoms with other diseases and the fact that the disease itself affects different people in a diversified manner. Until today, a definitive diagnosis of AD is only possible *post-mortem*,[29] nonetheless a diagnosis during life can be given with almost 90% certainty, based on the criteria described below.[30]

The AD diagnostic criteria were initially established by the NINCDS– ADRDA[1] in 1994 and were revised in 2011 by the NIA–AA[2], in order to provide a more sensitive and specific diagnosis in light of knowledge acquired since the initial report. Its main novelties were the distinction between the clinical disease and disease pathology that can occur prior to clinical alterations, and the use of biomarkers as a diagnosis tool. Moreover, these criteria led to the introduction of 3 disease stages (*Figure 2*) [5,31,32]:

Asymptomatic/preclinical: These individuals do not have any clinical symptoms yet, but already demonstrate some alterations, like changes of cerebrospinal fluid (CSF) biomarkers, which can indicate the disease presence.[5] This preclinical stage can be further subdivided into 3 stages, where stage 1 begins with cerebral amyloidosis, in stage 2 biomarkers for neurodegeneration are also detectable, and in stage 3 there is a combination of amyloidosis, neurodegeneration and subtle cognitive defects that are not sufficient to meet the mild cognitive impairment (MCI) criteria.[33]

Predementia stage: These individuals already have some clinical symptoms, although they are still in the mild stage, meaning they are detectable but not severe.[5] This state is commonly denominated MCI, and it is estimated that 10% to 20% of people over 65 years have MCI.[34]

Dementia stage: The neurological alterations in brains of these individuals affect their day-to-day normal activity and result in memory, behavioural and thinking impairments.[5]

Usually the initial memory loss is mostly related with the short-term memory, and not as much with immediate- or long-term memory, but these can also be progressively affected.[2] The typical patient evolves from a memory dysfunction to impairments in executive function, semantic processing and visuospatial skills, which in some cases can also evolve into psychiatric symptoms

[1] NINCDS-ADRDA - National Institute of Neurological and Communicative Disorders and Stroke and Alzheimer's Disease and Related Disorders Association.
[2] NIA-AA - National Institute on Aging–Alzheimer's Association.

like psychosis, mood disturbances and depression. Having a typical slow progression, AD ends up being fatal, usually within 3 to 9 years after appearance of the first symptoms.[2,29] Besides these criteria, supplementary tests can be used to provide a more conclusive diagnosis, like the presence of a genetic mutation or alterations in biomarkers, as indicated by the new NINCDS–ADRDA criteria described above. Examples of biomarkers are described in the next section.

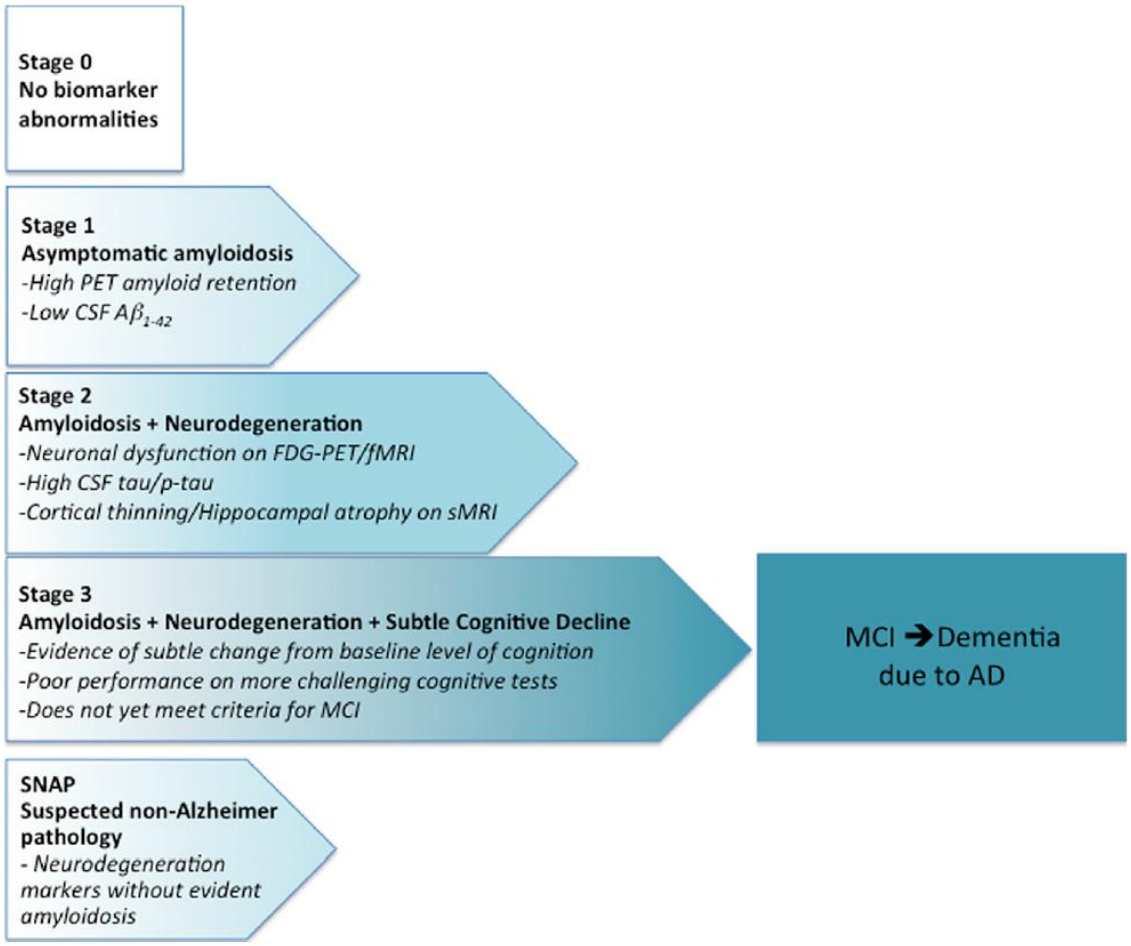

Figure 2 - Graphical representation of AD stages. The asymptomatic phase can be subdivided into three different stages that may evolve into the predementia phase (MCI due to AD) and eventually progress to the dementia stage. AD – Alzheimer's disease, PET – positron emission tomography, CSF – cerebrospinal fluid, Aβ – amyloid-β, FDG – ^{18}F fluorodeoxyglucose , fMRI – functional magnetic resonance imaging, t-tau – total tau, P-tau – phosphorylated tau, sMRI – structural magnetic resonance imaging, MCI – mild cognitive impairment (Adapted from Sperling, R. et al.,(2014)[33]).

3.1 BIOMARKERS

Biomarker or biological marker was defined by the National Institutes of Health Biomarkers - Definitions Working Group as "a characteristic that is objectively measured and evaluated as an indicator of normal biological processes, pathogenic processes, or pharmacologic responses to a therapeutic intervention".[35] Therefore, identification of proper biomarkers is crucial not only to

provide a more certain diagnosis but also to determine the risk of disease development and the effect of therapeutic interventions on the disease process.[7]

Several biomarkers are already in use to help in the diagnosis of AD and in the monitoring of the pharmacodynamics effect of disease-modifying strategies. AD biomarkers can be subdivided in plasma biomarkers, CSF biomarkers and neuroimaging biomarkers.[7]

3.1.1 Plasma Biomarkers

The fact that plasma Aß derives from peripheral tissues, which does not reflect Aß metabolism in the brain makes the use of Aß plasma levels as a diagnostic biomarker very controversial, as several studies present contradicting data.[36,37] Moreover, Aß measurements in the plasma can be further affected by other plasma proteins masking the epitopes, due to the hydrophobic nature of the peptide.[37]

Other blood-based protein biomarkers have been associated with AD-phenotypes and were even replicated in several studies, such as α-1-antitrypsin, α -2-macroglobulin, apolipoprotein E (ApoE), and complement C3, bur further studies are required before their consideration for diagnostic biomarkers.[38]

3.1.2 CSF Biomarkers

CSF can originate from several sites, but it is mainly from the choroid plexus of the lateral, third ventricle and fourth ventricle, and a smaller percentage from the subarachnoid space through the pial-glial membrane on the external surface of the parenchyma.[39] CSF runs from the lateral ventricle to the third ventricle, and then into the fourth ventricle, from where it goes into the subarachnoid space. It is still unclear what the source of Aß in CSF is, but it seems that production in and clearance from the brain might be the main source, since alterations in brain Aß are reflected by CSF Aß levels.[7,40]

The most studied CSF biomarkers are $Aß_{1-42}$, total tau (T-tau) and phosphorylated tau (p-tau).[37] To complement the analysis and increase the specificity of the diagnosis, evaluation of truncated Aß isoforms, like $Aß_{37}$, $Aß_{38}$ and $Aß_{40}$ can also be performed.[41] Different stages of NFT development can also be investigated taking advantage of the different tau phosphorylation epitopes. For example, in earlier stages of NFT, P-tau S262 or P-tau T181 are elevated, while P-tau S396 is found elevated in later stages of NFT development when there is extracellular tau accumulation.[42]

In AD, CSF $A\beta_{1-42}$ levels are decreased, and T-tau and P-tau levels are found increased when compared with cognitively normal individuals. [43] Studies using various enzyme-linked immunosorbent assays (ELISAs) have demonstrated a mean CSF $A\beta_{1-42}$ reduction of approximately 50% in AD individuals when compared with age-matched cognitively normal individuals.[43] Although the explanation is not clear, $A\beta_{42}$ levels are thought to be decreased due to its deposition into plaques in the brain. On the other hand, there are some pathological conditions where there are no plaques but CSF $A\beta_{42}$ levels are decreased as well, like plaque-negative Creutzfeldt-Jakob disease.[44] Studies using ELISA for T-tau or P-tau, found T- and P-tau to be approximately 300% increased in AD patients, when compared with age-matched cognitively normal individuals.[43] P-tau levels are thought to reflect tau phosphorylation state and NFT formation, while T-tau would reflect the intensity of neuronal damage and neurodegeneration, as it is associated with the progression from MCI to AD and with a faster cognitive decline.[44,45]

Recently, evidence is accumulating that the ratio between Aß42/Aß40 can provide additional value in discriminating between AD, healthy controls and patients with other dementias. Aß40 peptide is the most abundant peptide in the brain, therefore its levels in CSF may be considered to most closely reflect Aß total levels in the brain. Additionally it is important to consider that there is a large inter-individual variability in Aß load in both AD and healthy individuals, existing high and low amyloid-producing individuals in both cases. Therefore, the use of the Aß42/Aß40 ratio can more accurately reflect the changes in Aß metabolism in AD than Aß42 alone, as it corrects for individual baseline differences. Furthermore, the high variation in Aß levels between individuals makes it is more difficult to establish the cut-off values for a single peptide, so the use if the ratio also provides a solution for than problem. [46–49]

3.1.3 Neuroimaging

Neuroimaging has allowed *ante mortem* assessment of the altered neurochemistry and physiology, even prior to anatomical changes and appearance of the neuropathological hallmarks of AD. [50]

Within the neuroimaging methods, structural magnetic resonance imaging (MRI) is the most commonly utilized. This technique allows the evaluation of parenchymal and vascular anatomic variability in health and disease.[50]

Progressive neurodegeneration with the loss of neurons and their processes is visible in the AD brain as an atrophy of some specific areas.[50] LOAD is characterized by atrophy in the medial

temporal lobe, more specifically in the parahippocampus and the amygdala. In FAD brain atrophy can spread more posteriorly and may affect the posterior cortex, occipital lobes, posterior cingulate and precuneus. Atrophy in the hippocampus together with entorhinal cortex atrophy correlates with cognitive decline.[7] Additionally, atrophy also correlates with Braak NFT stage and with tau immunostaining burden, however it does not show an association with Aß deposition, suggesting that MRI outcomes function as a measure of tau-associated neurodegeneration.[51]

Although hippocampal atrophy has a very strong association with AD, many of the changes present in AD brain are not specific for AD. [50] However, there is evidence that some of the structural MRI biomarkers might have some discriminative diagnostic power. Individuals with MCI that progress into LOAD have higher hippocampal, and inferior and middle temporal gyri atrophy than those who do not progress. Atrophy in the anterior region of corpus callosum may help distinguish between AD and frontotemporal dementia.[7] Generalized atrophic progression is also accepted as an indicator of progression from MCI to AD.[52]

Cerebral blood flow may also be reduced in AD, which can be evaluated by arterial spin labelling (ASL)-MRI. This blood flow alteration can help to predict cognitive decline, differentiate and predict the progression from MCI to AD.[7]

Positron emission tomography (PET) and single-photon emission computed tomography (SPECT) imaging are widely used to assist in the diagnosis of dementia, and there are several ligands being investigated which specifically measure Aß, tau or metabolic activity.[7] Generally, PET radioligands targeting Aß are more specific and sensitive in distinguishing cognitively normal and AD and other conditions, than other neuroimaging techniques like MRI or SPECT. [50]

Pittsburgh compound B ([^{11}C]-PIB) is a PET ligand that selectively binds cortical and striatal amyloid plaques. This ligand shows a positive correlation with AD diagnosis and fibrillar amyloid plaques at autopsy.[53–56] However, cognitively normal individuals may also have plaques and therefore also retain the PIB ligand, this binding increases from less than 10% under 70 years, up to 40% at the age of 80.[50]

One disadvantage of PIB ligand is the short half-life of [^{11}C] (approximately 20 minutes), to surpass this labelling of PET probes with 18F, which as a half-life of 110 minutes have been developed. Some examples are the [^{18}F]-3'-FPIB (flutemetamol), [^{18}F]-AV-45 (florbetapir) and [^{18}F]-AV-1 (florbetaben) which so far have showed similar clinical performances to PIB.[57,58]

^{18}F-fluorodeoxyglucose (FDG)-PET is used to evaluate cerebral glucose metabolism. Several studies have shown that in MCI and AD there is a reduction in regional cerebral glucose metabolism, when compared with healthy controls. These results strongly correlate with cognitive impairment and may be able to predict progression from MCI to AD. Although FDG-PET has a very high sensitivity (94%) it presents a low specificity (approximately 76%) in the diagnosis of dementia. FDG-PET and ASL-MRI information may be combined, resulting in a more efficient differentiation between AD and healthy controls. [7,50]

3.1.4 Model of dynamic biomarkers in AD

Several biomarkers are already in use to help in the diagnosis of AD and considering their target measures, the major AD biomarkers can be subdivided into two categories: measuring amyloid deposition (CSF Aβ_{42} and amyloid PET) and measuring neurodegeneration (CSF T-tau, FDG PET, structural MRI).[51,59,60]

According to the model of dynamic biomarkers (*Figure 3*), these biomarkers become abnormal in a temporally ordered manner, first CSF Aβ_{42} and then amyloid PET, followed by CSF tau, and very closely by FDG PET and structural MRI, and only later the clinical symptoms. As disease progresses, all the biomarkers will become simultaneously abnormal, each following a sigmoid-shaped change rate and eventually reaching a plateau.[51]At each time point (shown at "T" in the graph) there are several possible cognitive outcomes depending on environmental and life style factors. High risk individuals might have genetic risk alleles, low cognitive reserve or be exposed to non-genetic risk factors and are more likely to develop cognitive impairment. On the other hand, low risk individuals with for example high cognitive reserve, low lifestyle risks or protective genetic profile, might have a normal cognitive function while already demonstrating AD-pathophysiological changes. [51]

This model also recognizes that there might be alterations in biomarker levels that are beneath the detection threshold of *in vivo* biomarkers. These would explain why in some studies, tau immunostaining is detected prior to Aß alterations. This initial tauopathy could be independent from the Aß pathophysiological changes, however once the Aß changes begin, they would promote the acceleration of the tauopathy until it finally reaches the threshold of detection *in vivo*. There might be several possible pathways leading to the development of sporadic AD, and with each pathway a slightly different biomarker model may arise. [51]

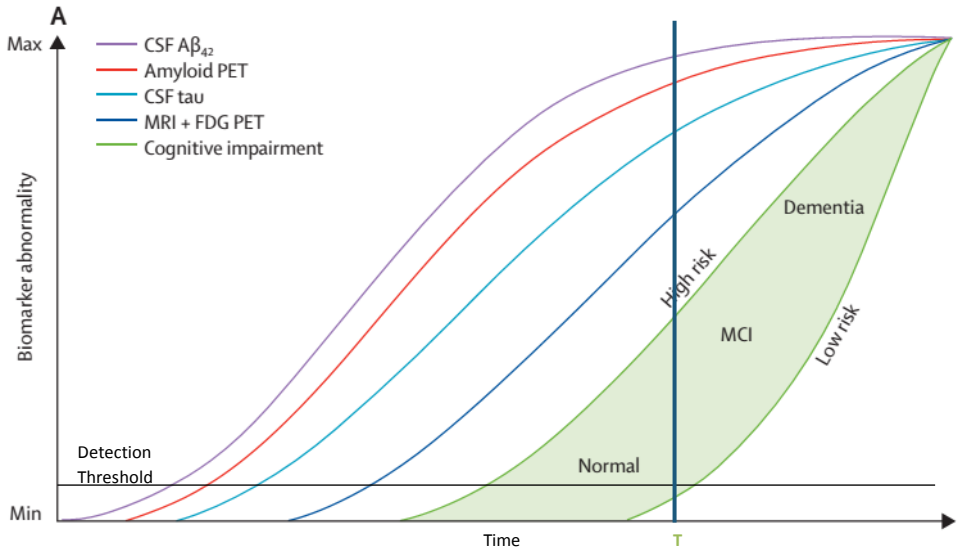

Figure 3 - Revised model of dynamic biomarkers of Alzheimer's disease. The dynamic biomarker model has in the horizontal axis the absolute time in years needed to transverse the disease pathway from left to right, taking into account that the age of disease onset varies among individuals. The vertical axis corresponds to a minimum to maximum scale, so that each biomarker is scaled considering its own dynamic profile. MCI – mild cognitive impairment, Aβ – amyloid-ß , CSF – cerebrospinal fluid, PET – positron emission tomography, MRI – magnetic resonance imaging, FDG – fluorodeoxyglucose (Adapted from Jack, C. R. et al., (2013)[51]).

Importantly, Aß$_{42}$ is not sufficient but is essential for development of the clinical symptoms. Cognitive decline does not correlate with amyloid biomarkers, but rather correlates with the neurodegenerative biomarkers. It is also important to take into consideration that AD often coexists with other pathophysiologies, like cerebrovascular disease, that might highly contribute to inter-individual variation. [51]

There is a clear need to discover new biomarkers that allow further testing of different hypotheses for AD pathogenesis, and also to help track relevant pathophysiological processes. Besides, it is also crucial to investigate proper cohorts to evaluate biomarker evolution. Most cohorts so far include only middle-aged individuals, therefore missing the onset of biomarker abnormalities, and do not include individuals in end-stage dementia. Additionally long-term within-subject longitudinal data is also lacking, although studies are being done to address this question. [51,61]

4 GENETICS OF ALZHEIMER'S DISEASE

Almost 99% of the AD patients are attributed to sporadic causes, probably resulting from a combination of environmental factors and genetic susceptibility. Associations were found with risk factors like cerebrovascular disease, hypertension, metabolic dysfunctions such as diabetes and metabolic syndrome, smoking, traumatic brain injury, among many others. The most

important risk factor however is age and most of these patients develop a characteristically LOAD (over 60 years old). The remaining 1% of the patients have been found to have transmission of AD as an autosomal dominant disease (FAD), and have a characteristic early onset, usually between 30 and 60 years of age.[7]

Mutations in three genes are known for causing FAD: amyloid precursor protein (*APP*), Presenilin 1 (*PSEN1*) and its homologue Presenilin 2 (*PSEN2*), found on chromosomes 21, 14 and 1, respectively. These mutations affect the age of onset but have little or no effect on the disease duration when comparing with LOAD. The high set of similarities between FAD and LOAD support the transposition of FAD-related insights to the general AD population.[28,29,62]

4.1 APP

Mutations in the APP gene were the first ones to be linked with inherited AD. The APP gene is located on chromosome 21 (21q21.2-3) and is part of a small gene family which contains APP, amyloid precursor-like protein 1 (APLP1) and amyloid precursor-like protein 2 (APLP2) (human). From this family only APP contains a sequence encoding for the Aß peptide.[63]

The Aß peptide – key component of the AD-amyloid plaques - is generated through the sequential cleavage of APP by the ß-site APP cleaving enzyme (BACE) and the γ-secretase complex. The peptide can have different lengths, with $Aß_{1-42}$ most abundantly deposited in AD brain.[63]

So far, more than 30 missense mutations have been identified in the APP gene, from which 25 are pathogenic, and the remaining are thought to be non-pathogenic.[64] Some are autosomal dominant (e.g. K670N;M671L (Swedish) double mutation, E693Q (Dutch)), some are autosomal recessive (e.g. A673V) and some have a protective effect (e.g. A673T).[65,66] Several of the FAD-related mutations are found near secretase cleavage sites, and are believed to turn APP into a more suitable substrate for endoproteolysis, resulting in the overproduction of Aß.[65] Additional mutations are found within the Aß sequence, and are thought to promote the self-aggregation of Aß into amyloid fibrils.[67]

Interestingly, a mutation (E682K) on the 11th residue of the Aß peptide, the ß'-cleavage site, acts through shifting the cleavage at the ß'-site to the ß-site, resulting in increased full-length Aß production and also increased $Aß_{1-42}/Aß_{1-40}$ ratio.[68] APP duplication and Down's syndrome (trisomy) lead to Aß deposition and AD caused by an excess of APP.[29]

4.2 PSEN 1 AND PSEN 2

γ-secretase is a multi-subunit complex, responsible for the cleavage of APP transmembrane domain, leading to the release of the Aß peptide. This complex integrates four different transmembrane proteins: PSEN, nicastrin, anterior pharynx defective 1 (APH-1) and Presenilin enhancer 2 (PEN2). PSEN is an aspartyl protease, which only becomes active when combined with the other multi-subunit components, forming the catalytical site of the γ-secretase complex.[28,29]

The human genome contains 2 genes for Presenilin (*PSEN1* and *PSEN2*), located on chromosome 14q24.3 and 1q31-q42, respectively.[29] So far, more than 180 mutations in *PSEN1* have been identified. These mutations, mainly missense ones, account for 18-50% of FAD, and have a highly heterogenic phenotype. Several of these mutations have a tendency to affect a specific ethnic group, for example the A431E mutation that is associated with FAD in Mexican families.[29]

PSEN1 mutations result in an increase in $Aß_{42}$ generation. This might be explained by the model of sequential cleavage of APP by γ-secretase. If the *PSEN1* mutations result in a less efficient γ-secretase cleavage then a less complete processing of APP would be performed, resulting in increased production of the longer and amyloidogenic $Aß_{42}$ form.[69]

PSEN2 mutations are rarer, and in general result in an older age of onset than *PSEN1* mutations.[29,70] Similarly to PSEN1, PSEN2 can also be integrated into the γ-secretase complex. Its role in FAD is thought to be driven by a similar mechanism as for PSEN1 mutations. A recent study demonstrated that PSEN2 also increases ß-secretase activity through reactive oxygen species-dependent activation of extracellular signal regulated kinases.[71]

4.3 APOE AND OTHER GENETIC RISK FACTORS IN AD

Although there has not been identified a genetic cause-effect mechanism in the much more common sporadic LOAD, there are many genetic risk factors which may contribute to the development of the pathology. Many studies have demonstrated that the presence of ε4 allele of the ApoE gene is a major risk factor for LOAD, which is present in almost 40% of AD patients.[72] More recently, genome-wide association studies (GWASs) have identified several other candidate genetic risk factors.[29]

ApoE is located on chromosome 19q13.2, and single nucleotide polymorphisms at exon 4 result in three common alleles (ε2, ε3, ε4).[29,73] ApoEε4 is the allele associated with LOAD. The presence of one ε4 allele increases AD risk by 3 fold, and two ε4 alleles increases AD risk by 12 fold,

resulting in an earlier age of onset. On the other hand, the presence of ε2 allele results in a decreased risk for AD development and a later age of onset.[73] Interestingly, both ε2 and ε4 increase the risk for CAA, by increasing the Aß deposition in the cerebral vasculature.[74]

ApoE is primarily synthetized by astrocytes and microglia and is associated with cholesterol transport, neuroplasticity and inflammation.[75,76] ApoE can form lipoprotein particles by being lipidated by the ABCA1 transporter, and when lipidated can bind to the soluble Aß peptide in an isoform-dependent pattern (ε2 > ε3 > ε4), facilitating its uptake through cell surface receptors like low-density lipoprotein receptor-related protein 1 (LRP1) and low-density lipoprotein receptor (LDLR), inducing its clearance. Studies have demonstrated that the efficiency of this complex formation also follows the order ε2 > ε3 > ε4, leading to the hypothesis that ApoEε4 may be less efficient on the clearance of Aß. [72,73]

In addition, ApoE was shown to directly enhance microglia- and astrocyte-mediated Aß clearance. Also in an isoform dependent manner (ε4 > ε3 > ε2), ApoE was shown to decrease the transport of Aß across the blood-brain barrier (BBB), promoting Aß accumulation in the brain. Additional theories for ApoE role in AD are related with ApoE involvement in oxidative stress, lipid metabolism and inflammatory response.[72,75,76]

Since 2009, GWAS have identified several potential genetic risk factors besides the ApoE gene. So far, single nucleotide polymorphisms (SNPs) in 21 additional loci have been associated with LOAD: CR1, HLA-DRB5-DRB1, INPP5D, MEF2C, CD33, MS4A4, CLU, ABCA7, EPHA1, , PICALM, CD2AP, SORL1, CASS4, CELF1, DSG2, FERMT2, NME8, PTK2B, SLC24H4-RIN3, ZCWPW1. In general the identified genes seem to be involved in three main functions: lipid metabolism, immune response, and endocytosis, although their specific role in the pathogenesis has yet to be determined. [8,29,73]

In addition to the genes mentioned above, variants in APP, APP-modifying genes (PSEN1, PSEN2 and a desintegrin and metalloproteinase 10 (ADAM10)), and triggering receptor expressed on myeloid cells 2 (TREM2) were identified, and are associated with either protection or increased risk to develop LOAD.[73]

Mutations in APP are usually only associated with FAD, with the exception of the rare variant N660Y which is associated with SAD.[77] However, more recently, an A673T substitution on APP was shown to have a protective role against development of AD, and that this protection of cognitive function was even extended to elderly without AD. A673T is localized at position 2 in the Aß peptide, and since the usual BACE1 cleavage site is localized at the first position of the

peptide, this alteration is thought to impair ß-secretase-mediated APP cleavage, leading to a significant reduction in Aß peptide production. *In vitro* studies indeed revealed that presence of the A673T mutation results in approximately 40% reduction in the production of amyloidogenic peptides. The strong protective role of this variant supports the idea that reducing BACE1 cleavage of APP may protect against AD.[66]

PSEN1 E318G, a polymorphism in PSEN1, is associated with a 10-fold increase risk in carriers of ApoEε4 allele, and ADAM10 Q170H and R181G shift APP processing towards the amyloidogenic pathway. These results indicate that besides causing FAD, variants of APP and APP-modifying genes, can also alter the risk for LOAD.[73]

5 PATHOGENESIS

5.1 AMYLOID CASCADE HYPOTHESIS

When it was first described in 1992 the Amyloid cascade hypothesis stated that: "deposition of Aß protein (AßP), the main component of the plaques, is the causative agent of Alzheimer's pathology and the neurofibrillary tangles, cell loss, vascular damage, and dementia follow as a direct result of this deposition".[78] Although there are many experimental data supporting the fundament of this hypothesis, there are also several limitations, which are described below. Nowadays, we know that the initial hypothesis was not completely correct and that some links are still missing.

This hypothesis resulted from two main observations: Aß is the main constituent of the amyloid plaques, and all the mutations found causing Familial Alzheimer's disease (FAD), which are localized on APP, PSEN 1 or PSEN 2 genes, give rise to alterations in Aß production.[79] These mutations were found to promote the amyloidogenic pathway, therefore favouring the production of Aß. Also supporting this hypothesis, several of the found genetic risk factors for LOAD, from which ApoE4 is the main one, also influence Aß processing and/or clearance.[79,80]

Mutations on the tau gene can cause autosomal dominant frontotemporal lobe dementia with parkinsonism, which is characterized by the presence of NFTs, in resemblance to AD, but in the absence of amyloid plaques, suggesting that although it is capable of causing neuronal loss, tau pathology itself is not sufficient to induce the amyloid plaques characteristic of AD.[2] In addition, transgenic mice overexpressing both mutant human APP and mutant human tau display increased NFTs compared to tau single transgenic mice, whereas the number and structure of their amyloid plaques does not change compared to APP transgenic mice, supporting the idea of

Aß deposition as the initial trigger.[67] Moreover, studies in APP-transgenic mice have also reported that a reduction in the endogenous levels of tau can improve some of the Aß-mediated consequences.[24]

Although the exact mechanism by which Aß deposition results in tau pathology is not clear, several studies have already shown that FAD-related mutations can alter tau phosphorylation, inducing its hyperphosphorylation and detachment from microtubules.[80] This allied to the reports that Aß-mediated toxicity is tau dependent and highly supports the amyloid cascade hypothesis.[23,81,82]

Several studies put tau as a downstream event of Aß,[82] therefore it would seem reasonable to assume a sequence of events where FAD mutations lead to overproduction of Aß, that by a yet to be clarified mechanism would induce NFTs formation, which would in turn lead to cell death and ultimately dementia. Since FAD and LOAD have a similar neuropathological phenotype, it is assumed that they would both result from a similar sequence of events. [79]

In recent years, several limitations of the amyloid cascade hypothesis have been described. Firstly, amyloid plaques and NFTs may be a consequence of neurodegeneration in AD rather than its cause, since both Aß deposition and NFT were found increased in individuals who suffered from head trauma or other kinds of brain injury.[83,84] In addition, intrathecal or intraparenchymal injection of toxins results in increased APP levels in hippocampal neurons, suggesting that APP production can be specific to the loss of functional innervation of the cortex, but not a specific phenomenon of AD. [80]

Secondly, this hypothesis also does not explain why there exists such a low correlation between the accumulation of Aß in plaques and the presence of NFTs, neuronal loss, and dementia,[85,86] and the *post-mortem* findings of significant Aß accumulation in the brains of elderly who were cognitively normal. Although Aß accumulation in cognitively normal individuals could be explained with the existence of individuals with high and low risk of developing AD as suggested by the dynamic model of AD biomarkers. Several studies have also reported that SP density declines with advancing age, possibly as a result of plaque removal by glial cells. This suggests that Aß deposition cannot certainly predict or cause AD, since SP may accumulate over a period of time and then stabilize or even decline with age, but again this lack of cause-effect in some individuals can be explained by the dynamic biomarker model, as different risk groups will have different responses to biomarker abnormalities. [87]

Additionally, the lack of positive results from Aß-targeted disease modifying strategies in clinical trials has also contributed to the scepticism related to the amyloid cascade hypothesis.[87,88] Interestingly, a recent clinical trial, with an anti-amyloid antibody – Aducanumab - had very positive results and appears to both remove amyloid plaques and stop disease progression, which supports the amyloid cascade hypothesis.[89]

Clearly, additional investigation about the mechanisms by which Aß accumulation results in the formation of PHFs and NFTs, and later in neuronal loss is required for further support and approval of this hypothesis. [80] But despite the limitations, the supporting data set is still extensive enough to make this a widely accepted hypothesis.[79]

The lack of correlation between Aß deposition and AD symptoms has led to the suggestion to insert a new component in the initial hypothesis. The modified amyloid cascade hypothesis (*Figure 4*), follows the same principles of the primary hypothesis but includes the presence of Aß-derived diffusible ligands or soluble toxic oligomers, which would account for the main Aß-mediated neurotoxicity.[79,90]

These intermediary forms would stand between the soluble monomer Aß and the insoluble fibrils, and would be able to directly affect neurotransmission.[91] This new link has been supported by the isolation of several different Aß oligomeric forms, which display toxic activity from transgenic mouse brain[92] and the human brain.[91] Since the mechanisms of their toxicity are not fully understood, they are referred to as 'aggregate stress', and are hypothesized to contribute to development of tau pathology and ultimately neuronal loss together with the deposited Aß.[79] It is however important to note that a single selective neurotoxic oligomer acting at a specific stage is yet to be found.[90]

Several studies have reported some of the possible mechanisms by which Aß oligomers can be toxic: disruption of calcium signalling,[93] induction of oxidative stress,[94] and mitochondrial dysfunction.[95] Aß dimers and oligomers have also been linked with synaptic dysfunction: inhibiting hippocampal long-term potentiation (LTP),[96,97] affecting N-methyl-D-aspartate (NMDA) receptor proper functioning,[98,99] and reducing postsynaptic receptors and disrupting synapse morphology.[100] Interestingly, tau-dependent microtubule disassembly can result from exposure to prefibrillary Aß, and this could help explain why Aß aggregation precedes NFT formation.[101]

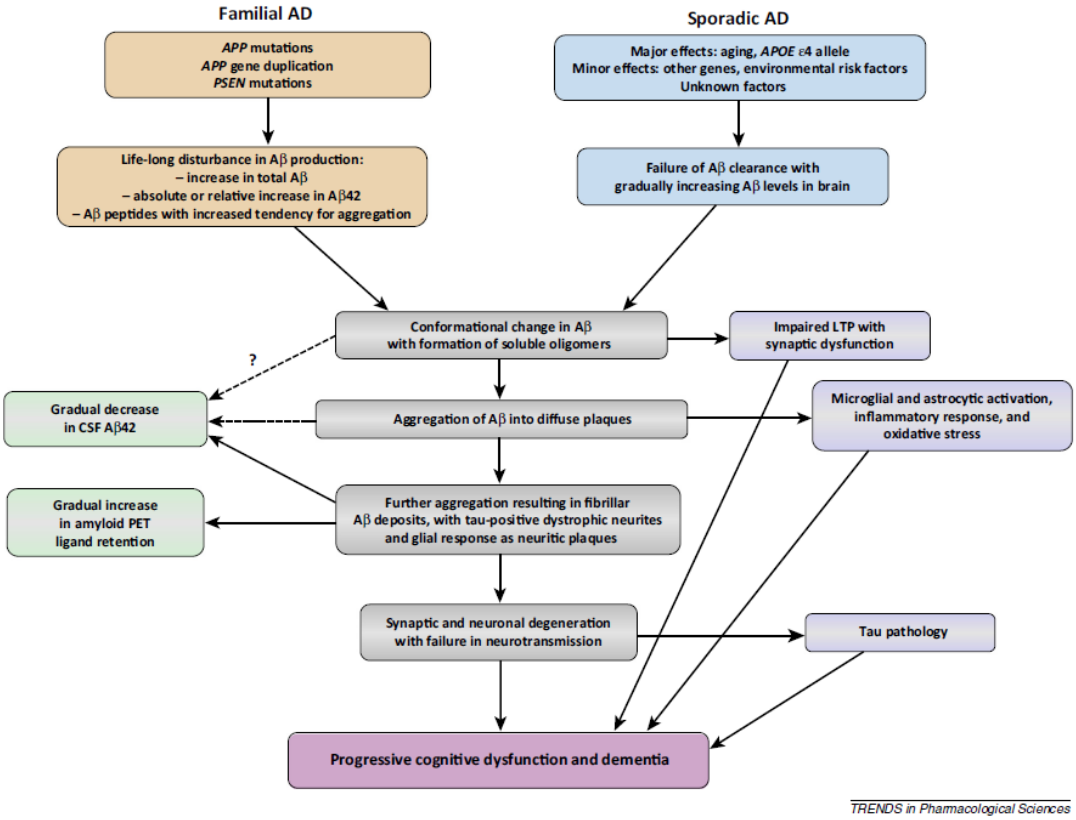

Figure 4 - The modified amyloid cascade hypothesis. APP – amyloid precursor protein, PSEN – Presenilin, Aβ – amyloid-β, LTP –Long Term Potentiation, CSF – Cerebrospinal fluid, PET – Positron Emission Tomography, NFT – neurofibrillary tangle. (Adapted from Blennow K., et al. (2015)[47])

More recent studies have provided additional insights, which might complement the modified amyloid cascade hypothesis:

- It was described that several transgenic mouse models accumulate intraneuronal Aß which might contribute to the initial steps of the disease process.[102,103] Intracellular Aß accumulates, both in mouse and humans with AD, before the amyloid plaque formation.[104–106]
- Aß deposits can directly activate the complement system, triggering an inflammatory response.[107] Neuroinflammation may promote tau phosphorylation, resulting in its intracellular aggregation, thus providing a possible explanation for the mechanism by which Aß promotes NFT formation.[108]
- Metal ions, namely Zn(II) and Cu(II), are a possible candidate for the initial trigger of Aß aggregation, by causing metal-induced aggregation. Since there is an overlap of the areas where amyloid plaques accumulate and the regions with a high density of glutamatergic terminals and free zinc vesicles (at least in some APP transgenic mice), this mechanism would explain the topographic selectivity of plaque formation in the AD brain.[27,109]
- Reduced brain blood flow can be found even in the preclinical disease. A chronic hypoperfusion and neurovascular dysfunction indicate that AD pathology not only results from Aß accumulation and Aß mediated-toxicity, but also from the impairment of the neurovascular

functioning, essential for neuronal cell survival. Though it is not clear if the reduction in blood flow is a cause or a consequence of AD.[110]

Overall, it appears that several factors related to the amyloid cascade hypothesis require further investigation. Nonetheless, the package of supporting evidence at current is convincing enough to drive the development of therapies targeting Aß for AD.

6 APP

APP is a type I transmembrane protein constituted of a large glycosylated extracellular N-terminal, an extracellular E1 and E2 domain, a transmembrane domain and a short C-terminal cytoplasmic domain containing 47 amino acid residues. The Aß peptide comprises the N-terminal juxtamembrane region (28 amino acid residues) and half of the transmembrane sequence. [111]

APP is expressed ubiquitously throughout the organism and in many cell and tissue types.[112] The APP transcript can be alternatively spliced into eight different isoforms from 365 to 770 amino acids long, and the three major isoforms are APP770, APP751 and APP695. In the brain, the predominant isoform is the APP695, which is the only that lacks a Kunitz protease inhibitor (KPI) domain in its extracellular domain.[113,114] Besides the alternative splicing, APP can also undergo a series of posttranslational modifications, such as glycosylation, phosphorylation and specific proteolytic cleavages.[1]

Deletion or knockdown of APP in mice is not lethal but gives rise to some cognitive and locomotor impairments and development of cerebral gliosis with age. In rat embryos, APP knockdown results in impaired migration of radial glial-guided immature neurons. The absence of a lethal phenotype is probably due to the mammalian expression of APP close homologous APLP1 and APLP2 which could compensate for the absence of APP. [1] Like APP, APLP2 is also ubiquitously expressed. On the other hand, APLP1 is only found in the brain. While both APP and APLP2 are mostly found in intracellular compartments, APLP1 is mainly found on the plasma membrane.[111]

6.1 APP PROTEOLYTIC PROCESSING

The maturation of APP happens through the constitutive secretory pathway from the endoplasmic reticulum (ER) to the plasma membrane.[115] APP is mainly found in the Golgi complex, and just a small part is located at the cell surface being rapidly internalized, due to the

endocytosis motif (YENPTY) localized in its cytoplasmic region, and sorted into early endosomes. Part of the internalized APP is then recycled, while the rest is directed to the lysosome for degradation.[116]

APP can be cleaved by two different proteolytic pathways – the non-amyloidogenic and the amyloidogenic pathway (*Figure 5*).[116,117]

In the non-amyloidogenic pathway, APP is first cleaved by α-secretase between Lys16 and Leu17 of the Aß peptide, leading to the formation of a secreted APP fragment (sAPPα) and a C83 transmembrane fragment. The transmembrane fragment is then cleaved by γ-secretase, yielding an extracellular p3 fragment and an APP intracellular domain (AICD), being the latter rapidly degraded.[116–118]

In the amyloidogenic pathway APP is sequentially cleaved by ß-secretase, or ß-site APP cleaving enzyme 1 (BACE1) at the 1st (ß-site) residue, followed by the γ-secretase cleavage. The first cleavage results in formation of 2 fragments – a secreted APP fragment (sAPPß) and a C99 (ß-site) transmembrane fragment. The latter is further cleaved by γ-secretase into an Aß peptide and the AICD.[116,117]

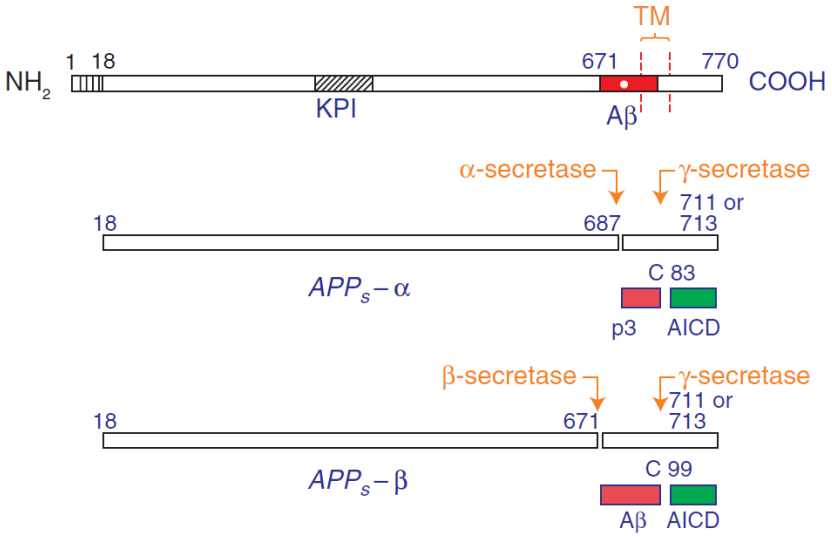

Figure 5 - Schematic representation of APP and its main processing pathways. (Middle) Non-amyloidogenic processing, where APP undergoes cleavage by α-secretase (residue 687) and then cleavage by γ-secretase (residue 711 or 713) giving rise to sAPPα, p3 and AICD. (bottom) Amyloidogenic processing of APP by β-secretase (residue 671) followed by γ-secretase, generating sAPPβ, the Aβ peptide and AICD. APP – amyloid precursor protein, APPs – secreted APP fragment, AICD – APP intracellular domain, Aβ- amyloid-β. (Adapted from Selkoe, D. J. (2011)[1])

Under physiological conditions, the non-amyloidogenic pathway accounts for more than 90% of APP processing, and since α-secretase cleaves within the Aß peptide region, this does not lead to Aß production. In the AD brain however, Aß accumulation is suggested to be caused by an

imbalance between the non-amyloidogenic and the amyloidogenic pathways and/or a deficit in clearing Aß from brain.[119]

While α-secretase is predominantly present on the cell surface, BACE1 is mostly found in the intracellular compartments, i.e., in the Trans Golgi Network (TGN) and endosomes. BACE1 location corresponds to the fact that the enzyme is optimally active at more acidic pH, which is not usually found on the cell surface.[116,120] Further cleavage by the γ-secretase complex requires the transmembrane fragment to be further transported into areas where the γ-complex is present, like the cell surface.[116]

Therefore, it is very likely that the two proteolytic pathways occur at different subcellular localizations. While the non-amyloidogenic pathway takes place on the cell surface, where the α-secretase is anchored,[121] the amyloidogenic pathway probably occurs within intracellular compartments, including the ER/ER-Golgi intermediate compartment, the Golgi during APP biosynthetic transport, and the endosome/lysosome after endocytosis occurs.[122] This is corroborated by the fact that impairing APP trafficking to the cell surface or enhancing APP internalization results in increased amyloidogenic processing, while doing the reverse leads to increased non-amyloidogenic processing. [122]

6.2 A-SECRETASE

α-secretase is a member of the ADAM family of membrane-anchored zinc metalloproteases. This family is constituted of type I integral membrane proteins, and have been associated with the shedding of several substrates such as APP,[123] Notch receptors and ligands,[124] cytokines (e.g. tumour necrosis factor (TNF)-α),[125] and growth factors (e.g. epidermal growth factor (EGF) family members).[126]

In the AD context, α-secretase is responsible for the non-amyloidogenic processing of APP, cleaving it on the 17th residue between Lys16 and Leu17 of the Aß peptide (Figure 6).[117] Processing by α-secretase occurs mainly at the cell surface, since these proteases are bound to the plasma membrane. So far, several members of the ADAMs family have been identified as having α-secretase activity – ADAM9, ADAM10, ADAM17, and ADAM 19.[123,127]

Regarding the APP processing, studies have suggested that ADAM10 would be responsible for the constitutive proteolytic cleavage by α-secretase, while ADAM9/17/19 would be more related with the regulated cleavage, i.e., the protein kinase C-dependent APP processing, rather than the constitutive one.[128]

6.3 ß-SECRETASE

In 1999, BACE1 was identified as being responsible for ß-secretase activity.[120,129] BACE1 is a type I transmembrane aspartyl protease, which has the active site located on the extracellular side of the membrane.[117] Having an optimal pH of 4.0-5.5, BACE1 is mostly found in perinuclear post-Golgi membranes and vesicular structures throughout the cytoplasm (endosomes and lysosomes), a small proportion can also be found on the cell surface.[117,120] BACE1 is synthesized in the ER, as a precursor with an N-terminal signal peptide (residues 1-21), a pro-domain (residues 22-45), a protease domain (residues 46-460) which contains the two active sites (residues 93-96 and 289-292), and is inserted in the cellular membrane through a transmembrane domain (residues 461-477), followed by a short cytosolic domain (478-501).[130]

After synthesis, BACE1 undergoes a process of maturation throughout the trafficking in the Golgi apparatus. During maturation several modifications occur: the pro-domain is cleaved probably by proprotein convertases (PC),[115,131] N-glycosylation as well as sulfation can occur at four sites (Asparagine residues 153, 172, 223 and 354),[132,133] and reversible acetylation in a cluster of seven lysine residues is possible which increases the protein stability and allows its transportation throughout the secretory pathway.[130] Besides these modifications, the cytosolic domain is particularly prone to various post-translational modifications such as palmytoylation,[133] phosphorylation,[130] and ubiquitination, [134] which affect BACE1 cellular trafficking.

In the Golgi apparatus, BACE1 is sorted by golgi-localized γ-ear-containing ARF-binding protein (GGAs), a family of monomeric clatherin-adaptor proteins, that will facilitate the sorting of BACE1 from the TGN to the endosomes, which is its primary site of location and activity.[130] From the endosomes it can recycle to the TGN or go to the plasma membrane, where it concentrates as a dimer in lipid rafts. The dimeric form of BACE1 is more active than the monomeric soluble form, and therefore produces higher amounts of Aß peptide.[135] From the plasma membrane, BACE1 undergoes internalization into specialized early endosomes under the control of GGA1 and ADP-ribosylation factor 6 (ARF6).[116,130] After internalization it can follow two paths: recycling from the early endosome to the TGN, which is favoured by phosphorylation at Ser498, and subsequent re-delivery to the plasma membrane, or retrograde trafficking from the early endosome to the TGN, which is controlled by the retromer complex. GGA3 can recognize endosomal ubiquitinated-BACE1 and target it for lysosomal degradation.[116,130]

There are several isoforms of BACE1 resulting from alternative splicing. However, only splice-variant with 501 amino acids (BACE1-501) has the particular ß-cleavage activity responsible for Aß peptide production.[117] BACE1 is ubiquitously expressed, having a higher level in the brain and pancreas, although the alternative splice-variant present in the pancreas has a reduced APP-cleavage activity.[136]

BACE1 also has a homolog, BACE2. This homolog has a low expression in the brain and is more predominant in glial cells, while BACE1 is more expressed on neuronal cells, although astrocytic expression of BACE1 increases with age. Interestingly, it was shown in transgenic mice that after amyloid plaques were formed, BACE1 would become selectively expressed in the activated astrocytes that surround the amyloid deposits, probably activated due to the Aß-mediated toxicity.[117,137] Nonetheless, although BACE2 can generate Aß *in vitro*, its main cleavage site is within the Aß peptide. [138] Therefore BACE2 is thought to exert an opposite effect to BACE1, having an anti-amyloidogenic activity in the glial cells.[128]

Additionally, BACE2 is involved in the processing of a pigment protein – the pigment cell-specific melanocyte protein (PMEL) substrate - which is essential for the formation of the amyloid matrix that supports the melanosomes. BACE2 has also a role in regulating pancreatic ß cell mass and function, through the shedding of Tmem27, a proproliferative protein.[65]

Besides the cleavage at the 1st residue, BACE1 can also cleave APP on the 11th (ß'-site) residue of Aß (Figure 6). Cleavage at ß- or ß'-site strongly depends on the APP sequence near the ß-cleavage sites, on the subcellular localization of BACE1, and on BACE1 expression levels. Targeting BACE1 to the ER or lipid rafts results in a preferential cleavage of the ß-site, whereas targeting it to TGN, lysosomal system and downstream apparatus of the ER promote a preferential cleavage of the ß'-site. Additionally, when BACE1 levels are low, the ß-site cleavage and its Aß1-x product are predominant, and when BACE1 levels increase, the ß'-site cleavage and its $Aß_{11-x}$ product become more abundant. [46,116] Though the functional significance of this alternative cleavage is not yet clear it is thought to have a possible anti-amyloidogenic effect, since a mutation at the ß'-site cleavage (E682K), shifts the cleavage towards the ß-site and is associated with an early onset of AD.[68,117]

BACE1 protein levels and enzymatic activity are described to be increased in AD populations in some studies, at least in the frontal and temporal cortices.[139–141] However, half of the AD patients do not present increased BACE1 levels.[130] The increase may be associated with post-translational and post-transcriptional changes (e.g. decreased levels of miRNA-29a/b or increase

in an antisense transcript which stabilizes BACE1 messenger RNA (mRNA)), rather than alterations in gene expression.

Aß production is completely blocked in BACE1 knockout mice,[142] making BACE1 one of the main targets for Aß-targeted therapies. Nonetheless, for consideration as a therapeutic target, it is also essential to investigate the effect of BACE1 inhibition on the other physiological functions of BACE1 and to minimize potential side effects. Besides the already described APP and APP homologs, BACE1 has several other substrates.[65]

6.3.1 BACE1 substrates

The BACE1$^{-/-}$ mice were initially thought to be viable, fertile and have no particular phenotype. Further investigation allowed to uncover complex neurological phenotypes, which are in accordance with BACE1 elevated central nervous system (CNS) expression and presynaptic localization. These phenotypes include hypomyelination, axon guidance impairment, disrupted muscle spindle maintenance, memory deficits, age-related neurodegeneration, schizophrenia endophenotypes, retinal pathology, spine number reduction, decreased neurogenesis and increased astrogenesis abnormalities, neurochemical deficits, among others. Such phenotypes are likely a result of a deficient BACE1 processing of its substrates.[138]

In the peripheral nervous system (PNS), BACE1 has been associated with the regulation of axonal myelination, where it was shown to proteolytically process Neuregulin-1 (NRG1), which is involved in promoting Schwann cells-mediated myelination. BACE1$^{-/-}$ animals present a PNS hypomyelination phenotype and a highly disturbed formation of Remak bundles. So far, BACE1 myelination-related function does not appear to participate in CNS myelination.[65]

Recent proteomic studies allowed the identification of novel BACE1 substrates involved in several neuronal functions, and that can be mainly subdivided into two groups: those involved in synaptic function and those involved in modulating axonal outgrowth and migration. The first group consists of neurexin 1α, the neuroligin family, and the latrophilin family. Neurexin-1α and latrophilins are presynaptic and can interact with each other, or with neuroligins, which are postsynaptic, allowing a proper synaptic functioning. The second group includes L1, close homolog L1 (CHL1), contactin-2, and SEZ6 family.[65,138]

Many other substrates of BACE1 have been identified such as the peptidyl amidating monooxygenase (PAM), type II a-2,6-sialyltransferase, JAG1, platelet selectin glycoprotein ligand-1, Aß itself, and the interleukin-like receptor type II, although the relevance of some of these cleavages is still unknown.[65,138,143]

While some of these substrate cleavages are completely dependent on BACE1, like SEZ6, and a BACE1-deficiency results in the non-cleavage of this substrate, other substrates can be cleaved by other proteases and as a result are only partially affected by the absence of BACE1. As an example, in the absence of BACE1, APP is proteolytically processed by α-secretase.[65,138]

6.4 γ-SECRETASE

In both the amyloidogenic and the non-amyloidogenic pathway, the remaining transmembrane carboxy-terminal fragments (CTFs) are cleaved by γ-secretase. γ-secretase-mediated proteolysis is performed by a multi-subunit complex of proteins, being constituted by four main subunits – nicastrin, APH1a or APH1b, PSEN1 or PSEN2 and the PEN2.[28,117,128]

The human genome contains 2 genes for Presenilin (PSEN1 and PSEN2) and 2 genes for Aph1 (Aph1a and Aph1b), so there are at least 4 different γ-secretase complexes that can be formed. The γ-secretase complex has many proteolytic substrates besides APP, and different combinations appear to be important for different activities, for example while the Aph1a/PSEN1 are essential for Notch signalling, embryonically and in the adulthood, the Aph1b is associated with the neuregulin processing.[28,144] Of note, APP itself can regulate PSEN1, and therefore γ-secretase cellular trafficking, distribution and activity.[117]

APP can be cleaved at several sites by γ-secretase. This cleavage is suggested to happen in a sequential manner, resulting in the production of Aß peptides and AICDs with several lengths.[145,146] The intramembrane proteolytic cleavage is suggested to begin by the ε-cleavage sites (after aa 49/48), followed by cleavage at ζ-cleavage sites (after aa 46/45), ending with the γ-cleavage site (after aa 42/40 (usually), or after aa 37, 38, 39 and 43) (Figure 6). The generation of the main

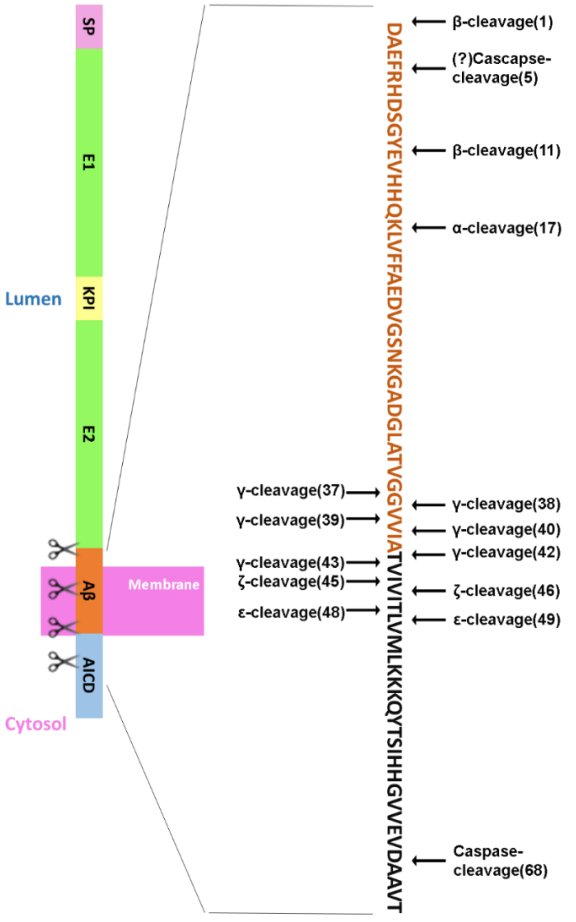

Figure 6 - APP main proteolytic cleavages. APP – amyloid precursor protein, SP – signal peptide , KPI- kunitz protease inhibitor, Aβ – amyloid-β, AICD – APP intracellular domain. (Adapted from Zhang, H., et al. (2012)[117]).

products ($Aß_{42}$ and $Aß_{40}$) is suggested to follow different cleavage sequences. $Aß_{42}$ may result from sequential cleavage of ε-48, then ζ-45 and finally $γ\text{-}_{42}$, whereas $Aß_{40}$ may result from cleavage of ε-49, ζ-46, γ-43 and finally γ-40.[145,146]

6.5 ADDITIONAL CLEAVAGES

Besides secretase-mediated cleavage, APP also undergoes cleavage by caspases, in the AICD region (*Figure 6*). This cleavage results in the release of a short tail containing the last 31 amino acids of APP (C31 fragment). Studies suggest that this caspase-mediated cleavage is toxic, since this fragment displays cytotoxic activity through the potentiation of apoptosis by a mechanism involving activation of caspase 8 and 9.[147,148]

Several other proteases have also been suggested to cleave the Aß peptide in the N-terminal region. Aminopeptidase A and Meprin-ß have been associated with the generation of Aß2-x; Neprilysin (NEP) has been associated with the production of Aß3-x,Aß4-x, Aß6-x. The latter, Aß6-x, can also be produced by plasmin-mediated cleavage. Moreover, myelin basic protein and the angiotensin-converting enzyme are associated with Aß5-x and Aß8-x production, respectively.[149]

6.6 FUNCTION OF APP AND APP-DERIVED FRAGMENTS

6.6.1 APP

The normal APP function is not yet clarified, and throughout the years it has been associated with a variety of mechanisms. This is mainly because APP owns a range of functional domains: metal binding, extracellular matrix (ECM) (heparin, collagen and laminin) binding, neurotrophic and adhesion domains, and protease inhibition (through the KPI domain). The most accepted functions of APP and its metabolites are regulation of synapse formation and proper functioning, and neuronal growth through promotion of cell movement and neurite outgrowth.[113,114,119,150]

In the peripheral nervous system, mammalian APPs are required in motor neurons and muscles to ensure a functional neuromuscular junction (NMJ). However the mechanisms by which this is mediated are not clear.[151] In CNS, APP appears to be also related with synapse formation, since its absence results in impairment of LTP and a decrease in the number of dendritic spines.[152] This phenotype can be rescued by sAPPα, suggesting an important role for the non-amyloidogenic processing of APP.[153] Some studies also indicate a role for APP in learning and memory, but again the mechanisms are not yet clarified.[154,155]

Through its interaction with the ECM components APP has been shown to promote neurite outgrowth and enhance cell migration and movement. Several other APP-binding proteins have

corroborated this promotion of cell movement, for example Fe65 is an adapter protein that binds the intracytoplasmic tail of APP and also binds a second protein, mammalian homologue of Drosophila enabled (MENA), which in turn binds profilin and enhances actin filament formation.[113]

Several studies suggest that APP, both in the full length and in the secreted form, may act as a co-receptor transducing several extracellular motility signals that would converge on kinase activation, and would regulate neuronal cytoskeleton, allowing its remodelling, neurite outgrowth and cell movement.[150]

6.6.2 sAPPα and sAPPß

sAPPα has been suggested to exert neuroprotective activity, being also associated with neurite outgrowth, synaptogenesis and cell adhesion. Some studies have also shown that it can act as a growth factor that regulates the proliferation of embryonic and adult neural stem cells.[117] It was demonstrated that sAPPα interacts with Semaphorin 3A, a secreted axonal outgrowth inhibitor, inhibiting semaphorin 3A-induced growth cone collapse.[156] sAPPα has also been linked with learning and memory promotion in animal models.[157,158]

Contrary to the neuroprotective activity of sAPPα, a fragment of sAPPß – the amino terminal fragment of APP (N-APP) - has been suggested to activate caspase-6, stimulating axonal pruning and neuronal cell death.[159]

6.6.3 CTF

APP-CTFs are generated through processing of APP by α-secretase or ß-secretases or even other proteases, and might contribute for the development of AD. Transgenic mice overexpressing.[160] So far, CTFs were associated with calcium homeostasis disruption, and memory and learning impairments through the LTP prevention. Additionally, CTF also promote neuroinflammation through MAPKs and NF-κB-dependent astrocytosis and inducible nitric oxide synthase (iNOS) induction.[160,161]

6.6.4 AICD

Due to the alternative sites for γ-secretase cleavage of APP, AICD fragments with several lengths can be formed. But because they are quickly degraded, their specific function is still poorly defined.[117] Nonetheless, several proteins have been identified to bind AICD: Fe65, JIP, Numb, Clathrin, mDab1, Shc among many others. So it is possible that AICD has different functions when interacting with different proteins.[117]

One of the generally accepted functions for AICD is the formation of a complex with Fe65, and through this latter with tip60. In this complex, AICD can be translocated to the nucleus, and regulate the expression of several genes, e.g. LRP1, p53, NEP, GSK-3ß and EGFR.[117] Although some studies suggest that AICD has to be translocated to the nucleus to regulate transcription, other studies propose that the conformational alteration of Fe65 induced by AICD is sufficient for the transcriptional regulation.[162]

Several studies also suggested that AICD has cytotoxic activity, through for example the C31 fragment, mentioned above, which may have the capacity to activate caspase-3 and further cell death.[147,148] However, it is possible that cytotoxic effects are sometimes mediated by its interacting partners (e.g. JIP is a scaffolding protein of the JNK pathway, which is involved in apoptosis; AICD-mediated activation of p53 may lead to apoptosis activation), rather than just by AICD itself.[163,164]

6.6.5 Aß peptide

The Aß fragment is usually constituted of 40 or 42 amino acid residues, but it can also be 37, 38, 39 and 43 amino acids length.[128] In the AD brain, N-truncated forms, $Aß_{X-40/42}$, can also be found, and are associated with a very high amyloidogenic propensity and toxicity.[165]

$Aß_{1-40}$ is produced in the highest amount in the human brain, but it is generally accepted that $Aß_{1-42}$ is the fragment critically associated with AD development. Most mutations associated with AD development are associated with an increase in the ratio $Aß_{42}$/ $Aß_{40}$.[28,117]

Studies have shown that $Aß_{40}$ possibly protects against $Aß_{42}$-mediated toxicity, and in normal physiological conditions may promote synaptic plasticity and memory.[166,167] Nonetheless, Aß monomers tend to spontaneously aggregate due to their amphipathic nature, leading to the formation of larger soluble forms – oligomers or protofibrils. The continuous assembly results in the formation of the insoluble fibrils that will eventually deposit in the brain forming the so called amyloid plaques, which are one of AD's hallmarks.[85,117]

Several studies have shown that excess of Aß peptide results in neurotoxicity, NFT formation, synaptic impairment and eventually neuronal cell death.[117] The neurotoxic effects can probably be attributed to both oligomeric as well as fibrillar forms of Aß. Oligomeric Aß has gained more attention in recent years as being the most toxic species, resulting in impaired LTP and synaptic dysfunction. On the other hand, Aß fibrils and plaques are associated with microglial and astrocytic activation, induction of inflammatory response, neuronal/synaptic dysfunction, and alteration of the kinase/phosphatase activity which in turn can contribute to NFT

formation.[168,169] Interestingly, studies suggest that the levels and distribution of the soluble forms of Aß (monomers, oligomers, protofibrils) correlate much better with disease progression and severity than the insoluble fibrils.[85]

Studies have also shown N-truncation and modification of the Aß peptide to cause increased neurotoxicy and enhanced aggregation into plaques. It has also been suggested that N-truncated peptides may be the trigger for Aß plaque formation, and it is generally accepted they are highly abundant in SAD and FAD brains. N-truncated species starting at AßpE3-x and Aß4-x are reported to be the abundant species in the SP of AD individuals.[149,170,171] The pyroglutaminylation of N-truncated species, like $Aß_{pE3-x}$ and $Aß_{pE11-x}$, has been shown to increase aggregation propensity. This modification has been speculated to make the fragments more degradation-resistant.[149,172] Comparable to the rest of the N-truncated forms, Aß5-x is also thought to be a highly toxic isoform due to the capacity to rapidly form stable aggregates. Aß5-x is found deposited in several pathological lesions such as the ones associated with CAA, but is also found in association with amyloid extracellular plaques.[165,173]

Regarding Aß degradation, several proteases have been associated with this process: NEP, Insulin degrading enzyme (IDE), angiotensin converting enzyme (ACE), endothelian converting enzyme (ECE1,2), matrix metalloproteinases (MMP9, MMP2), plasmin and cathepsin B. Some reports suggest that some of these proteases are upregulated in AD, but this increase does not appear to be sufficient to prevent further Aß accumulation. Another important mechanism for Aß degradation is through its interaction with ApoE, which is involved in cholesterol homeostasis and trafficking.[28,169]

Aß peptides are transported across the BBB, mainly through the low-density lipoprotein receptor-related protein (LRP) on the brain side and the receptor for advanced glycation end products (RAGE) on the blood side. Interfering with this mechanism increases the amount of Aß in the brain and may potentiate further deposition.[114,168]

More recently, increasing evidence indicates that misfolded Aß oligomers might be able to spread throughout the brain in a similar manner as misfolded prion protein. This theory states that the misfolded peptide, when taken up by neurons, can promote normal Aß misfolding and then further spreading of the toxic oligomers into other brain regions. This is supported by the Aß spreading along its axonally connected regions.[20,174]

7 MODELS TO STUDY AD

Having a proper disease model is crucial not only for the study of AD pathogenesis, genetic interactions and risk factors, but also for the evaluation of possible therapeutic drug-candidates.[175] Animal models of AD ideally should fulfil three main characteristics:

- Face validity: Display pathophysiological (plaques, NFTs, neuronal loss) and behavioral (including cognitive deficits) markers representative for AD.[175]
- Construct validity: Development of the disease traits (pathophysiological and behavioral) in a similar manner to the human AD.[175]
- Predictive validity: Provide predictive value for AD pathogenesis, allowing extrapolation of the data obtained of an experimental manipulation.[175]

Because the etiology of LOAD is not entirely known, many animal models have been developed using genetic mutations associated with FAD, based on the principle that these mutations would trigger the downstream events of AD. And although many models present some of the characteristics of AD, none of the currently available models is complete in mimicking all aspects of the AD pathology.[176]

Although there are invertebrate models (*Drosophila Melanogaster* and *C. elegans*) and non-mammalian vertebrate models (chickens, *Xenopus laevis* and *Danio Rerio* (Zebrafish)) that are used for the study of some mechanisms of AD, the most utilized models are the mammalian ones, which can be subdivided into transgenic, interventional and natural models.[176,177]

7.1 TRANSGENIC MODELS OF AD

Transgenic mice have been the most widely used transgenic models in AD research. These models have been helpful in improving the understanding of the molecular mechanisms associated with Aß production, deposition and clearance, the effects of Aß on the neuronal level and correlation with the development of cognitive decline. The transgenic mouse models have also given important information about the role of inflammation, mitochondrial dysfunction and oxidative stress in the pathogenesis of AD.[177,178]

It is important to take into account that rodent APP differs from human APP in the region of the Aß peptide, and this difference makes rodent Aß less prone to aggregation. Therefore, models using rodents require the over-expression of human APP and/or other proteins involved in AD to give rise to development of plaque pathology.[179]

The first transgenic models of AD were generated by overexpression of mutant human APP in an attempt to reproduce amyloid pathology.[180] Some of these models were the PDAPP mice, the Tg2576 line and the APP23 mice. These models developed amyloid plaques in the hippocampus and cortical areas.[180,181]

Following the identification of pathogenic mutations in the PSEN genes in AD, transgenic animal models have been generated to address the role of PSEN1 and PSEN2 in APP processing *in vivo*.[181] These PSEN-models showed increased levels of $Aß_{42}$, but this did not seem to be sufficient for plaque development.[182] Introduction of several transgenes, like in the double transgenic mice (expressing mutant human APP and mutant human PSEN1), can significantly accelerate plaque deposition. [182]

Although some of the models presented abnormal tau phosphorylation, most of them did not develop NFTs. With the aim of studying tau pathology, tau-mutant mice were developed, and more recently, triple transgenic mice, expressing mutant human APP, PSEN1, and tau, were generated, allowing the development of the majority of AD hallmarks.[182]

The histopathological hallmarks of AD, like amyloid plaques and NFT, have been reproduced in several animal models. Aspects like inflammation, plaque deposition, the role of presenilins in APP processing and the importance of phosphorylation in tau aggregation have been shown. However, it seems to be difficult to achieve massive cell loss in the mouse, either due to the short lifespan of the animal, or because mouse neurons may be less vulnerable.[181]

Nowadays, among the created transgenic mouse models we can find APP models , CTF models, Aß models, PSEN1/PSEN2 models, APP+PSEN models, Tau models, and triple (APP+PSEN+Tau) models (summarized in *Table 1*). [175,183,184]

More recently, rat transgenic models have also been developed. Rat brain is approximately six times larger than mouse brain, making it more suitable for some studies, such us evaluation of imaging biomarkers by PET, sampling tissue and CSF for histological or biochemical studies, and for electrophysiological measurements.[185–187] The closer evolutionary distance between humans and rats, when compared with mice, may also suggest that rat models may be better for AD-related studies.[185] Additionally, rats also have a more complex behavior that is better characterized, which may make them more suitable for the assessment of therapeutics on cognitive functions. Still, rat transgenic models also have some disadvantages when compared with mice: there is a low survival rate of the embryos following injection of transgene,[188] there are less available tools for rat genome manipulation,[189] and rat one-cell embryos have less visible

pronuclei and more flexible plasma pronuclear membranes making the transgene injection process more complicated.[188]

Table 1 – Transgenic AD mouse models (Adapted from Lee J. and Han P. 2013[175])

Type of Model	Model examples	Transgene	Phenotype
APP models	PDAPP	APP695, 751, 770-V717F	Plaque deposition (6-9m); behavioural defects (13-15m)
	Tg2576	APP695-K670N/M671L	Plaque deposition (9m); behavioural defects (6m)
	TgAPP23	APP751-K670N/M671L	Plaque deposition (6m), synaptic degeneration and tau hyperphosphorylation; behavioural defects (10m)
CTF models	CTF104	CTF 104 of APP591-695	Plaque deposition (8-10m); cognitive deficits (8m); neuronal loss (18-22m)
	TgCTF99	ßCTF99	No plaques; cognitive deficits (11-14m); neuronal loss (16-18m)
Aß-models	BRI-$Aß_{42}$	C-terminus of the BRI protein	Compact plaques (3m), diffuse plaques (12m)
PSEN1/2 models	Tg-PSEN1 M146L or M146V	PSEN1-M146L or M146V	Increased $Aß_{42}$ levels; No plaques
	Tg-pNSE-hPS2	PSEN2 -N141I	Increased $Aß_{42}$ levels; No plaques
APP and PSEN transgenic models	Tg-APPswe/PS1dE9	APP695-K670N/M671L, PSEN1-M146L	Increased $Aß_{42}$ levels; Extensive plaque deposition (6-8m); behavioural deficits (6-8m); No NFT or neuronal loss
	5XFAD	APP695-K670N/M671L, I716V, V717I, PSEN1-M146L, L286V	Plaque deposition (2m); cognitive deficits (4-6m)
Tau models	JNPL3	FTDP-17 - P301L	NFT (6.5m)
	Tau V337M	FTDP-17 - V337M	NFT (11m); hippocampal neuronal loss (11m)
Triple transgenic models	3xTg-AD	APP695-K670N/M671L, PSEN1-M146V, Tau- P301L	Plaque deposition (6m); NFT (12m); synaptic dysfunction; memory deficits (4.5m)

*m-months, AD – Alzheimer's disease, APP – Amyloid precursor protein, PSEN – presenlin, Aß – amyloid-ß peptide, NFT – Neurofibrillary tangles, CTF – carboxy-terminal fragment.

Some examples of rat models are the triple transgenic (Tg478/Tg1116/Tg11587) model,[186] the double transgenic (TgF344-AD) expressing mutant human APP and PS1,[185] and Tg2576 (similar to the mouse Tg2576).[187] These models manifest age-dependent amyloid plaques deposition, NFT, apoptosis, neuronal loss and present cognitive impairments.[185–187] Interestingly, the TgF344-AD rat model displays tau pathology in the absence of mutant human tau, which allows a more physiological investigation into Aß-mediated tauopathy. This is probably due to the higher resemblance of the tau protein between human and rat, and to the higher levels of Aß1-40/42 and soluble oligomeric Aß species of this specific model.[185]

It is important to take into account the predictive value of translating the obtained data on drug effects from the models to the patients, since many compounds have been shown to decrease Aß deposition in preclinical models, but failed to have an effect on cognitive measures in clinical trials. This might be related to several factors like over-expression of Aß in the preclinical

models, faster development of plaques in transgenic mice , poor translation of cognitive tests performed in mice to the clinic, inter-species differences in pharmacokinetics et cetera.[169,190]

In addition, it is also crucial to remember that these are incomplete models of the disease. Although most of the models display some features of AD neuropathology, they do not develop extensive progressive neuronal loss in the hippocampus or in other specific areas, suggesting that the memory deficits may result from other neuronal alterations.[169] The described limitations are important to take into account when interpreting the results from studies in transgenic animals.

7.2 INTERVENTIONAL ANIMAL MODELS

Interventional models are generated through the introduction of pharmacological or chemical substances into the brain (e.g. Aß peptide introduction, scopolamine-induced amnesia, endotoxins-induced inflammation) or by the induction of lesions in specific brain regions like cholinergic (e.g. nucleus basalis magnocellularis in rodents) or cognition-related regions (e.g. hippocampus). Some of the animals commonly used are the rats or rhesus monkeys. These models show some of the clinical features, but they do not directly replicate AD's pathology and therefore the progression of disease and other aspects are difficult to study. [177,191]

The interventional models can be induced to: mimic amyloid pathology by direct intracerebral injection of Aß; mimic tau pathology by inducing the hyperphosphorylation of tau through activation of caspases or inhibition of phosphatases (e.g. Okadaic acid); or mimicking other characteristics of AD like oxidative stress, mitochondrial dysfunction, microglia activation, neuroinflammation, and cell cycle aberration.[178,191] A disadvantage of the lesion models is the non-specificity of the lesion and the wide range of variability between animals, which would be influenced by the site of injection, the model protocol, concentration and volumes of substances among other parameters. [178]

As a disease model, interventional models are generally used for the identification of symptomatic or corrective treatments, rather than disease-modifying treatments.[177,178]

7.3 NATURAL ANIMAL MODELS OF AD

Some animals, like dogs, some rodent species, and non-human primates, can naturally develop AD-like neuropathological features.[177] This type of model can be very useful to monitor brain and CSF levels of Aß after acute treatment, and may provide more physiologically relevant models for LOAD than transgenic or interventional models.[176]

Non-human primates, such as aged Rhesus monkeys (over 19 years old), develop amyloid-plaque lesions in areas associated with cognitive function; however, monkeys do not develop an Alzheimer's-like syndrome or even a rapid cognitive decline. Although this model could be useful to identify diagnostic markers and to develop effective and safe therapeutics for AD as it is evolutionary most close to humans, disadvantages are the old age when pathology develops, low reproductive output and expensive maintenance as well as ethical considerations.[177,191]

Among the non-human primates, the mouse lemurs have a similar ageing process to humans, developing Aß plaques, NFTs, neurodegeneration and/or loss of cholinergic neurons.[192] Like humans, there is also a decline in declarative memory and executive function, while procedural memory is maintained in both cases.[193] However, Aß deposits and plaques display a different distribution: in humans plaques are abundantly found in the hippocampus, while in the mouse lemur the hippocampus appears to have a significant resistance to plaque development.[194,195]

Dogs are among the species that can also spontaneously develop Aß plaques with age. There is a very high homology between human and canine APP and the Aß peptide has a fully conserved sequence between human and dog.[196] Additionally, it also been shown that there is a very high degree of resemblance between the Aß CSF profile in dogs and humans.[197]

Among the breeds, beagles are the most used, and a beagle with 10 years of age corresponds to a 66-96 years old human. These models exhibit diffuse amyloid deposits, and the extent of the plaques correlates with the decline of some cognitive functions. However, dogs do not develop NFTs, possibly due to the interspecies differences in tau protein sequence. Dog models can be used to evaluate therapeutics aimed to reduce Aß production, deposition and subsequent cognitive improvement, like was shown for active immunization with $Aß_{1-42}$ and antioxidants.[191,198]

The Octodon degu, a South American rodent, also develops spontaneous AD-related neuropathology with age. This model strongly mimics human AD characteristics like development of both intracellular and extracellular amyloid deposits, intracellular NFTs, extensive astrogliosis, cholinergic neuronal degeneration and cognitive impairment.[177,191] This high similarity is probably due to the high interspecies homology (97,5%) of the $Aß_{42}$ peptides.[199]

Although natural models have the advantage of mimicking AD-like characteristics without any external induction, their usage is limited by availability, economical and ethical reasons, and often older age at which the pathology develops, making them very difficult to use in a laboratory environment.[191]

8 CURRENT THERAPIES AND DISEASE-MODIFYING APPROACHES UNDER INVESTIGATION

So far, there are only five FDA-approved drugs for AD: four acetylcholinesterase inhibitors (donezepil, rivastigmine, tacrine and galantamine) and one NMDA receptor antagonist (memantine). All these drugs provide symptomatic treatment, having no effect on the eventual progression of the disease.[85,200] Disease-modifying treatments are currently not available but are a topic of intense research.

Since so many activities and processes are found disrupted in AD, it is difficult to obtain a drug to target them all. According to the amyloid cascade hypothesis, the most relevant target for AD would be the Aß peptide, however many drug trials targeting this peptide have failed to produce significant clinical benefit for AD patients, and although this raises some questions about the validity of the amyloid theory, it may be simply possible that the theory has not been adequately tested in those clinical trials.[200]

Some of the possible explanations to why drug trials have failed are the non-optimal drugs or the incomplete understanding of the drug's pharmacokinetics and bioavailability.[87,200] Additionally, the lack of translation from animal results to human patients can also be partly attributed to the inappropriate timing, since many trials included individuals that are too advanced in their disease progression and therefore unlikely to benefit from the drug.[88] The population heterogeneity can also contribute to different responsiveness to the drug by different individuals and this in turn can contribute to an "ineffective" conclusion on the compound effects.[200]

The main disease-modifying approaches that are being investigated are amyloid-based therapeutics, tau-based therapeutics, modulation of neurotransmission, anti-inflammatory therapeutics and others like reduction of oxidative stress and multi-targeted ligands, which can be found described in further detail on several reviews, for example, on the work by Hampel, *et al*. (2015)[201], and Anand *et al.*(2014).[200]

Focusing on the amyloid-targeted disease-modifying approaches, which are the topic for the current project, there are several mechanisms of action under investigation: preventing amyloid aggregation, promote its clearance or reduce Aß levels by using Aß-based immunotherapy, and modulate the secretase enzymes responsible for Aß generation (e.g. BACE1 inhibitors, γ-secretase inhibitors or modulators). [202,203]

8.1 TARGETING AMYLOID AGGREGATION

Aggregation inhibitors are an attractive approach for AD treatment, since theoretically they would prevent Aß-Aß interactions and the assembly of Aß oligomeric species and the further deposition into plaques. Potential issues are the need for high concentrations in brain because unlike enzyme inhibitors the ratio has to be 1:1 to prevent the physical interaction of Aß peptides. Also, side effects can be expected based on the fact that other protein interactions could also be affected.[204]

Tramiprosate is a nonpeptidic compound, reported to bind to monomeric Aß and prevent oligomerization and aggregation that progressed into Phase III trials but failed to demonstrate efficacy. Secondary data analysis suggested probable benefits of Tramisoprate administration, like domain specific cognitive improvement and reduction in hippocampal atrophy in drug-treated subjects, but it also showed that Tramisoprate lead to unexpected tau aggregation. ELND005 is another compound reported to prevent Aß oligomerization, and is currently in Phase II trials.[200,202] Metal chelators or metal complexing agents have also been investigated, as metals like Zn and Cu can promote oligomerization into fibrils. Clioquinol (PBT2) induces metal ions redistribuition to neurons promoting MMP expression and inducing Aß degradation.[205]

8.2 SECRETASE INHIBITION AND MODULATION

8.2.1 γ-secretase inhibitors or modulators

In an attempt to reduce Aß generation, γ-secretase inhibitors (GSIs) and modulators (GSMs) have been developed. GSIs completely block γ-secretase activity. Semagacestat is an example of a γ-secretase inhibitor that reached clinical settings, but had to be discontinued due to significant adverse effects, such as increased risk for skin cancer and infections, which were allied to a lack of significant positive results on cognition. These results could be related to the fact that γ-secretase has a role in processing over 40 different substrates, including Notch. Additionally, a complete γ-secretase inhibition leads to the accumulation of ß-CTF resultant from the continued BACE1-processing of APP, which has been proposed to have a toxic effect by itself.[206] Moreover, ß-CTF accumulation is thought to lead to a Aß rebound effect after the GSI concentration decreases.[207] To overcome this side-effects, Notch sparing GSIs were developed. Avegacestat is one example of a Notch-sparing GSI that reached clinical trials, but trials had to be halted due to side-effects such as increased rate of nonmelanoma skin cancers. Additionally the clinical trial in mild to moderate AD subjects showed cognitive worsening when compared with

placebo, while a clinical trial in prodromal AD showed a similar cognitive worsening to placebo.[208]

GSM alter γ-secretase activity towards the production of Aß shorter species instead of longer more amyloidogenic ones, such as Aß42.[209] This modulation allows that APP and other substrates continue to be processed, so it does not affect Notch signaling nor it leads to ß-CTF accumulation. Non-steroidal anti-inflammatory drugs (NSAID) were the first compounds to be investigated as GSM. The first generation of NSAID (e.g. flurbiprofen) had a problem associated with inhibition of cyclo-oxygenase 1 (COX1) activity, leading to gastrointestinal and renal toxicity. A second generation of NSAID, which modulate γ-secretase without COX1 inhibition was then investigated. An example is Flurizan™, which reached phase 3 clinical trial but was discontinued due to a lack of effect that was attributed to its low pharmacodynamics.[210] Despite the progress of GSM research still several questions need to clarified, such as their precise binding site and mechanism of action, or possible safety issues from chronic treatment.[211]

8.2.2 BACE1 inhibitors

BACE1 is the enzyme responsible for the first and rate-limiting APP cleavage of the amyloidogenic pathway, which will later give rise to the Aß peptide. This role in APP processing made BACE1 one of the main targets of AD therapeutics.[138] The discovery of a rare APP A673T protective mutation, which reduces BACE1 processing and has a protective effect against AD, accentuated the potential of decreasing BACE1-mediated cleavage of APP as a therapeutic approach for AD.[66]

BACE inhibition may have advantages when compared with γ-secretase inhibition/modulation. First it reduces Aß levels without resulting in ß-CTF accumulation which is believed to have toxic effects, and second it does not interfere with Notch signalling or other γ-secretase-processed substrates. On the other hand, BACE inhibition may interfere with the processing of other BACE substrates.[206]

Initial inhibitors of BACE1 were peptidomimetic molecules, and although they presented good effects *in vitro* this did not translate *in vivo* due to lack of oral bioavailability, long serum half-life, and poor BBB penetration. These results indicated the need to find a non-peptidic BACE1 inhibitor that is large enough to make sufficient contacts with the active site and to have high affinity, but also small enough to cross the BBB and have the desired pharmacokinetic profile.[138]

Some BACE inhibitors are now being tested in clinical trials. [212,213] The most advanced are MK-8931 (Merck & Co.) which is currently in a phase 2/3 clinical trial and E-2609 (Eisai) which is in

phase 1 and going for phase 2. On the results for MK-8931, presented in 2012 from the phase 1 trials, a single dose of 100 mg MK-8931 administered to healthy individuals, showed a reduction in CSF $Aß_{40}$ by 75%, with similar results for CSF $Aß_{42}$ and sAPPß. Moreover, after a single dose of 550 mg this reduction reached 92%. The E-2609 clinical trial in healthy individuals showed at the highest dose (400mg) of a multiple oral ascending dose study, a reduction in CSF Aß up to 85%.[138] For both compounds there was acceptable tolerability, with only headaches and dizziness as the most common adverse effects.[214]

LY-2886721 (Eli Lilly) also progressed into clinical trials, and showed translatable results in mice, dogs and humans in the phase I clinical trial in healthy human subjects, reducing CSF $Aß_{40}$, $Aß_{42}$ and sAPPß up to 74%. However, the development of this compound had to be terminated due to the observation of abnormal liver biochemistry values that were considered to be an off-target effect of the compound unrelated to BACE inhibition. [215]

JNJ-54861911 (Janssen Pharmaceutica) is another BACE inhibitor that is currently in a phase 2 clinical trial. So far, in a phase 1 trial with healthy elderly individuals, the inhibitor was reported to be safe and well tolerated, having entered the blood and CSF with favourable pharmacokinetics and pharmacodynamics, and dose-dependently reducing Aß species. Simultaneously to reduction of sAPPß, the levels of sAPPα were increased. A 5 mg dose was reported to reduce CSF Aβ concentration by half; 25 mg by 80 percent, 50 mg by 90 percent.[216]

Other compounds are now being tested in Phase I trials and in preclinical studies by various companies. The selected compounds are highly selective for BACE1 over other aspartyl proteases like cathepsin D, which is very important since loss of cathepsin D can result in lysosome dysfunction. However, most of the currently available BACE1 inhibitors are equipotent inhibitors of the human BACE2 enzyme.[65,138]

The equal inhibition of BACE1 and BACE2 has the potential to lead to specific side effects. BACE2 is involved in the processing of PMEL, which is essential for the formation of the amyloid matrix that supports the melanosomes. Additionally BACE2 is also associated with Tmem27 shedding. Inhibiting the cleavage of Tmem27 allows it to be active in ß cells, leading to an increase in pancreatic cell mass and function, which might indicate a potential risk for BACE inhibitors.[65] Therefore, effect of novel BACE inhibitors on these processes are closely monitored during drug development.

An alternative to small-molecule BACE1 inhibitors are the bi-functional inhibitory antibodies that bind both the transferrin receptor (Tfr) to increase BBB penetration and the BACE1 enzymatic

domain to inhibit BACE1 activity. These antibodies can selectively and potently inhibit BACE1-mediated APP processing in cells, and in transgenic APP mice it was shown that an anti-BACE1/TfR antibody was able to reduce peripheral Aß by approximately 50%, and also reduce Aß in the brain by 15-22%.[217] The capability of binding to the transferrin-receptor increases the BBB penetrance by approximately 5-fold.[218] Aside from its high penetrance, one of the main advantages of this antibody is its high selectivity for BACE1 over other aspartyl proteases including BACE2.[65] Although on initial studies on mice, the animals developed acute clinical reactions, such as profound lethargy and lack of responsiveness, and a reduction of reticulocytes, recent studies in nonhuman primates showed no side-effects, encouraging the further development of this approach .[219,220]

Besides the selectivity for BACE1 over BACE2, there is also the need to take into consideration the fact that BACE1 has two different cleavage sites in APP – the ß-site and the ß'-site – which are assumed to be both affected by BACE1 inhibitors. Kinetic data indicate that BACE1 has a higher enzymatic efficiency for peptides containing the ß-site, suggesting that a BACE1 inhibitor might have different effects on the two different sites depending on the concentrations used. Therefore studies are warranted to evaluate BACE1 inhibitor effects on the Aß $_{11\text{-}40\,/\,42}$ as well as the effects on the Aß $_{1\text{-}40\,/\,42}$ peptide levels.[68]

Considering the BACE1$^{-/-}$ phenotype, possible side effects of BACE1 inhibition might be muscle spindle maintenance impairment[221] and synaptic dysfunctions specific to the CA3 pyramidal neurons (localized in the hippocampus).[222] Additional side effects of BACE1 inhibition may include hypomyelination, increased astrogenesis and decreased neurogenesis, axonal guidance defects, memory deficits, retinal pathology, and seizures, among others. However, an important question is if these phenotypes arise from the BACE1 deficiency during development or in the adult. Several studies of BACE inhibitors in adult animals have revealed already that BACE1 blockage can impair synaptic plasticity by reducing the number of dentritic spines,[223] can affect muscle spindles and consequently motor coordination,[221] and can even result in retinal pathology.[224]

Clearly, there is a need for further comprehension of the adult BACE1 functions, and also further evaluation if any more of the observed phenotypes found in BACE1 null animal models are predictive of possible side-effects of BACE1 inhibitors in humans.[138]

Reduction of CSF Aß and sAPPß levels indicates target engagement of BACE inhibitors. Additionally sAPPα can have increased levels, due to a shift in APP processing to the non-

amyloidogenic pathway. [225] It was also shown that upon BACE1 inhibition, there was a reduction in CSF $Aß_{1-34}$ levels and an increase in $Aß_{5-40}$ levels, this pattern was present in APP transfected cellular models, dog-treated CSF, and in human clinical trials. These data suggest that the $Aß_{5-40}/Aß_{1-34}$ ratio may provide complementary information on the changes in the Aß and APP metabolism.[226,227]

8.3 PROMOTING AMYLOID CLEARANCE

Several enzymes have been identified as mediators of Aß degradation, such as NEP, IDE and plasmin. However, achieving drug-mediated enzyme activation can be a difficult task, and the fact that this is a non-specific approach increases the risks for side effects, and therefore requires further evaluation. [200,202]

Modulation of Aß transport can be another mechanism to stimulate Aß clearance, by promoting Aß movement from the CNS to the periphery. The RAGE receptor binds Aß with high affinity and facilitates its influx into the CNS. Antagonizing RAGE activity could therefore promote Aß presence in the periphery. [200,202] With that aim, soluble RAGE receptor analogues were created to serve as a decoy receptor, such as FPS-ZM1 that so far showed reduced amyloid deposition, improvement in cognitive and cerebrovascular parameters and significant BBB clearance in a mouse model.[228]

8.3.1 Anti-Aß immunotherapy

Immunotherapy allows the generation of antibodies that can target a wide variety of mechanisms and molecules for therapeutic purposes. In AD, the mechanism of action of a particular antibody will be influenced by its target binding. If it binds to soluble Aß, it may increase clearance and shift the equilibrium between Aß uptake and removal from the brain, whereas if it binds to insoluble forms it may need microglia activation to promote the clearance. Antibodies may also regulate Aß aggregation, disrupt Aß interaction with other molecules, bind to immune effectors regulating neuroinflammation, and even be internalized in cells or enter the synaptic cleft interfering with cell-to-cell transmission of Aß and its aggregates.[85]

So far, there are no known active transport mechanisms for antibodies of immunoglobulin (Ig)G isotype into the CNS. Consequently, only a small fraction (roughly 0.1%) of the antibodies introduced into the peripheral circulation eventually reach the brain or the CSF by passive diffusion.[85]

Both active immunization and passive immunization approaches are pursued for treatment of AD. In both cases, the effects can be blocked by anti-idiotype antibodies (neutralizing antibodies).[85] Active immunization involves the activation of the patient's immune system through the administration of a vaccine containing antigens or other stimuli, leading to the production of target-specific antibodies.[85,225] Passive immunization involves the delivery of monoclonal target-specific antibodies, which are not its own, to the patient. These antibodies can be human or humanized murine monoclonal antibodies produced in the laboratory.[85,225]

The first clinical trial on Aß immunotherapy was using AN1792, an active vaccine containing full-length aggregated $Aß_{1-42}$ with the QS-21 adjuvant. However, the trial had to be discontinued due to the development of meningoencephalites by approximately 6% of the patients, which was due to a strong T-helper (Th) cell-mediated immune system activation. This finding led to the attempt of developing vaccines that would trigger a humoral response, or that involved Th2 rather than Th1. For that reason, an alternative active immunotherapy approach was developed, through the coupling of synthetic fragments of Aß with carrier proteins.[229]

ACC-001 a vaccine composed of an Aß1-6 fragment attached to a QS-21 carrier protein; was discontinued after a phase 2 clinical trial with mild to moderate AD, where a serious adverse effect of vasculitis in the skin was encountered. [85,230]

There are at least two vaccines that have reached phase II clinical trials: Cad106, which consists of an Aß1-6 fragment coupled to the virus-like particle QB and has been shown to block plaque formation in the brain of animal models;[231] and AFFITOPE AD02, consisting of the amino-terminal B-cell epitope of Aß avoiding this way Th-mediated response. CAD-106 showed no unexpected safety findings in two phase 2a trials, indicating that antibody maturation and safety even after seven injections and follow-up of two and a half years. [232] AFFITOPE AD02 showed favorable safety and tolerability in a phase 1 clinical trial with mild to moderate AD subjects, although primary data from the phase 2 trial with early diagnosed AD subjects indicated that the antibody failed to reach primary and secondary outcome measures.[233]

Passive immunization is nowadays the main approach used in immunotherapy for AD, and so far several antibodies have advanced into clinical trials.

Bapineuzumab, which targets both fibrillar and soluble forms of Aß, showed in clinical trials a small but significant reduction in CSF levels of P-tau but no alterations in CSF $Aß_{1-40}$ or $Aß_{1-42}$. The lack of significant benefit in cognitive or functional performance and the development of amyloid-related imaging abnormalities, specifically with parenchymal oedema (ARIA-E), led to

its termination.[85,225] In phase I trials, Gantenerumab, an antibody mainly targeting aggregated Aß, was shown to decrease amyloid plaques in AD subjects by 11% when compared placebo-treated AD subjects. Some patients on higher doses also developed ARIA-E.[85,234] Currently a Phase III trial in patients with mild AD is ongoing. Some hypothesize that immunotherapies cause blood vessels to become leaky due to the movement of Aβ from brain plaques across blood vessel walls, which might explain why ARIAs occur in areas of highest plaque removal.[235]

Intravenous immunoglobulin (IVIG) is a purified immunoglobulin preparation obtained from the blood plasma of thousands of healthy donors. IVIG contains most of IgG antibodies present in humans, and 0.5% of that antibodies are against conformational epitopes for Aß oligomers, fibrils and also monomeric Aß.[236,237] This therapy is based on the hypothesis that AD patients present lower blood levels of anti-Aß antibodies when compared with the healthy individuals.[238] So far at least two preparations were under development for AD therapy, Octagam (Octapharma) and Gammagard (Baxter), although Gammagard was discontinued in 2013 due to no significant positive clinical effect.[225,239]

With the objective of targeting a specific Aß species, like the protofibrils, conformation-dependent antibodies are being developed as well. The humanized BAN2401 is one of the anti-Aß protofibril antibodies, which is currently under phase IIb trials. [85]

Another antibody under development is Creneuzumab, which is a fully humanized IgG4 monoclonal anti-Aß antibody that binds monomeric and oligomeric Aß, inhibiting its aggregation and promoting disaggregation. Due to its IgG4 subclass, it does not promote Fc-mediated phagocytosis, possibly resulting in lower inflammation.[85]

Furthermore, targeting soluble Aß, Ponezumab and Solaneuzumab (Lilly) have been developed. The first has been discontinued due to a failure to reach primary endpoints in Aß reduction, [225] the second showed in preclinical studies that it is able to reduce plaque burden and increase (1000 fold) plasma Aß levels in transgenic mice.[225] A phase II trial in mild-to-moderate AD showed an increase in total (free and antibody-bound) $Aß_{42}$ and $Aß_{40}$ plasma levels. CSF level of free $Aß_{42}$ was also increased, while free $Aß_{40}$ remained unchanged, when compared with placebo.[240] Solaneuzumab was not effective in reaching cognitive and functional primary endpoints in the overall patient population with mild-to-moderate AD. Subgroup analyses of pooled data across both studies showed a statistically significant slowing of cognitive decline in patients with mild Alzheimer's disease, but not in patients with moderate AD. Studies in mild AD are currently ongoing.[85,190]

Very recently, Aducanumab (Biogen), a high affinity anti-Aß antibody specifically targeting fibrillar forms of Aß, showed encouraging pre-results on a phase 1b trial enrolling 166 individuals with prodromal or mild AD. Aducanumab was shown to dose-dependently reduce Aß deposition in 6 cortical regions of the brain, and after 1 year the highest dose (10mg/kg) reduced cortical amyloid close to the cutpoint of positivity. Additionally Aducanumab also appears to dose-dependently reduce cognitive decline in both MMSE and CDR-SB cognitive tests. ARIA-E was observed as a side effect and correlated with increasing dose and ApoE4 genotype. The positive results on cognition and plaque load have pushed the antibody into a Phase 3 trial.[241 ,

Of notice, several antibodies, such Solaneuzumab, Crenezumab and Gantenerumab have been enrolled in prevention trials by the Collaboration for Alzheimer's Prevention (CAP) group, formed by the Dominantly Inherited Alzheimer Network (DIAN), Alzheimer's Prevention Initiative (API), and Anti-Amyloid Treatment in Asymptomatic Alzheimer's Disease (A4) trial platforms, which intends to show clinical benefit in individuals with no symptoms.[242]

Although much is being done towards the finding of a disease-modifying AD therapeutic, there are still many questions to be answered, such as what is the most appropriate time for a therapeutic intervention, what degree of Aß reduction is needed so a clinical effect is obtained, and which are the most appropriate targets (monomers, oligomers, fibrils) for the anti-amyloid therapy. These questions are actively pursued to reach the goal of developing an effective therapeutic for AD.

9 BIOMARKERS IN PRECLINICAL STUDIES AND CLINICAL TRIALS

Biomarkers are of crucial importance in AD clinical trials, where they can improve the accuracy of the diagnosis in trial participants, allow AD patient stratification, monitor the safety profile of the drug candidate, evaluate the drug pharmacodynamic behaviour, and also participate in monitoring of drug effects.[225]

So far, the majority of amyloid-targeted disease-modifying approaches have been tested in populations with more advanced stages of the disease. However, these therapies are very likely to have better results on the earlier rather than on the later disease stages, where there is already advanced plaque deposits and neurodegeneration. Therefore, testing of drug candidates in early disease stages can be very important. Since these earlier stages are difficult to diagnose and prognose based on clinical symptoms, the use of biomarkers has become a crucial tool in identifying patients which are eligible for participation in trials of early AD.[225]

Biomarkers to identify patients that will progress from MCI to AD are elevated CSF T-tau and P-tau, and low CSF $Aß_{1-42}$. The combination of these markers has a high sensitivity to identify prodromal AD cases, with a specificity of 90% when compared with controls, and 80% when compared with stable MCI. Additionally imaging biomarkers, such as sMRI and amyloid PET can also be used. Plasma biomarkers are still very controversial regarding its use as preclinical diagnosis biomarker. [225]

Biomarkers can also be of use in AD patient stratification. For example, individuals with high binding of amyloid tracers on PET or higher reduction of CSF $Aß_{42}$ might be more responsive to anti-Aß drugs, while individuals with elevated P-tau, might be more responsive to drugs that reduce tau phosphorylation. [43]

Another application of biomarkers is safety monitoring of drug candidates, which is particularly important in de-risking the therapies. This type of approach can be used for example to exclude that an immunotherapy drug candidate has adverse immune effects.[225] Identification and monitoring of inflammatory processes in the CNS can be done through CSF cell count, IgG or IgM Index, and IgG or IgM oligoclonal bands. Disturbances in the BBB on the other hand, which can lead to cerebral oedema, can be detected by the CSF-serum albumin ratio. [43] CSF samples taken at baseline (prior to drug administration) can be compared with CSF samples taken during the study period. Another example is detection of amyloid-related imaging abnormalities (ARIA) by the use of MRI.[243]

Finally, another key application of biomarkers is monitoring the effects of drug candidates on the pathology. Within this field, biomarkers can be subdivided into primary and downstream biomarkers. Primary biomarkers are used to identify and monitor the pharmacodynamic effect of the drug, allowing assessing target engagement. For anti-Aß therapies amyloid PET and CSF and plasma levels of $Aß_{42,}$ $Aß_{40}$, sAPPß, and sAPPα, as well as other Aß isoforms are utilized. Downstream biomarkers can be used to evaluate subsequent effects, like for example neuronal loss. For that purpose, CSF T-tau levels or the levels of other neuronal proteins like heart-type fatty acid-binding protein (H-FABP) can be used. [43,225] , Additional downstream markers for anti-amyloid therapy may include brain atrophy (sMRI), brain metabolism (FDG-PET) and tau phosphorylation state (CSF p-tau).[225]

9.1 CSF Aß BIOMARKERS IN PRECLINICAL AND CLINICAL TRIALS

CSF biomarkers have been and are widely used in clinical trials, as is summarized in *Table 2*. Regarding the study of BACE1 inhibitors, CSF Aß and sAPP biomarkers can be used to monitor

target engagement. For these studies, both core and truncated Aß peptide biomarkers have been used. A correct engagement of the inhibitor will translate into a reduction in Aß and sAPPß levels. Interestingly, an increase in Aß5-x species upon BACE inhibition was recently shown.[227] In studies involving γ-secretase inhibitors and modulators, CSF biomarkers have also been used to show target engagement. In the case of γ-secretase inhibition, a decrease in Aß1-38, Aß1-40, and $Aß_{1-42}$, together with an increase in Aß1-15 and/or Aß1-16 represent a characteristic CSF profile. [46,244]

In immunotherapy trials, data on CSF Aß biomarkers for demonstration of target engagement can be trickier to interpret. Data from active immunization (AN1792 and CAD-106), showed a reduction in CSF tau levels, while $Aß_{1-42}$ levels remained unaltered although there was a reduction in Aß deposition. These data suggest that CSF $Aß_{1-42}$ levels do not always reflect changes in fibrillary Aß. Aß-biomarkers have also been used in immunotherapy trials to measure disease modifying effects of drug-administration and in some cases as patient-inclusion criteria (low CSF $Aß_{1-42}$ levels).[244] It remains to be demonstrated whether CSF biomarker changes can predict a clinical benefit in the patient.

9.1.1 N-truncated Aß species as possible biomarkers of target engagement

Besides the classically investigated Aß1-40 and Aß1-42 species, several other Aß species have been identified in human CSF, and are being investigated as possible biomarkers of target engagement. N- and C-terminally truncated species such Aß1-14, Aß1-15, Aß1-16, Aß1-37, Aß1-38, Aß1-39, Aß5-40, Aß11-40, Aß11-42 and Aß11-30, are among those.[46,244]Ileo

Studies comparing full length Aß to N-terminally truncated Aß have suggested that these two pools can behave differently upon Aß-targeted modifying therapies. For example, BACE1 inhibitors have been shown to have a higher effect on $Aß_{1-40}$ than on $Aß_{X-40}$ concentrations in neuroblastoma and primary neuronal cultures.[245,246]

Research on specific N-truncated species, revealed differential effects upon BACE1 inhibition, where Aß1-x were decreased, but Aß2-x and Aß5-x were increased in neuroblastoma cell cultures.[247] Moreover after BACE1 inhibition Aß1-34 levels decreased, together with an increase in Aß5-34 levels in preclinical models (APP-transfected cells and dog CSF) and in CSF of healthy individuals.[227,248]

Table 2 - Clinical trials of anti-Aß disease-modifying therapies (From Lleó, A. et al. (2014)[244])

Drug	Population	Trial phase	CSF biomarker use	Effects of therapy on biomarkers	References*
APP synthesis inhibitors					
(+)-Phenserine	MCI	I	Target engagement	↓sAPPα, ↓sAPPß, ↓t-tau	Maccecchini *et al.*[249]
ß-Secretase inhibitors					
MK-8931	Healthy volunteers, patients with prodromal AD, and patients with mild to moderate AD	III	Target engagement	↓$Aß_{1–40}$, ↓$Aß_{1–42}$, ↓sAPPß	NCT01496170 NCT01739348 NCT01953601
E2609	Healthy volunteers and patients with MCI due to AD	I	Target engagement	↓Aß, ↓sAPPß	NCT01511783 NCT01600859 Lai *et al.*[250]
LY2811376 LY2886721	Healthy volunteers	I	Target engagement	↓Aß, ↑$Aß_{5-40}$, ↓$Aß_{1–34}$, ↓sAPPß	May *et al.*[251] Portelius *et al.*[252]
PF-05297909	Healthy volunteers	I	Target engagement	↓Aß, ↓sAPPß	NCT01462851 Bell *et al.*[253]
γ-Secretase inhibitors and modulators					
LY450139 (semagacestat)	Patients with mild to moderate AD	III	Target engagement	↓$Aß_{1–38}$, ↓$Aß_{1–40}$, ↓$Aß_{1–42}$, ↑$Aß_{1–15/16}$	Doody *et al.*[254] Fleisher *et al.*[255] Siemers *et al.*[256] Portelius *et al.*[257] Bateman *et al.*[258]
BMS-708163 (avagacestat)	Patients with mild to moderate AD or prodromal AD	II	Target engagement, sample enrichment	↓$Aß_{1–38}$, ↓$Aß_{1–40}$, ↓$Aß_{1–42}$, ↑$Aß_{1–14/15/16}$	NCT00890890 Tong *et al.*[259] Coric *et al.*[260]
PF-3084014	Healthy volunteers	I	Target engagement	↓Aß	Mangialasche *et al.*[261]
ELND006	Healthy volunteers	I	Target engagement	↓Aß	Hopkins *et al.*[262]
Tarenflurbil	Healthy volunteers	I	Target engagement	= $Aß_{1–42}$	Galasko *et al.*[263]
CHF5074	Healthy volunteers	II	Target engagement	= $Aß_{1–40}$, = $Aß_{1–42}$, ↓CD40	NCT01203384 NCT01303744 Imbimbo *et al.*[264] Ross *et al.*[265]
Aß aggregation inhibitors					
Tramiprosate (3APS)	Patients with mild AD	II	Target engagement	↓$Aß_{1–42}$, = $Aß_{1–40}$	Aisen *et al.*[266]
PBT1 (clioquinol)	Patients with mild to moderate AD	I	Target engagement	↑t-tau, GAP43	Reglan *et al.*[267]
PBT2	Patients with mild AD	II	Target engagement	↓$Aß_{1–42}$	Lannfelt *et al.*[268]
ELND005 (scyllo-inositol)	Patients with mild to moderate AD	II	Target engagement	↓$Aß_{1–42}$	Salloway *et al.*[269]
PQ912	Healthy volunteers	I	Target engagement	↓Glutaminyl cyclase activity	Black *et al.*[270]
Aß immunotherapy					
AN1792 + QS21	Patients with mild to moderate AD	II	Target engagement, disease modification	= $Aß_{1–42}$, ↓t-tau	Gilman *et al.*[229]

ACC-001	Patients with mild to moderate or early AD	II	Target engagement, disease modification	NA	NCT00479557 NCT01227564 NCT01284387
CAD-106	Patients with mild to moderate AD	II	Target engagement, disease modification	= $Aß_{1–42}$, = t-tau, ↓p-tau (antibody responders)	Winblad *et al.*[271] NCT01097096
Bapineuzumab	Patients with mild to moderate AD	III	Target engagement, disease modification	= $Aß_{1–42}$, = $Aß_{1–40}$, ↓p-tau	Blennow *et al.*[272] Salloway *et al.*[273]
Solanezumab	Patients with mild to moderate AD, or autosomal dominant AD	III	Target engagement, disease modification	↑Total Aß1–$_{42}$, ↑total $Aß_{1–40}$, = t-tau, = p-tau	Doody *et al.*[274] Farlow *et al.*[240] Siemers *et al.*[275]
Gantenerumab (RO4909832)	Patients with mild to moderate AD, prodromal AD or autosomal dominant AD	III	Target engagement, disease modification, sample enrichment	NA	NCT00531804 NCT01656525 NCT01224106 NCT01760005 NCT02051608
Ponezumab (PF-04360365)	Patients with mild to moderate AD	II	Target engagement, disease modification	↑$Aß_{1–x}$	Landen et al.[276] NCT00945672 NCT00722046
MABT5102A (crenezumab)	Patients with mild to moderate AD, or autosomal dominant AD	II	Target engagement, disease modification	NA	NCT01397578 NCT01723826 NCT01998841
BAN2401	Patients with mild to moderate AD, or early AD	II	Target engagement, disease modification	NA	NCT01767311 NCT01230853
Intravenous immunoglobulin	Patients with mild to moderate AD or MCI	III	Target engagement	↑Anti-Aß antibody levels, = $Aß_{1–42}$	Dodel et al.[277] Relkin et al.[278]

*Some trials are cited with ClinicalTrials.gov identifiers. ↑ - increased, ↓ - reduced, = - unchanged, Aß - amyloid-ß, AD - Alzheimer's disease, APP - amyloid precursor protein, CSF - cerebrospinal fluid, GAP-43 - growth-associated protein 43, MCI - mild cognitive impairment, NA - not available, p-tau - phosphorylated tau, sAPP - soluble APP, t-tau -total tau.

Additionally it has also been shown that between *in vivo* models, such as rodents and dogs, the $Aß_{1-40}/Aß_{x-40}$ ratio may vary, with $Aß_{1-40}$ corresponding to different percentages of the total Aß pool. Moreover, BACE inhibition may result in different effects in full length and n/truncated species, so it becomes of interest the simultaneous study of $Aß_{1-x}$ and $Aß_{x-40/42}$ across different models.[279]

Importantly, it was shown in BACE1 KO mice that there is still an $Aß_{x-40}$ pool present, while Aß1-40 is completely reduced. This suggests that this remaining pool might result from other protease-mediated APP processing. [245,280]

9.2 Methodology and Other variables – The need for standardization

The use of CSF biomarkers in preclinical and clinical trials of AD requires a strict standardization of the reference conditions and methodologies used. A quality control program involving over 90

laboratories worldwide has been running for 5 years with the goal to identify factors that induce variability and ultimately contribute to standardization. Until now, studies regarding CSF biomarkers have always reported high variability between and within clinical centres and laboratories, which have been associated with pre-analytical (e.g. sample collection, handling and storage), analytical (e.g. different assays and protocols), post-analytical (e.g. different data analysis methods) and even assay-related factors (e.g. batch variations) (*Table 3*). [44,244]

Another important factor to consider is dilution linearity of samples in a particular assay. Lack of dilution linearity is usually associated with matrix-effects, due to the presence of proteins or other components in CSF.[281] A possible solution for the non-linearity is the denaturation of the sample in high concentrations of guanidine hydrochloride and reverse-phase HPLC (RP-HPLC). This process would purify the sample for the desired analyte and allow a measurement without matrix interference. Unfortunately, studies comparing CSF $Aß_{42}$ levels in crude and in HPLC-enriched sample revealed that although $Aß_{42}$ levels are higher in the HPLC-enriched samples, diagnostic power is reduced when comparing AD and control individuals. Diagnostic power is recovered when the $Aß_{42}$/Aß40 ratio is determined. [282,283]

Table 3 - Possible sources of variability in CSF biomarker studies (From Blennow, K. et al. (2014) [44])

Source	**Cause**
Pre-analytical	Subject selection and diagnostic criteria
	LP technique (e.g., time of day/diurnal variation, artifacts due to binding of proteins to collection tube)
	Specimen shipment or storage (e.g., freeze/thaw effects, artifacts due to oxidation of proteins or binding of proteins to storage tubes)
Analytical	Assay kit handling and storage
	Laboratory equipment (e.g., calibration of pipettes, maintenance of ELISA reader)
	Analytical variation (e.g., pipetting errors, use of internal QC samples, acceptance criteria for assay)
Post-analytical	Data-handling differences (e.g., type of curve fitting used, software for data calculation)
Assay manufacturing	Method optimization (e.g., antibody cross-reactivity, assay linearity, and LLOQ)
	Within-assay and lot-to-lot variability due to reagents and manufacturing (e.g., variation in antibody plate coating, purity of antibodies, quantification, and stability of assay calibrators)

Abbreviations: CSF, cerebrospinal fluid; LP, lumbar puncture; SOP, standard operating procedure; ELISA, enzyme-linked immunosorbent assay; QC, quality control; LLOQ, lower limit of quantification.

Chapter II. Objectives

The main objective of this project is the preclinical evaluation of disease-modifying treatments that aim at reducing Aß accumulation and deposition in the brain. We will focus on the effects and therapeutic potential of BACE1 inhibitors, γ-secretase inhibitors and γ-secretase modulators. To fulfil this objective, biomarkers related with APP/Aß metabolism are essential, allowing assessment of a drug effect on a specific pathogenic process by comparing baseline biomarker levels with biomarker levels after treatment. The specific goals of the project are:

- Characterization of monoclonal antibodies against $Aß_{11-x}$ and development of specific and sensitive immunoassay methods for accurate quantification of this peptide in cell culture supernatant, dog and human CSF.
- Monitor the effects of novel experimental drugs (BACE1 inhibitors, γ-secretase inhibitors and γ-secretase modulators) on different APP fragments ($Aß_{1-37/38/40/42/x}$, $Aß_{X-37/38/40/42}$, $Aß_{11-x}$) through evaluation of biomarker levels in cell culture supernatant, and in CSF of beagle dogs and human healthy volunteers.
- Evaluation of matrix interference in $Aß_{1-42}$ measurements and diagnostic value, through the comparison of crude and HPLC-enriched human CSF.
- Comparison of the diagnostic value of individual Aß peptides ($Aß_{1-42}$) and peptide ratios in AD and non-AD individuals.

Chapter III. Materials and Methods

1 CELLULAR STUDIES

SK-N-BE(2) human neuroblastoma cells expressing WT APP695 were utilized. SK-N-BE(2) cells were cultured in Falcon 175 flasks in culture medium, containing Dulbecco's modified Eagle medium with L-glutamine (DMEM) supplemented with 10% (v/v) heat-inactivated fetal bovine serum (FBS) and 1% antibiotics (penicillin, streptomycin).

Near confluent flasks (80-90%) of SK-N-BE (2) cells were trypsinized and seeded into 384-well polypropylene plates containing a concentration range of the compounds summarized in *Table 4*. Cells were added to a final concentration of 10000 cells/well, and incubated overnight (18h) at 37°C. Upon cell addition, compounds are present in a final concentration of 0.3% DMSO. Cells treated with 100% DMSO were used to define baseline levels and were seeded on the same plates as compound-treated cells. Upon compound-incubation cell supernatant was collected into 384-well polypropylene plates, placed immediately in dry ice, and stored at -80°C prior to analysis.

Table 4 Compounds tested in the cellular assay using SK-N-BE (2) human neuroblastoma cells expressing wild-type hAPP695

Compound	Dose (M)
GSI A (Semagacestat) / B (Begacestat)	9.01E-06 2.25E-06 5.62E-07 1.41E-07
GSM C / D (JNJ-42601572) / E (E2012)	3.51E-08 8.80E-09 2.20E-09
BACEi 1-24 BACEi 11 (MK8931) / BACEi 15 (LY2811376) / BACEi 22 (LY2886721) / BACEi 24 (AZD3839)	5.50E-10 1.38E-10 3.42E-11

GSI – γ-secretase inhibitor, GSM – γ-secretase modulator, BACEi – ß-secretase inhibitor

2 ANIMAL STUDIES

All animals were housed in an animal facility that is fully compliant with European policy on the use of Laboratory Animals. Experimental protocols were approved by the Institutional Review Committee of Janssen Pharmaceutica (Beerse, Belgium), and meet the European and Belgian guidelines on animal experimentation.

In vivo studies were performed in beagle dogs, and the respective details of each study are described below. CSF was collected into polypropylene tubes (Micronic 1.4 mL non-coded tubes U-bottom with caps from FluidX, Split TPE Capcluster Blue (Falcon®), placed immediately in dry ice, and stored at -80°C prior to analysis. Samples were thawed on ice on the day of analysis and refrozen as soon as possible.

2.1 STUDY 1 – COMPARISON OF CSF COLLECTION SITES

The study was performed in 16 male and female untreated beagle dogs. First, CSF from the animals was sampled when awake from the lateral ventricle. With a period of at least one week in between, CSF was collected a second time and now from the cisterna magna under anesthesia (0.2ml medetomidine IV (Domitor®) and 2ml propofol IV (Propovet®)).

2.2 STUDY 2 – GSM F

The study was performed in 24 beagle dogs (12 females, 12 males), subdivided into the following groups:

- Vehicle group 0mg/kg: 6 dogs (3 females, 3 males), 20% HP-ß-CD;
- Dosing 2.5mg/kg GSM F (low dose(L)): 6 dogs (3 females, 3 males);
- Dosing 5mg/kg GSM F (medium dose(M)): 6 dogs (3 females, 3 males);
- Dosing 20mg/kg GSM F (high dose(H)): 6 dogs (3 females, 3 males).

Dogs were dosed orally (by gavage) daily, in the morning, on an empty stomach for a period of 7 days. CSF was sampled from the cisterna magna under anesthesia (0.2ml medetomidine IV (Domitor®) and 2ml propofol IV (Propovet®)). before dosing (pre-dose), at 8 and 25h post dose on day 1, and at day 7 at 8 and 25h. After dosing, animals got access to their regular meal, except on day 1 and 7, where the meal was given after the 8h sampling time point.

2.3 STUDY 3 – BACEI 25

The study was performed in a group of 16 beagle dogs (8 females and 8 males), subdivided into the following groups:

- Vehicle group 0mg/kg: 4 dogs (2 females, 2 males) (20% HP-ß-CD);
- Dosing 0.63mg/kg (low dose (L)): 4 dogs (2 females, 2 males);
- Dosing 2.5 mg/kg (medium dose (M)): 4 dogs (2 females, 2 males);
- Dosing 10 mg/kg (high dose (H)): 4 dogs (2 females, 2 males).

Dogs were fasted overnight, and in the morning received a single dose orally (by gavage) on an empty stomach. Animals got access to their regular meal 8h after dosing. CSF was sampled from the cisterna magna under anesthesia (0.2ml medetomidine IV (Domitor®) and 2ml propofol IV (Propovet®))., before dosing (pre-dose), and at 8 and 25h after dosing.

3 HUMAN STUDIES

3.1 STUDY 1 – EVALUATION OF MATRIX-EFFECTS ON AD DIAGNOSTIC ASSAY

The study was performed in a group of 40 patients who sought medical advice due to cognitive impairment. They were designated as AD (n=20) and non-AD (n=20) according to CSF biomarker levels obtained using Innotest ELISAs (Fugirebio, Ghent, Belgium). The cutoff values are summarized in *Table 5.*

Table 5 AD and NC diagnostic criteria

Sample	Aß1-42 (ng/L)	T-tau (ng/L)	p-tau(181) (ng/L)
NC	> 600	< 350	≤ 79
AD	< 600	> 350	≥ 80

Aß – amyloid-ß peptide, T-tau – total tau, p-tau – phosphorylated tau, AD – Alzheimer's disease, NC – non-AD

CSF was collected by lumbar puncture through the L3/L4 or L4/L5 interspace. CSF was collected into a polypropylene tube. Immediately, CSF was centrifuged at 2000g at 4°C for 10min. Supernatant was pipetted off, mixed to avoid gradient effects, aliquoted and stored at -80°C.

For each individual 3 different samples were evaluated:

- Crude CSF – containing neat CSF
- HPLC 40 CSF – containing CSF enriched for $Aß_{1-40}$
- HPLC42 CSF – containing CSF enriched for $Aß_{1-42}$.

For Aß enrichment, the biological samples were denaturated using a solution with a high concentration of guanidine hydrochloride (6M GuHCl) and then reverse-phase-HPLC was employed. A detailed description of these procedures can be found in Slemmon J. R. *et al.* (2012)[282]

3.2 STUDY 2 – BACEI 26

A double-blind, placebo-controlled, randomized, multiple-ascending dose study was performed and CSF samples from 17 elderly healthy subjects (55-85 years) were evaluated. Subjects were treated with various doses of BACEi 26 (5 or 6 individuals per cohort):

- Cohort 1: 6 individuals, dosed with 5mg;
- Cohort 2: 5 individuals, dosed with 50mg;
- Cohort 3: 6 individuals, dosed with 90mg.

CSF was sampled by lumbar puncture before dosing (pre-dose), at 2 and 10h of day 14, and at 24h of day 15. [284]

4 MONOCLONAL ANTIBODIES

An overview of the monoclonal antibodies used as capture antibodies, detection antibodies, and antibodies of the Alpha-LISA assay, is presented in *Table 6*.

Table 6 Characteristics of the monoclonal antibodies utilized as capture antibodies, detection antibodies, and used in Alpha-lisa assays. Isotype, antigen specificity, species reactivity, source of the antibody, and assays in which the antibodies were used.

Capture antibodies

Monoclonal Antibody	Isotype	Specificity	Reactivity	Source	Assay
JRD/Aß37/3	IgG2b/κ	C-terminus of Aß peptide, ending at residue 37	Human, Canine, Rodent	Janssen Research & Development	MSD
J&JPRD/Aß38/5	IgG1/κ	C-terminus of Aß peptide, ending at residue 38	Human, Canine, Rodent	Janssen Research & Development	MSD
JRF/cAß40/28	IgG1/κ	C-terminus of Aß peptide, ending at residue 40	Human, Canine, Rodent	Janssen Research & Development	MSD / ELISA
JRF/cAß42/26	IgG1/κ	C-terminus of Aß peptide, ending at residue 42	Human, Canine, Rodent	Janssen Research & Development	MSD / ELISA
J&JPRD/hAß11/1	IgG1/K	N-terminus of Aß peptide, starting at residue 11	Human, Canine	Janssen Research & Development	MSD / ELISA

Detection antibodies

Monoclonal Antibody	Labelling	Isotype	Specificity	Reactivity	Source	Assay
JRF/cAß40/28	SULFO-TAG	IgG1/κ	C-terminus of Aß peptide, ending at residue 40	Human, Canine, Rodent	Janssen Research & Development	MSD
	HRPO					ELISA
JRF/cAß42/26	SULFO-TAG	IgG1/κ	C-terminus of Aß peptide, ending at residue 42	Human, Canine, Rodent	Janssen Research & Development	MSD
	HRPO					ELISA
JRF/AßN/25	SULFO-TAG	IgG1/κ	N-terminus of full-size Aß peptide (end-specific)	Human, Canine	Janssen Research & Development	MSD
J&JPRD/hAß11/1	SULFO-TAG	IgG1, K	N-terminus of Aß peptide, starting at residue 11 (end-specific)	Human, Canine	Janssen Research & Development	MSD
4G8	SULFO-TAG	IgG2b	Residues 17-23 of Aß peptide	Human, canine, Rodent	Meso Scale Discovery	MSD
6E10	SULFO-TAG	IgG1	Residues 3-8 of Aß peptide	Human, canine	Meso Scale Discovery	MSD
3D6	Biotinylated	IgG2b	N-terminus of full-size Aß peptide (end-specific)	Human, Canine	Fujirebio	Innotest (Aß1-42)

Additional antibodies

Monoclonal Antibody	Labelling	Isotype	Specificity	Reactivity	Source	Assay
JRF/cAß42/26	Biotinylated	IgG1/κ	C-terminus of Aß peptide, ending at residue 42	Human, Canine, Rodent	Janssen Research & Development	Alpha-lisa
JRF/AßN/25	Coupled to acceptor Beads	IgG1/κ	N-terminus of full-size Aß peptide	Human, Canine	Janssen Research & Development	Alpha-lisa
4G8	Biotinylated	IgG2b	Residues 17-24 of Aß peptide	Human, Rodent	Covance	Alpha-lisa

Aß- Amyloid-ß peptide, MSD – Meso Scale Discovery, ELISA – enzyme-linked immunosorbent assay, HRPO – horseradish peroxidase

5 SANDWICH ENZYME-LINKED IMMUNOSORBENT ASSAY (ELISA)

ELISA is one of the most commonly used immunoassays. For this study, sandwich ELISAs were performed. Sandwich ELISAs involve the coating of a capture antibody onto a plate that upon sample adding will capture the analyte of interest. Detection of the analyte is then done by a labelled (e.g Horseradish peroxidase (HRPO)) detection antibody.

5.1 MEASUREMENTS OF Aß LEVELS

ELISAs were performed in 96 well plates (Maxisorb ELISA plates, NUNC™ 430341 (Thermo Scientific, Nunc™, Roskilde, Denmark). Capture antibody was diluted in coating buffer (10mM NaCl, 10mM Tris, pH=8.5) to a final concentration of 3µg/ml, transferred to the ELISA plate and incubated overnight at 4°C. After incubation, plates were washed 5 times with washing buffer (Phosphate Buffered Saline (PBS) with 0.05% Tween-20), and blocked with 0.1% casein in PBS, for 1-4 hours, at room temperature with shaking (600rpm). After blocking, plates were washed 5 times with washing buffer, and tapped dry. Previously prepared standards and samples were then added in duplicate.

Standards consisted of human Aß synthetic peptides (Anaspec, Inc., San Jose, CA, USA). Peptides were dissolved in DMSO to a concentration of 0.1mg/ml and stored at -80°C. Standards were diluted in 0.1% casein in PBS to a starting concentration of 500pg/ml followed by sequential dilution steps until 7.81pg/ml. Samples were also diluted in 0.1% casein in PBS. Standard curves were added to the plate within 1 hour after preparation. Standard and samples were mixed with the detection antibody and incubated overnight at 4°C (no shaking). Following incubation, plates were washed 5 times with washing buffer and reading substrate was added.

Several substrates were used: QuantaBlu™ Fluorogenic Peroxidase substrate kit (Thermo Scientific, Pierce, Rockford, USA), TMB Substrate kit (Thermo Scientific), and 1-Step™ Ultra TMB-ELISA Substrate Solution (Thermo Scientific). QuantaBlu is a chemifluorescent substrate for ELISA that generates a blue fluorescent product upon reaction with peroxidase. TMB substrate is a chromogenic substrate that yields a blue color upon reaction with HRP. Unlike the TMB, which consists of a 2 component mixture, the Ultra-TMB is only composed of 1 reagent with no need to prepare the substrate. Ultra-TMB is the most sensitive of the chromogenic substrates.[285]

For all substrates used, signals were measured in the EnVision 2012 Multilabel Reader (PerkinElmer, USA). The excitation and emission for QuantaBlu Substrate was 325nm and 420nm, respectively. For TMB and 1-step Ultra TMB absorbance was measured at 450nm.

5.2 SPIKE-AND-RECOVERY ASSAYS

To evaluate cross-reactivity of the assay, individual human CSF samples were spiked with $Aß_{1-40}$ peptide at final concentrations of 2500pg/ml, 5000pg/ml and 10000pg/ml. The samples were diluted 4 or 8 times and measured simultaneously with unspiked samples of the same individuals, in one analytical run with ELISA assay using J&JPRD/hAß11/1 coating antibody and JRF/cAß40/48-HRPO detection antibody, following the previously described ELISA protocol.

To evaluate the assay accuracy individual human CSF samples were spiked with $Aß_{11-40}$ peptides at different concentrations, using as final spike concentrations 30pg/ml and 60pg/ml. Samples were diluted 4 and 8 times and measured simultaneously with unspiked samples of the same individuals, in one analytical run with ELISA assay using J&JPRD/hAß11/1 coating antibody and JRF/cAß40/48-HRPO detection antibody, following the previously described ELISA protocol.

5.3 ELISA DATA ANALYSIS

ELISA data analysis was done in GraphPad Prism 6 software (GraphPad software, Inc., CA, USA). Standard curves were generated using a non-linear regression (curve fit) for a sigmoidal standard curve, and concentrations in samples were obtained by interpolation from the standard curve.

Acceptance criteria of standard curve were as follows:

- Calculated concentration % Coefficient of variation (CV) between duplicates is lower than 20%, otherwise point is excluded. (CV criterion does not apply to standard 0pg/ml);
- % recovery (calculated concentration/expected concentration x 100), should fall between 80 and 120%, and between 75 and 125% for the highest and lowest non-zero calibrators, if not point is to be excluded.
- Calibration curve should consist of at least 5 valid non-zero calibration standards;
- It is not allowed to exclude two adjacent non-zero calibration samples from the curve.

Acceptance criteria of samples (if not met sample is to be excluded):

- Calculated concentration % CV between duplicates is lower than 20%;
- Samples concentrations should be obtained within the quantifiable range that is determined by the limits of quantification. For the lower limit of quantification, it is defined as the lowest calibrator (with the exception of 0pg/ml), that meets the acceptance criteria (%CV <20% and % recovery between 80 and 120%).

6 INNOTEST® ß-AMYLOID(1-42)

6.1 MEASUREMENTS OF Aß LEVELS

The Innotest® $Aß_{1-42}$ (Fujirebio, Guent, Belgium) kit is a solid phase enzyme immunoassay for the quantitative determination of $Aß_{1-42}$ in human CSF, in which the Aß peptide is captured by the 21F12 antibody. CSF samples are then added and incubated with a biotinylated 3D6 antibody. The complex is then detected by peroxidase-labeled streptavidin that develops a color upon substrate working solution addition.

The kit was used according to manufacturer's instructions. Standards, controls, and samples were prepared and added together to the assay plates. Plates were read within 15 minutes, at 450nm (single wavelength) in EnVision 2012 Multilabel Reader (PerkinElmer, USA).

6.2 INNOTEST DATA ANALYSIS

Innotest $Aß_{1-42}$ data analysis was done in GraphPad Prism 6 software (GraphPad software, Inc., CA, USA). Standard curve values were created using a non-linear regression (curve fit) for a sigmoidal standard curve, and sample values were interpolated from the standard curve.

Acceptance criteria of standard curve (repeat experiment if criterion is not met):

- Absorbance of the lowest calibration point should be lower than 0.300 OD, and highest calibration point should be higher than 1.700 OD.
- Run controls should be within the defined concentrations of the kit.
- %CV for duplicate measures of calibration curve points and controls should be lower than 20%.

Acceptance criteria of samples (if not met sample is to be excluded):

- %CV for duplicate measures of samples should be lower than 20%.
- Absorbance is within the limits of the calibration curve.

7 INVITROGEN™ ELISA Aß40

7.1 MEASUREMENTS OF Aß LEVELS

The Invitrogen™ Human Aß40 ELISA kit (Invitrogen, Carlsbad, California) is a solid phase sandwich ELISA and is used for the determination of $Aß_{1-40}$ levels in CSF samples. A monoclonal antibody

specific for the N-terminus of human $Aß_{1-40}$ is used as capture antibody and is pre-coated into the kit plates. CSF samples, controls and standards, are then incubated together with the detection antibody, which is specific for the C-terminus of the Aß1-40 peptide. The complex is then detected by a HRPO-labelled anti-rabbit antibody that upon substrate solution addition produces a color. The intensity of the colored product is proportional to the concentration of human Aß1-40 peptide present in the samples.

The kit was used according to manufacturer instructions. Standards, controls, and samples were prepared and added together to the plates. Plates were read at 450nm in EnVision 2012 Multilabel Reader (PerkinElmer, USA).

7.2 INVITROGEN ELISA Aß40 DATA ANALYSIS

Invitrogen ELISA Aß40 data analysis was done in GraphPad Prism 6 software (GraphPad software, Inc., CA, USA). Standard curve values were created using a non-linear regression (curve fit) for a sigmoidal standard curve, and sample values were interpolated from the standard curve.

Acceptance/exclusion of standard curve and samples followed the same criteria as for ELISA (Section 5.3).

8 ALPHALISA

Total Aß ($Aß_{1-x}$) and $Aß_{1–42}$ in cell supernatant were measured by sandwich Alphalisa – a bead-based homogenous proximity assay. In the presence of the target analyte, the beads come in close proximity, and upon excitation of the donor beads, singlet oxygen molecules are released triggering a cascade of energy transfer to the acceptor bead, resulting in light emission.

8.1 MEASUREMENTS OF Aß LEVELS

Alphalisa was performed in a 384-well Optiplate (PerkinElmer Inc., Waltham, Mass., USA). Standards consisted of human synthetic peptides (Anaspec, Inc., San Jose, CA, USA). Peptides were dissolved in DMSO to a concentration of 0.1mg/ml and stored at -80°C. Standard curves ranged from 0pg/ml to 2400pg/ml for $Aß_{1–42}$, and from 0pg/ml to 12800pg/ml for Aß total assays. Standards and samples were added simultaneously to the Optiplate in duplicate. The antibody mix, containing the conjugated acceptor beads (2ug/ml ($Aß_{1-42}$), 3µg/ml (Aß total)) and biotinylated antibody (0.261nM ($Aß_{1-42}$), 0.25nM (Aß total)), was then added to the Optiplate,

followed by 1h incubation at room temperature. After incubation, streptavidin donor beads (10 µg/ml) were added to the plate, followed by 1 h incubation at room temperature in the dark. Light emission was measured (Excitation 650nm, Emission 615nm) using the EnVision 2012 Multilabel Reader (PerkinElmer, USA).

Alongside samples, low and high controls are also measured. High controls (HC) correspond to cells treated with 100% DMSO, and low controls (LC) correspond to cells treated with 100% DMSO but without biotinylated antibody.

8.2 DATA ANALYSIS

Standard curve values were created using a linear curve with logarithms of both concentration and response (formula below), and sample values were then interpolated from the standard curve.

$$\ln Y_i = B_0 + B_1 \ln x_i$$

Data acceptance criteria:

- Non-linear points in standard curves (lowest and/or highest concentrations) are rejected.
- Z prime should be higher than 0.5. When a control (HC or LC) value deviates 20% or more from the median of all control values, the value can be rejected. A plate is rejected if more than 40% of the control values need to be disapproved to reach a z prime of 0.5.
- In each experiment different "reference" compounds are tested. The pIC50 of these compounds should be within 0.5 log range. An experiment is rejected if more than 25% of the reference compounds are out of range.

9 MESO SCALE DISCOVERY TECHNOLOGY (MSD)

MSD technology (Gaithersburg, MSD, USA) is based on electrochemiluminescence (ECL) detection (*Figure 7*). The detection antibody utilized is conjugated with electrochemiluminescent labels (MSD SULFO-TAG™) that emit light at ~ 620 nanometers after electrochemical stimulation. This technology uses microplates with carbon electrodes integrated into the bottom of the plate. Analytes in the sample bind to the capture antibody which is immobilized on the electrode surface. Further addition of the detection antibody allows the analyte detection. Addition of MSD reading buffer provides the proper environment for the

electrochemiluminescent reaction. In the imager, a voltage is placed across the plate-associated electrodes, resulting in a series of electrically induced chemical reactions leading to the generation of a luminescent signal. The multiple excitation cycles of each label amplify the signal to enhance light levels and improve sensitivity.

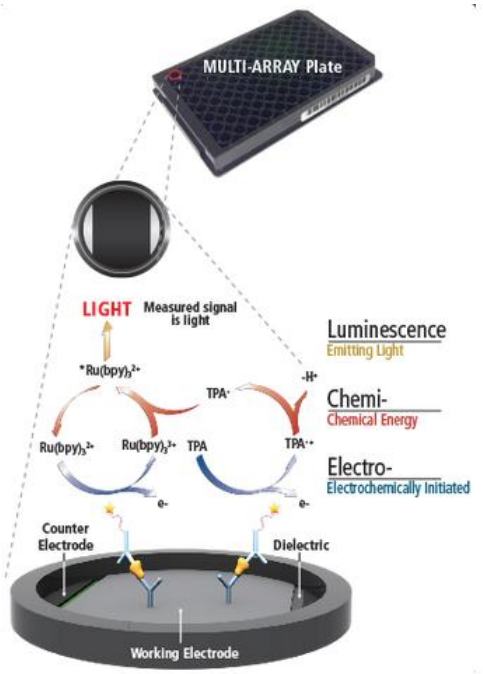

Figure 7 Schematic representation of Meso Scale Discovery technology and assay. (www.mesoscale.com).

9.1 ANTIBODY LABELLING

Detection antibodies for MSD assays were labelled with MSD SULFO-TAG NHS Ester. The label is an amine-reactive, N-hydroxysuccinimidine ester which readily couples to primary amines (randomly) under mildly basic conditions to form a stable amide bond.

The lyophilized MSD SULFO-TAG was reconstituted in ice cold water (3nmol/µl) and conjugated to the antibody in a ratio of 15:1 for JRF/AßN/25, and a ratio of 15:1 and 20:1 for J&JPRD/hAß11/1 antibody. Antibodies were diluted to a final concentration of 1.5mg/ml in PBS (pH=7.9). The mixture was then incubated for 2h, at room temperature, in the dark. Labelled antibody was then isolated using ZEBA spin desalting columns (Thermo Scientific), 40K, MWCO, to dialyze-out the free label. The labelled antibody was then filtered using a 0.22µm filter (Millex-GV SLGV013SL (Merck Millipore ®, Darmstadt, Germany), and stored at 4°C.

9.2 MSD Aß 4-PLEX

9.2.1 Measurements of Aß levels

In the J&J Aß 4-plex assay, 4 distinct peptides can be detected simultaneously. Each well of the 96-well plate contains four spatially distinct spots, each coated with a specific antibody (300µg/ml) for the capture of Aßx-37 (coated with JRD/Aß37/3), Aßx-38 (coated with J&JPRD/Aß38/5), Aßx-40 (coated with JRF/cAß40/28), and Aßx-42 (coated with JRF/cAß42/26).

The coated plates were blocked with 0.1% casein in PBS, during 1h at room temperature with shaking (600rpm), after which plates were washed 5 times with washing buffer (PBS with 0.05% Tween). After washing, samples and standards are added to the plate in duplicate.

Standards consisted of human synthetic peptides (Anaspec, Inc., San Jose, CA, USA). Peptides were dissolved in DMSO to a concentration of 0.1mg/ml and stored at -80°C. Standards were diluted in 0.1% casein in PBS to a starting concentration of 5000pg/ml followed by sequential dilution steps until 2.28pg/ml. Samples were also diluted in 0.1% casein in PBS. Standard curves were added to the plate within 1 hour after preparation. Standard and samples were mixed with the SULFO-TAG labelled detection antibody and incubated overnight at 4°C (no shaking). Following incubation, plates were washed 5 times with washing buffer and MSD Read buffer T with surfactant (MSD) was added to each well. Plates were immediately read in the MSD SECTOR Imager 6000 (MSD).

9.3 MSD SINGLEX

MSD Singlex assay follows the same principle of MSD detection. Capture antibodies are coated on 96-well Standard (L15XA) plates (MSD). For spot coated plates, 5µl of capture antibody, diluted in 0.1% casein in PBS, is dispensed directly onto the working electrode. For solution coating, 50µl of capture antibody, diluted in 0.1% casein in PBS, is dispensed into the well. Plates are then sealed and incubated overnight at 4°C.

The coated plates were blocked with 0.1% casein in PBS, during 1h at room temperature with shaking (600rpm), after which plates were washed 5 times with washing buffer (PBS with 0.05% Tween). After washing, samples and standards were added to the plate in duplicate. 3 methods of incubation were tested:

- In the 2-step incubation method samples were added to the coated plate and incubated at room temperature (RT) (1-2hours). Afterwards the plate was washed and the detection antibody was added and incubated at RT (1-2hours).
- In a 1 step incubation method the sample and detection antibody are added conjunctly to the coated plate. Incubation time can then be for 2-2.5hours at RT (with shaking) or overnight (ON) at 4°C (no shaking required).

Standards consisted of human synthetic peptides (Anaspec, Inc., San Jose, CA, USA). Peptides were dissolved in DMSO to a concentration of 0.1mg/ml and stored at -80°C. Standards were diluted in 0.1% casein in PBS to a starting concentration of 5000pg/ml followed by sequential dilution steps until 6.86 pg/ml. Samples were also diluted in 0.1% casein in PBS. Standard curves were added to the plate within 1 hour after preparation. Standard and samples were mixed with the SULFO-TAG labelled detection antibody and incubated overnight at 4°C (no shaking). Following incubation, plates were washed 5 times with washing buffer and MSD Read buffer T

with surfactant (MSD) was added to each well. Plates were immediately read in the MSD SECTOR Imager 6000 (MSD).

9.4 MSD DATA ANALYSIS

MSD data analysis was done in MSD Discovery Workbench software version 4.0.12 (MSD).

Acceptance criteria for standard curve and samples were the same as for ELISA (Section 5.3).

10 ALAMAR BLUE ASSAY

The Alamar Blue assay is based on the conversion of the non-fluorescent reagent (resazurin) to fluorescent product (resorufin) by metabolically active cells. Viable cells retain the ability to reduce resazurin into resorufin. Non-viable cells rapidly lose metabolic capacity, therefore not having the capacity to reduce the Alamar blue dye, resulting in no fluorescent signal.

The stock alamar blue solution is diluted 1.5 times in 0.1M potassium phosphate buffer (PPB), and added to the plate, followed by an incubation of 2-3h at 37°C, 5% CO_2. Fluorescence is then measured (Excitation 540nm, Emission 590nm) using the EnVision 2012 Multilabel Reader (PerkinElmer, USA).

11 STATISTICAL ANALYSIS

Statistical analysis was performed utilizing GraphPad Prism version 6 software (Prism, GraphPad Software San Diego, CA, USA). Statistical tests consisted of t-test, and $p < 0.05$ was set as statistically significant.

12 OVERVIEW OF ANTIBODY COMBINATIONS USED THROUGHOUT THE ASSAYS

Table 7 Overview of antibody combinations used throughout the assays, and respective antigens.

Assay	Coated Antibody	Detection antibody	Analyte
ELISA	J&JPRD/hAß11/1	JRF/cAß40/28 – HRPO	Aß11-40
		JRF/cAß42/26 – HRPO	Aß11-42
Innotest Aß1-42	21F12	3D6 – biotinylated	Aß1-42
Invitrogen ELISA Aß40	N-terminus specific	C-terminus specific	Aß1-40
Alphalisa	JRF/AßN/25 (donor beads)	4G8 (acceptor beads)	Aß Total (1-x)
		JRF/cAß42/26 (acceptor beads)	Aß1-42
MSD 4-Plex	JRD/Aß37/3	J&JPRD/hAß11/1 – SULFO-TAG	Aß11-40, Aß11-42
	J&JPRD/Aß38/5	JRF/AßN/25 – SULFO-TAG	Aß1-37, Aß1-38, Aß1-40, Aß1-42
	JRF/cAß40/28	4G8 – SULFO-TAG	Aßx-37, Aßx-38, Aßx-40, Aßx-42
	JRF/cAß42/26	6E10 – SULFO-TAG	
MSD Singlex	J&JPRD/hAß11/1	JRF/cAß40/28 – SULFO-TAG	Aß11-40
		JRF/cAß42/26 – SULFO-TAG	Aß11-42
	JRF/cAß40/28	J&JPRD/hAß11/1 – SULFO-TAG	Aß11-40
	JRF/cAß42/26		Aß11-42

ELISA – Enzyme-linked Immunosorbent assay, Aß – Amyloid-ß peptide, MSD – Meso Scale Discovery, HRPO – horseradish peroxidase.

Chapter IV. Results

1 ASSAY DEVELOPMENT FOR Aß$_{11-x}$ MEASUREMENTS

The first part of this project aimed at developing an assay that could measure Aß$_{11-x}$ levels in various types of samples, in a sensitive and specific manner. After optimization, this assay was used to assess the effect of specific compounds (GSM, GSI, and BACEi) on Aß$_{11-x}$ levels, by comparing levels post treatment with baseline measurements. For this purpose, MSD singlex and 4-plex, and ELISA assays were evaluated and optimized according to the parameters summarized in *Figure 8.*

Maximum sensitivity of each assay was defined as the lowest point of the standard curve meeting the following acceptance criteria: % CV between duplicate measures inferior to 20% and %recovery between 80 and 120%. %Recovery compares the input concentration of the standards to the calculated concentration obtained by backfitting the calibration curve (%recovery = Calculated concentration/Expected concentration*100).

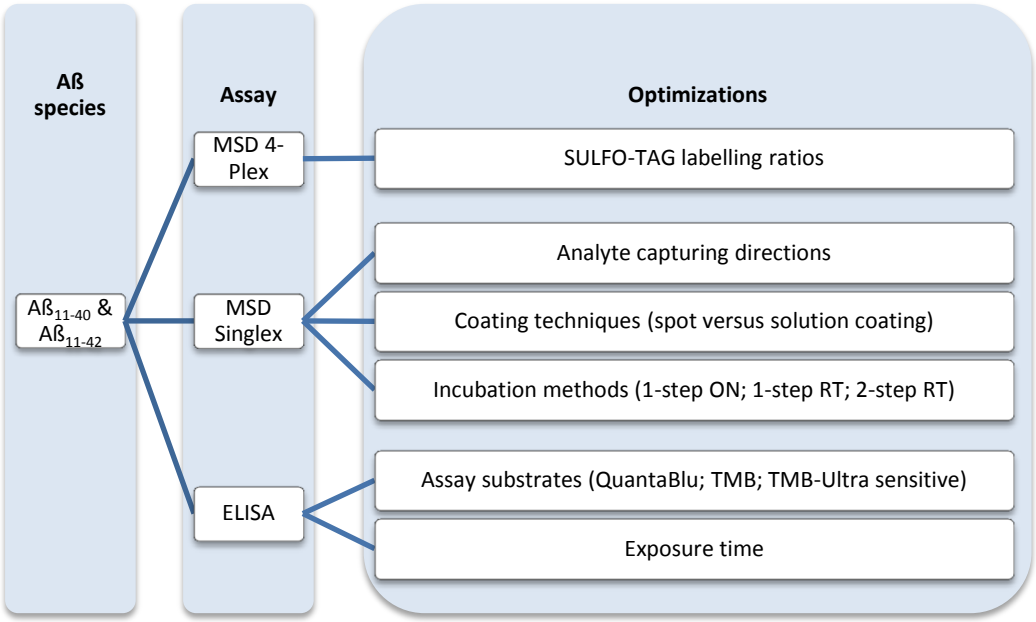

Figure 8 Schematic representation of assays and optimizations performed during assay development for Aß$_{11-x}$ measurement. Aß – amyloid-ß peptide, MSD – Meso Scale Discovery, ON – overnight, RT – Room Temperature.

1.1 MSD 4-PLEX

To evaluate the possibility of measuring both Aß$_{11-40}$ and Aß$_{11-42}$ simultaneously, the J&J Aß 4-plex assay was used.[286,287] This assay is a sandwich immunoassay with ECL detection. Since each well has four individually coated spots, it allows the detection of four Aß species simultaneously. As no appropriate synthetic Aß standards were available for Aß1$_{1-37}$ and Aß1$_{1-38}$, for this study only the Aß$_{x-40}$ and Aß$_{x-42}$ spots were evaluated.

Using human Aß$_{11-40}$ and Aß$_{11-42}$ as standards, and MSD SULFO-TAG labeled J&JPRD/hAß11/1[288] as detection antibody, this assay was optimized towards its maximum sensitivity.

For this assay the same purification lot of J&JPRD/hAß11/1 antibody was labelled with MSD SULFO-TAG, using two different antibody:SULFO-TAG challenge ratios (number of moles of SULFO-TAG per mole of protein in the reaction mixture) – 1:15 and 1:20. Both ratios showed the same assay sensitivity, but the 1:20 ratio yielded lower signal values, which lead to the use of the 1:15 ratio for further experiments.

Assay optimization led to a maximum sensitivity of 20.58pg/ml for detection of Aß$_{11-40}$, and 185.19 pg/ml for detection of Aß$_{11-42}$.

Evaluation of dog and human CSF pools in dilutions ranging from 1:2 to 1:256, revealed that the assay was not sensitive enough to detect Aß$_{11-40}$ and Aß$_{11-42}$ levels in CSF pools.

After testing CSF pools, CSF samples from individual dogs and humans were also tested. 5 individual human samples were tested, and no signal for Aß$_{11-42}$ was detected, and for Aß$_{11-40}$ a signal was detected at the lower dilutions of the samples (1:2 and 1:4), with an average of 151.11pg/ml (SD=68.53) at 4 times sample dilution. 4 individual dog samples were also tested, showing again no signal for Aß$_{11-42}$, while for Aß$_{11-40}$ the four samples had an average of 286.8pg/ml (SD=86.5) at 8 times sample dilution.

In both human and dog CSF the signals in the individual CSF samples were low and close to the Lower limit of quantification (LLOQ), making measurement of Aß$_{11-x}$ reductions after drug treatment unfeasible.

1.2 MSD SINGLEX

1.2.1 hAß11/1 as capture or detection antibody

The next assay tested was the MSD singlex assay. This assay uses the same detection technology as the MSD 4-plex, but detects a single analyte per well.

For detection of Aß$_{11-40/42}$ the two possible sandwich directions were tested:

- Plate coated with JRF/cAß40/28 or JRF/cAß42/26, which capture species terminating at residue 40 or 42 (Aß$_{x-40/42}$), respectively; Detection with J&JPRD/hAß11/1-SULFO-TAG labelled antibody, which will detect Aß species initiating at residue 11 (Aß$_{11-x}$) specifically.

- Plate coated with J&JPRD/hAß11/1, that captures Aß species starting at residue 11 ($Aß_{11\text{-}x}$); Detection with JRF/cAß40/28-SULFO-TAG or JRF/cAß42/26-SULFO-TAG labelled antibody, detecting species ending at residue 40 or 42 ($Aß_{x\text{-}40/42}$), respectively.

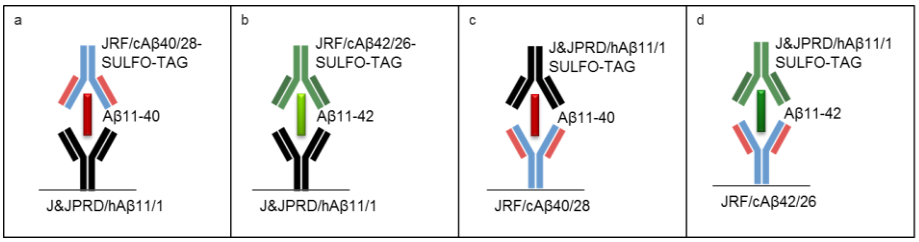

Figure 9 Schematic representation of $Aß_{11\text{-}40}$ and $Aß_{11\text{-}42}$ sandwich assay directions studied in MSD singlex assay. (a) and (b) represent coating with J&JPRD/hAß11/1 and detection with JRF/cAß40/48- or JRF/cAß42/26-SULFO-TAG for $Aß_{11\text{-}40}$ or $Aß_{11\text{-}42}$, respectively. Figures (c) and (d) represent the opposite direction to capture the peptides, capturing first species ending at residues 40 or 42, and then detecting the $Aß_{11\text{-}x}$ species with J&JPRD/hAß11/1-SULFO-TAG. Aß – amyloid-ß peptide.

From the set-ups depicted in *Figure 9,* (a) detected $Aß_{11\text{-}40}$ with a maximum sensitivity of 20.58pg/ml, while setup (b) detected $Aß_{11\text{-}42}$ with a maximum sensitivity of 185.19pg/ml. Setup (c) had a maximum sensitivity of 555.55pg/ml and (d) had a maximum sensitivity of 1666.67pg/ml. Therefore the capture of $Aß_{11\text{-}x}$ species first appears to be the best working sandwich direction to achieve maximal sensitivity.

1.2.2 Coating methods

We compared solution coating and spot coating on MSD single-spot plates (*Figure 10)*. In the first condition, the bottom of the well is completely covered with coating solution, and in the second only the working electrode is coated, which could provide a more sensitive assay.

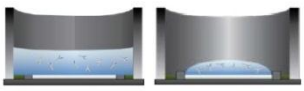

Figure 10 Coating patterns of MSD Singlex plates. The left image displays the solution coating and the right the spot coating technique (MSD).

Coating of 96-well standard plates with J&JPRD/hAß11/1 antibody, using both coating methods, and further detection with JRF/cAß40/28-SULFO-TAG, showed that spot coating did not increase the assay sensitivity as compared to solution coating. Maximum sensitivity obtained for both methods was 20.58pg/ml for detection of $Aß_{11\text{-}40}$, but spot coating resulted in slightly lower signals. The lack of increased sensitivity and the risk for higher variability (more complex coating method) led to the further use of solution coating.

1.2.3 Incubation methods

An additional parameter that can be optimized in MSD singlex assay method is the sample/detection antibody incubation method. From the three methods – 2 steps at RT, 1 step at RT or 1 step ON, the latter had the highest sensitivity. Maximum sensitivity for $Aß_{11\text{-}40}$

detection was 555.55pg/ml, 61.73pg/ml and 20.58pg/ml for the 2 steps RT, 1 step RT, and 1 step ON, respectively.

Overall, the use of MSD singlex method did not increase the sensitivity of $Aß_{11\text{-}40}$ detection when compared with MSD 4-plex.

1.3 ELISA

Based on MSD singlex assay results regarding use of J&JPRD/hAß11/1 as coating or detection antibody, the ELISA setup was defined to capture Aß species starting at residue 11 ($Aß_{11\text{-}x}$) and then detect species ending at the residue 40 or 42 ($Aß_{11\text{-}40/42}$) (*Figure 11)*.

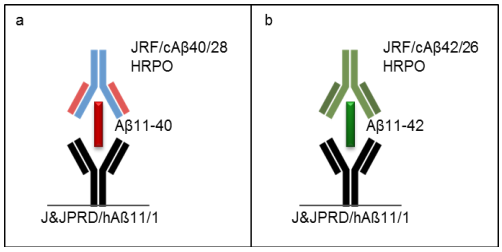

Figure 11 Schematic representation of $Aß_{11\text{-}40}$ and $Aß_{11\text{-}42}$ setup in sandwich ELISA assay. (a) and (b) represent coating with J&JPRD/hAß11/1 and detection with JRF/cAß40/48-HRPO or JRF/cAß42/26-HRPO for $Aß_{11\text{-}40}$ or $Aß_{11\text{-}42}$ analysis, respectively. Aß – amyloid-ß peptide, HRPO – horseradish peroxidase.

Different detection substrates were tested for this assay: QuantaBlue™ Fluorogenic Peroxidase substrate, TMB and 1-Step™ Ultra-TMB.

Using the QuantaBlue™ Fluorogenic Peroxidase substrate, the maximum obtained sensitivity for $Aß_{11\text{-}40}$ was 78.1pg/ml, after a 15 minutes exposure time.

Using the TMB Substrate, the sensitivity of the assay to detect $Aß_{11\text{-}40}$ was increased to 20.6pg/ml, using an exposure time of 20 minutes.

The 1-Step™ Ultra TMB-ELISA Substrate Solution was also tested since it is promoted as the most sensitive of the available chromogenic substrates. Results indeed showed an increase in assay sensitivity, with maximum sensitivity for $Aß_{11\text{-}40}$ detection of 6.86pg/ml, and for $Aß_{11\text{-}42}$ 15.63pg/ml (optimized exposure time of 8 minutes).

As the assay offered the highest sensitivity of all assays and conditions tested, the ELISA assay using the 1-Step ™ Ultra TMB-ELISA Substrate Solution was the selected assay for further assay validation.

1.3.1 ELISA Assay Validation

1.3.1.1 *Spike-recovery of synthetic Aß peptides in human CSF samples*

To evaluate cross-reactivity of the assay, individual human CSF samples of untreated subjects (n=6) were spiked with $Aß_{1\text{-}40}$ peptide. The % recovery of $Aß_{1\text{-}40}$ was below 1% in all spiked concentrations and in all samples, indicating minimal crossreactivity to full-length peptide (*Table 8)*.

To evaluate the assay accuracy individual human CSF samples (n=6) were spiked with $Aß_{11-40}$ peptides at different concentrations. The % recovery between 102 and 110% (*Table 8)*.

In conclusion, this ELISA assay has the capacity of accurately measuring $Aß_{11-x}$ levels in CSF samples, showing minimal cross-reactivity with the full length peptide $Aß_{1-40}$, which is the most physiologically abundant Aß peptide in CSF.

Table 8 Summary of spike and recovery results. Human CSF samples (n=6) were spiked with $Aß_{1-40}$ or $Aß_{11-40}$ to evaluate cross-reactivity with full length and assay accuracy, respectively. %recovery was calculates as (calculated concentration / expected concentration *100).

Peptide Spiked	Concentration of Peptide	Recovery (%) (1 : 4 Dilution)	Recovery (%) (1 : 8 Dilution)
$Aß_{11-40}$	60pg/ml	102 - 105	102 - 107
$Aß_{11-40}$	30pg/ml	109 - 110	108 - 109
$Aß_{1-40}$	10000pg/ml	0	0
$Aß_{1-40}$	5000pg/ml	0	0
$Aß_{1-40}$	2500pg/ml	0	0

Aß – amyloid-ß peptide

1.3.1.2 *Linearity between dilutions*

To complete the assay validation, experiments were performed to evaluate the dilution linearity in SK-N-BE(2) cell supernatant, dog CSF, and human CSF samples. Linearity is defined as concentration measurements between sample dilutions having a variation inferior to 20% (80-120% of reference dilution).These experiments additionally allowed to determine the optimal sample dilution for each sample type.

Cell supernatant from SK-N-BE(2) DMSO-treated cells, 4 dog CSF samples and 6 human CSF samples were diluted 2, 4, 8, 16, 32, 64, 128 and 512 times, and dilution linearity was assessed using the previously described ELISA setup.

Regarding $Aß_{11-40}$ measurements, the maximum sample dilution factor with detectable signal was 16 times for all samples, and there was dilution linearity between dilution factor 4 and 16 for most of them. For $Aß_{11-42}$ in dog and human CSF no signal was detectable at any dilution, while in cell supernatant signals were detectable and linear at 2 and 4 times sample dilution *(Table 9).*

We selected the following sample dilutions for next experiments based on dilution linearity and location of sample signal in the standard curve: for $Aß_{11-40}$ detection in dog CSF samples 8 times diluted, in human CSF 4 times diluted, and in cell supernatant 8 times diluted. For $Aß_{11-42}$ the selected working dilution for cell supernatant was 4 times *(Figure 12).*

Table 9 Dilution linearity in human and dog CSF and in cell supernatant. Linearity is defined as concentration measurements between sample dilutions having a variation inferior to 20%. Dilutions with variations higher than 20% are highlighted in grey. Note: Values correspond to the %variation between the dilution indicated in the respective line and the previous dilution.

	Human CSF						Dog CSF			Cell supernatant	
Analyte	$Aß_{11-40}$						$Aß_{11-40}$			$Aß_{11-40}$	$Aß_{11-42}$
Sample / *Dilution*	1	2	3	4	5	6	1	2	3	1	1
1:2							-	-	-		
1:4	10	51	54	08	66	14				6	5
1:8	16	7	2	5	8	18	24	23	13	13	BLLQ
1:16	03	26	17	23	15	10	12	04	09	2	BLLQ

Aß – Amyloid-ß peptide; BLLQ – below lower limit of quantification, '-' – dilution not tested.

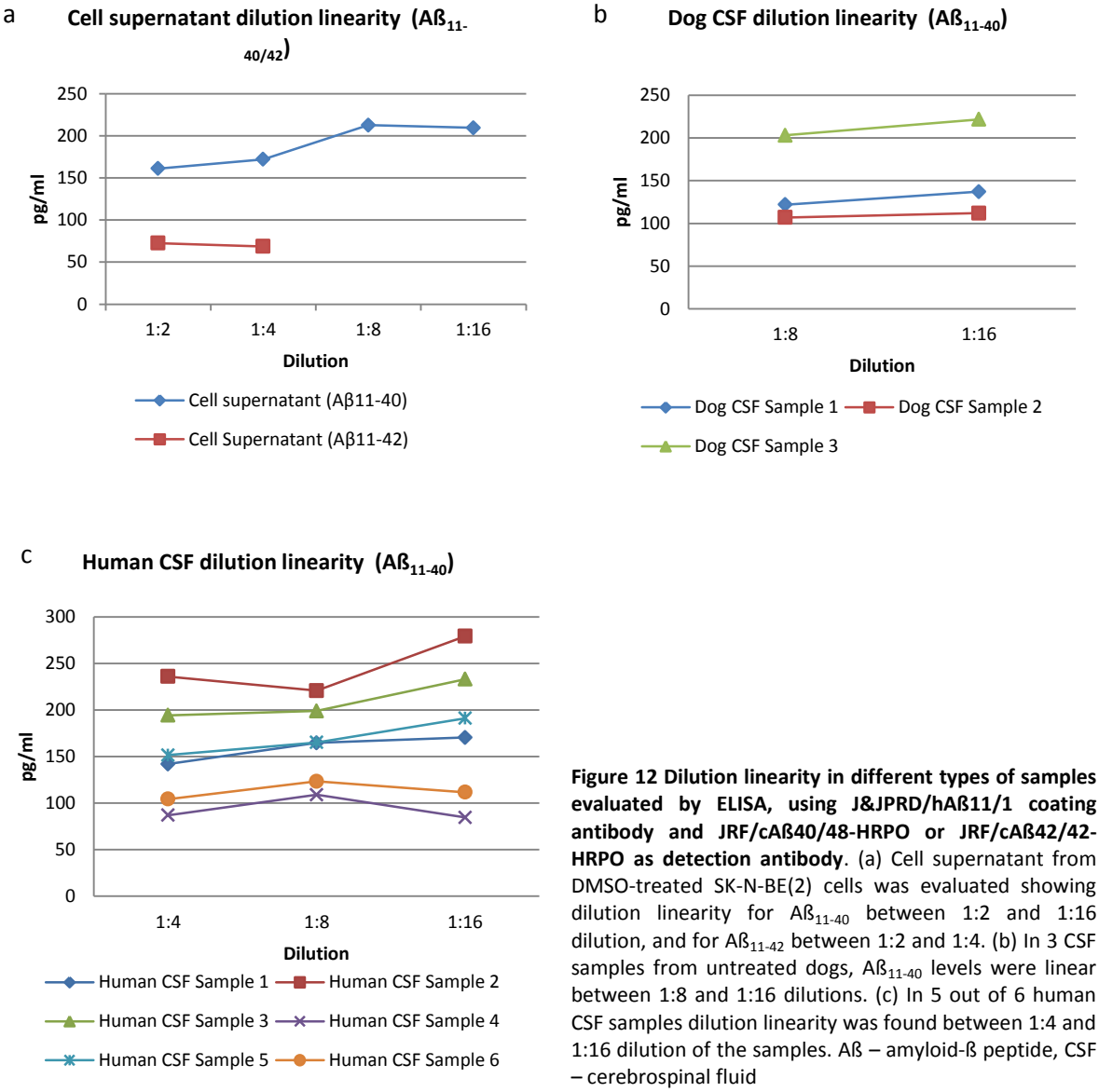

Figure 12 Dilution linearity in different types of samples evaluated by ELISA, using J&JPRD/hAß11/1 coating antibody and JRF/cAß40/48-HRPO or JRF/cAß42/42-HRPO as detection antibody. (a) Cell supernatant from DMSO-treated SK-N-BE(2) cells was evaluated showing dilution linearity for $Aß_{11-40}$ between 1:2 and 1:16 dilution, and for $Aß_{11-42}$ between 1:2 and 1:4. (b) In 3 CSF samples from untreated dogs, $Aß_{11-40}$ levels were linear between 1:8 and 1:16 dilutions. (c) In 5 out of 6 human CSF samples dilution linearity was found between 1:4 and 1:16 dilution of the samples. Aß – amyloid-ß peptide, CSF – cerebrospinal fluid

1.4 SUMMARY OF ASSAY DEVELOPMENT: ASSAY SENSITIVITY AND SAMPLE DILUTIONS

Throughout the immunoassays tested different antibody combination were tested, which are summarized in *Table 7*. Assay development lead to an ELISA using J&JPRD/hAß11/1 coating antibody and JRF/cAß40/28-HRPO or JRF/cAß42/26-HRPO detection antibody for $Aß_{11-40}$ or $Aß_{1-42}$ respectively *(Table 10)*. For this assay, the optimal dilution for each matrix – human and dog CSF, and cell supernatant – was also determined and is summarized in *Table 11.*

Table 10 Summary table of assays evaluated and respective maximum sensitivities (defined as the lowest point of the standard curve meeting the following acceptance criteria: %CV between duplicate measures inferior to 20% and %recovery between 80 and 120 %.)

Assay	Capture	Detection	$Aß_{11-40}$ (pg/ml)	$Aß_{11-42}$ (pg/ml)
ELISA: QuantaBlue	J&JPRD/hAß11/1;	JRF/cAß40/28-HRPO or JRF/cAß42/26-HRPO	78.1	----
TMB	J&JPRD/hAß11/1	JRF/cAß40/28-HRPO or JRF/cAß42/26-HRPO	20.58	----
TMB-Ultra	J&JPRD/hAß11/1	JRF/cAß40/28-HRPO or JRF/cAß42/26-HRPO	6.86	15.63
MSD Singlex:	JRF/cAß40/28 or JRF/cAß42/26	J&JPRD/hAß11/1-SULFO-TAG	555.55	1666.7
	J&JPRD/hAß11/1	JRF/cAß40/28- SULFO-TAG or JRF/cAß42/26- SULFO-TAG	20.58	185.19
MSD 4-plex		J&JPRD/hAß11/1-SULFO-TAG	20.58	185.19

ELISA – enzyme-linked immunosorbent assay, Aß – amyloid-ß peptide, MSD – Meso Scale Diagnostic, HRPO – Horseradish peroxidase

Table 11 Summary table of selected dilutions for each sample type

Sample Type	Sample Dilution	Analyte
Human CSF	1:4	$Aß_{11-40}$
Dog CSF	1:8	$Aß_{11-40}$
Cell Supernatant	1:8	$Aß_{11-40}$
Cell Supernatant	1:4	$Aß_{11-42}$

CSF – cerebrospinal fluid, Aß- amyloid-ß peptide

2 AMYLOID-ß MEASUREMENTS IN CELL SUPERNATANT

In the second part of this project, the developed assay was used to measure $Aß_{11-40}$ and $Aß_{11-42}$ levels in different types of samples, starting with cell supernatant. Assay results were compared with reductions measured on Aß Total levels ($Aß_{1-x}$), $Aß_{1-42}$ levels, and $Aß_{x-37/38/40/42}$ levels.

Three classes of compounds were tested for treatment of human neuroblastoma SK-N-BE(2) cells expressing wild type human APP (hAPP695): γ-secrfetase inhibitors (GSI), γ-secretase modulators (GSM) and BACE1 inhibitors (BACEi). Each compound was tested at 10 different concentrations, ranging from 9.01µM to 34.2pM.

Aß total (or 1-x) levels were measured by alphaLISA using the antibody pair JRF/hAßN/25 and 4G8. $Aß_{1-42}$ levels were also measured by alphaLISA using the antibody pair JRF/hAßN/25 and

JRF/cAß42/26. $Aß_{11\text{-}40}$ and $Aß_{11\text{-}42}$ levels were measured by ELISA using J&JPRD/hAß11/1 as capture antibody and JRF/cAß40/28-HRPO or JRF/cAß42/26-HRPO as detection antibodies, respectively.

$Aß_{x\text{-}37/38/40/42}$ levels were measured by MSD 4-plex using 4G8-SULFO-TAG as detection antibody, which binds to the 17th to 24th residue of Aß peptide, capturing full-length Aß, and species truncated up to the 17th residue.

Compound toxicity was determined through the Alamar Blue assay.

For all the assays, compound effect was measured based on the underneath formula:

$$\%\ effect = \frac{sample\ concentration(pg/ml)}{High\ control\ concentration(pg/ml)} * 100$$

Where the high control corresponds to DMSO-treated cells (i.e. no compound treatment) and is calculated by the average of high control values present per assay plate. All compound effects are compared to this value.

2.1 EVALUATION OF GSI AND GSM EFFECTS IN CELL SUPERNATANT

Two γ-secretase inhibitors (GSI A (Semagacestat) and GSI B (Begacestat)) were selected and their effect on Aß total, $Aß_{1\text{-}42}$ and $Aß_{11\text{-}40/42}$ levels was measured *(Figure 13)*. GSIs inhibit γ-secretase activity, thereby blocking APP proteolytic processing and the production of Aß species.

A dose-dependent response was seen for both compounds, and a near complete reduction of all peptides was observed between 9.01µM and 35.1nM concentrations, reaching a maximum reduction of 86% and 85% for $Aß_{1\text{-}42}$ levels in GSI A (Semagacestat) and GSI B (Begacestat), respectively. Aß total levels had a maximum reduction of 90% for both compounds. Of note, due to the sensitivity limits of the $Aß_{11\text{-}x}$ ELISA assays, it was estimated that for $Aß_{11\text{-}40}$ a reduction up until 88% could be quantified, while for $Aß_{11\text{-}42}$ a reduction of up until 50% could be quantified. Reductions that were beyond these numbers are represented in the graphs as 0% of baseline.

Between compound concentrations of 8.80nM and 34.2pM Aß total and $Aß_{1\text{-}42}$ levels return to baseline levels. $Aß_{11\text{-}40/42}$ levels showed an increase above baseline levels at these lower concentrations, particularly at 2.20nM, which reached 29% (GSI A) and 15% (GSI B) increase compared to baseline for $Aß_{11\text{-}40}$, and 50% (GSI A) and 43% (GSI B) for $Aß_{11\text{-}42}$. This increase pattern was replicated in a second independent experiment. At lower concentrations (<2.20nM) levels of $Aß_{11\text{-}40/42}$ returned to baseline levels.

Three γ-secretase modulators (GSM C, D (JNJ-42601572), and E (E2012)) were also selected and their effect on Aß total, $Aß_{1-42}$ and $Aß_{11-40/42}$ levels was measured *(Figure 13)*. GSMs intend to block selectively the production of longer Aß forms, including $Aß_{1-42}$, without affecting the cleavage of other substrates.

For GSM C, a dose–dependent response was observed, with a high reduction of $Aß_{1-42}$ (maximum reduction 85%) and $Aß_{11-42}$ levels (below 50%). Aß total had a maximum reduction of 33% and $Aß_{11-40}$ had a maximum reduction of 47%. This selectivity for $Aß_{x-42}$ species is likely related to the pharmacological properties of the compound itself.

GSM D (JNJ-42601572) and GSM E (E2012) showed a similar dose-dependent reduction pattern. At the highest concentrations of compound, several Aß species are reduced – $Aß_{1-42}$ (maximum reduction 84%, $Aß_{11-40}$ (below 12% of baseline) and $Aß_{11-42}$ (below 50% of baseline) – while Aß total levels remain stable compared to baseline levels. At lower compound concentrations (inferior to 8.80nM) all Aß levels return to baseline level.

Compound toxicity tests demonstrated that none of the compounds is significantly affecting cell viability, allowing to conclude that all registered Aß reductions are due to compound activity and not to compound-induced cellular death.

2.2 EVALUATION OF BACE INHIBITOR EFFECTS IN CELL SUPERNATANT

Twenty-four BACE1 inhibitors (BACEi 1 to 24) were selected and their effect on Aß total, $Aß_{1-42}$ and $Aß_{11-40}$ levels was measured in SK-N-BE(2) cell supernatant. BACEi block BACE1 activity, preventing APP proteolytic processing, and generation of Aß peptide. Aside from BACE cleavage at the 1st residue, there is also a cleavage site at the 11th residue. With this study we aim at studying if there is a differential effect on this two Aß species – Aß1-x and $Aß_{11-x}$ – upon BACE inhibition. Compounds with different potency and belonging to different chemical classes were selected to provide a broad spectrum of information regarding the BACEi effects *(Figure 14)*.

$Aß_{11-42}$ levels were no longer measured for this set of compounds due to the small detection range of the assay (a maximal reduction of only 50% could be detected). Nevertheless, it is expected that $Aß_{11-42}$ would have a similar reduction pattern as $Aß_{11-40}$ since BACE1 inhibition is expected to only affect the $Aß_{11-x}$ cleavage, and not the C-terminal cleavage by γ-secretase.

Besides Aß total, $Aß_{1-42}$ and $Aß_{11-40}$, $Aß_{x-37/38/40/42}$ species levels were also measured for a subset of the compounds (BACEi 16 to 24), to determine if those species were lowered in a similar manner as full-length $Aß_{1-x}$ species upon BACE1 inhibition.

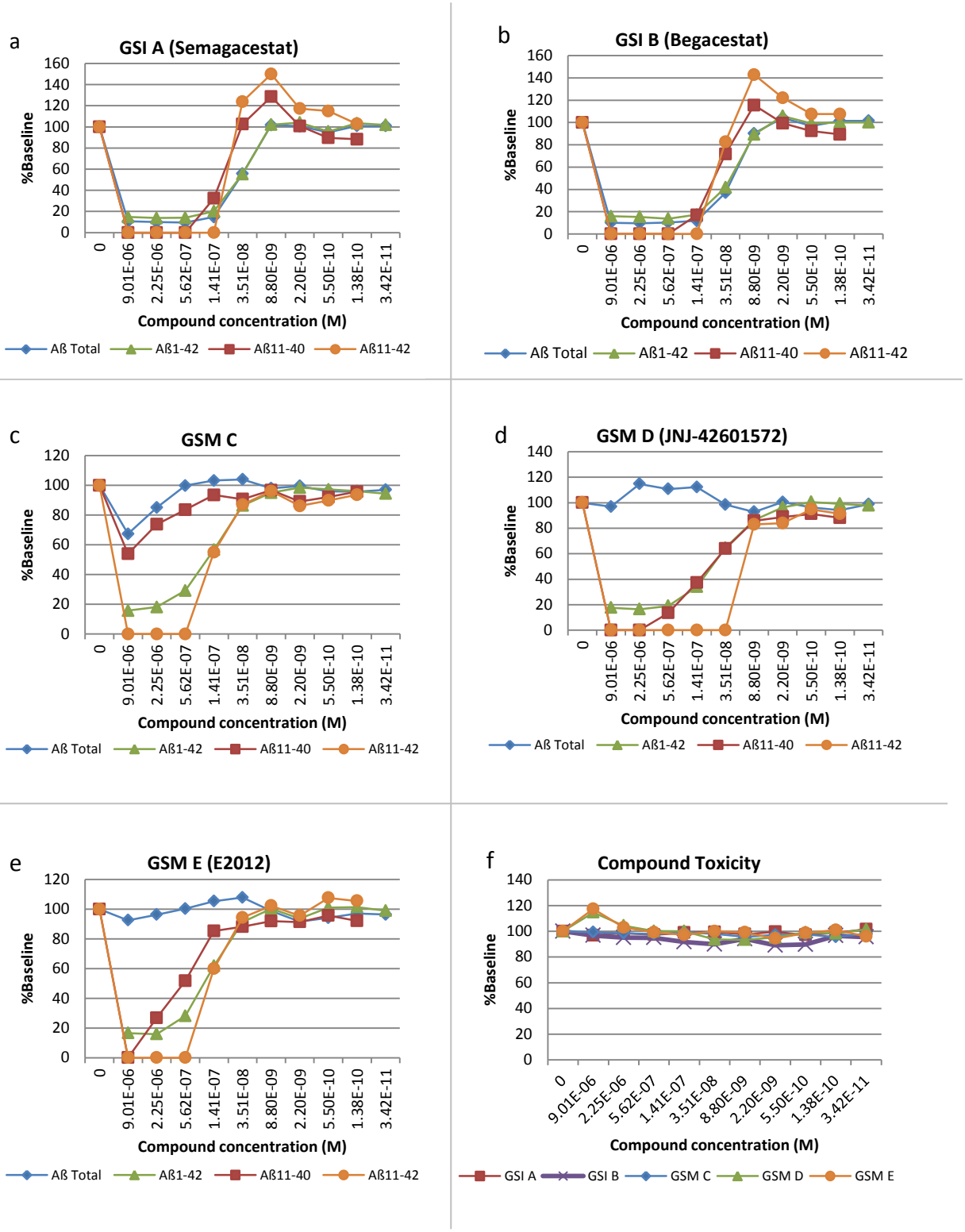

Figure 13 Effect of different GSI (A and B) and GSM (C, D and E), on Aß total, Aß$_{1-42}$, Aß1$_{1-40}$, and Aß1$_{1-42}$ levels in supernatant of human neuroblastoma cells (SK-N-BE(2)), expressing human wild type APP. In all panels "0" in the x-axis corresponds to DMSO- treated cells, and the measured concentration was used as 100% baseline (high control) value. Cells were treated with different compound doses, and the effects were calculated as %baseline (DMSO-treated cells). Aß total and Aß$_{1-42}$ were determined by alpha-LISA, using the antibody pairs JRF/hAßN/25-4G8 and JRF/hAßN/25- JRF/cAß42/26, respectively. Aß$_{11-40/42}$ levels were determined by ELISA using the antibody pairs J&JPRD/hAß11/1- JRF/cAß40/28 and J&JPRD/hAß11/1- JRF/cAß42/26, respectively. The last panel (f) represents compound toxicity which was determined using the Alamar Blue assay. Reductions that were beyond these numbers are represented in the graphs as 0% of baseline. GSI – γ-secretase inhibitor, GSM – γ-secretase modulator, Aß – amyloid-ß peptide.

A dose-dependent response was seen for all the compounds (except BACEi 20). Aß total, $Aß_{1-42}$ and $Aß_{11-40}$ levels were reduced to a similar extent for almost all compounds (21 out of 24). 3 of the BACEis - BACEi 16, 17 and 18 - $Aß_{11-40}$ showed an increase of 36%, 52% and 33% versus baseline at concentrations below 2.20nM, in contrast to Aß total and $Aß_{1-42}$ assays.

For all compounds maximum reduction occurred at the highest doses, and in general at compound concentrations inferior to 5.50nM measured levels of all Aß species returned to baseline levels. Of notice, for a few compounds, such as BACEi 11, 15, 22, and 23, $Aß_{11-40}$ levels return to baseline before Aß total and $Aß_{1-42}$ levels.

Evaluation of N-truncated species levels ($Aß_{x-37/38/40/42}$), showed a less pronounced effect of the BACEi on these species. Additionally there also appears to be a size- dependent effect with regard to the N-truncated species, where inhibition is stronger for the longer Aß species: $Aß_{x-42}$ > $Aß_{x-40}$ > $Aß_{x-38}$ > $Aß_{x-37}$.

$Aß_{x-37}$ and $Aß_{x-38}$ had very similar reduction pattern for all tested compounds. $Aß_{x-37}$ shows a maximum reduction inferior to 20% in most of the compounds, with a maximum reduction of 40% for BACEi 19. Similarly, $Aß_{x-38}$ shows a maximal reduction inferior to 25% for most compounds, reaching a maximum reduction of 33% for BACEi 22. For $Aß_{x-40}$ maximum reduction is higher than 35% for most compounds, reaching maximal 45% reduction in BACEi 18, and for $Aß_{x-42}$ maximum reduction is usually over 45%, reaching maximal 65% reduction in BACEi 16.

In conclusion, for all the compounds tested there is a dose-dependent effect on all Aß species tested. Importantly, Aß species starting at the 1st or 11th residues of Aß are significantly more reduced by BACE1 inhibition than N-truncated Aß species as measured by 4G8 detection.

Compound toxicity assays demonstrated that none of the compounds is significantly affecting cell viability (difference from baseline inferior to 20%, with the exception of one compound where viability reached 78% of baseline), allowing to conclude that all registered Aß reductions are due to compound activity and not due to compound-induced cellular death.

a

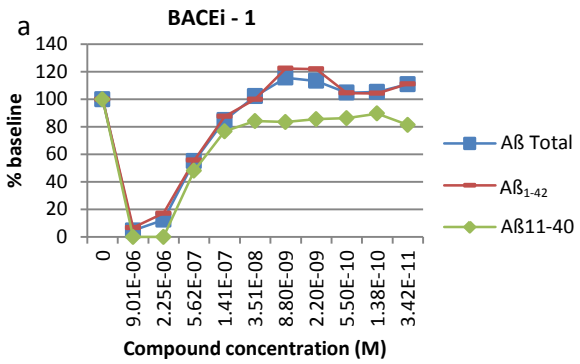
BACEi - 1
% baseline
0
20
40
60
80
100
120
140
0
9.01E-06
2.25E-06
5.62E-07
1.41E-07
3.51E-08
8.80E-09
2.20E-09
5.50E-10
1.38E-10
3.42E-11
Compound concentration (M)
Aß Total
Aß1-42
Aß11-40

b

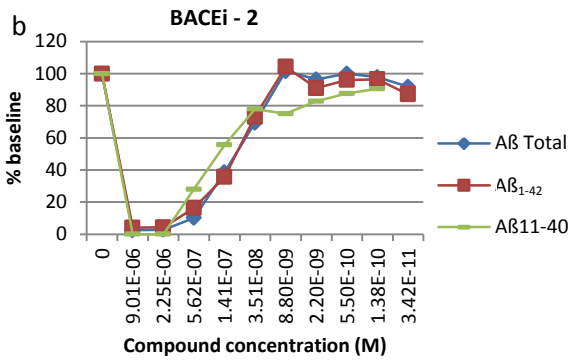
BACEi - 2
% baseline
0
20
40
60
80
100
120
0
9.01E-06
2.25E-06
5.62E-07
1.41E-07
3.51E-08
8.80E-09
2.20E-09
5.50E-10
1.38E-10
3.42E-11
Compound concentration (M)
Aß Total
Aß1-42
Aß11-40

c

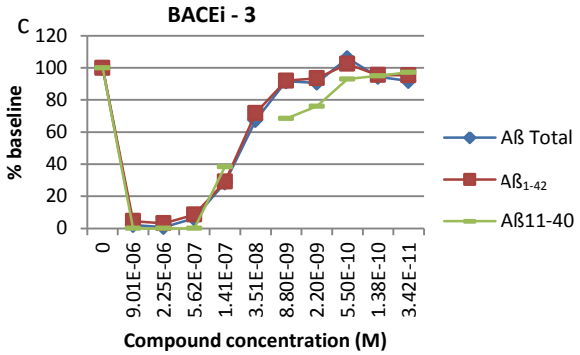
BACEi - 3
% baseline
0
20
40
60
80
100
120
0
9.01E-06
2.25E-06
5.62E-07
1.41E-07
3.51E-08
8.80E-09
2.20E-09
5.50E-10
1.38E-10
3.42E-11
Compound concentration (M)
Aß Total
Aß1-42
Aß11-40

d

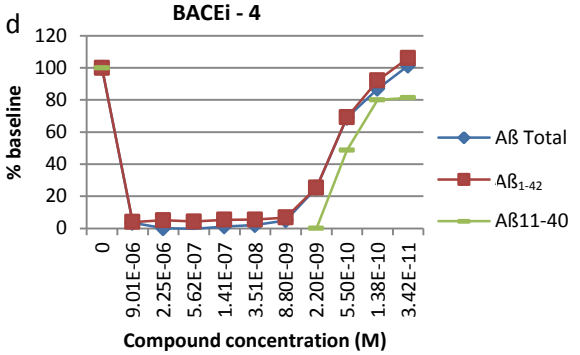
BACEi - 4
% baseline
0
20
40
60
80
100
120
0
9.01E-06
2.25E-06
5.62E-07
1.41E-07
3.51E-08
8.80E-09
2.20E-09
5.50E-10
1.38E-10
3.42E-11
Compound concentration (M)
Aß Total
Aß1-42
Aß11-40

e

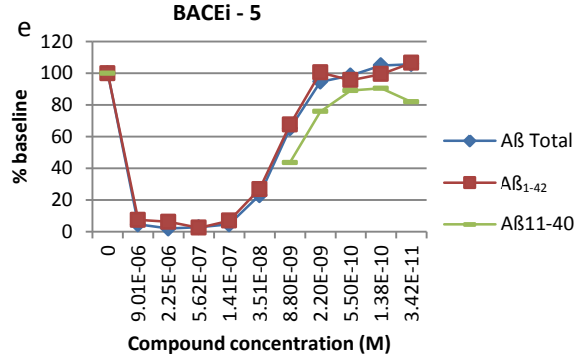
BACEi - 5
% baseline
0
20
40
60
80
100
120
0
9.01E-06
2.25E-06
5.62E-07
1.41E-07
3.51E-08
8.80E-09
2.20E-09
5.50E-10
1.38E-10
3.42E-11
Compound concentration (M)
Aß Total
Aß1-42
Aß11-40

f

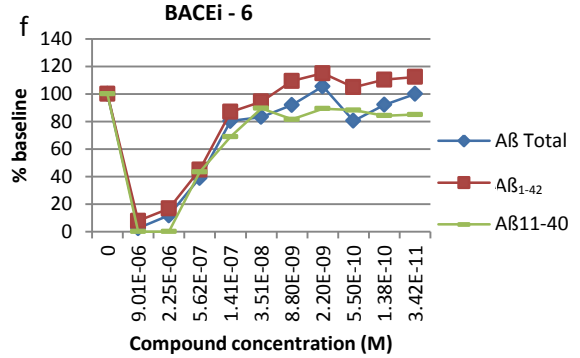
BACEi - 6
% baseline
0
20
40
60
80
100
120
140
0
9.01E-06
2.25E-06
5.62E-07
1.41E-07
3.51E-08
8.80E-09
2.20E-09
5.50E-10
1.38E-10
3.42E-11
Compound concentration (M)
Aß Total
Aß1-42
Aß11-40

g

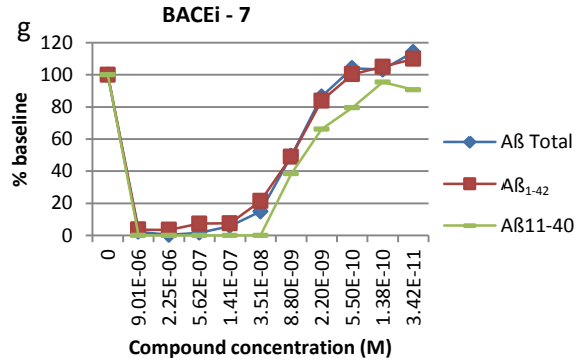
BACEi - 7
% baseline
0
20
40
60
80
100
120
0
9.01E-06
2.25E-06
5.62E-07
1.41E-07
3.51E-08
8.80E-09
2.20E-09
5.50E-10
1.38E-10
3.42E-11
Compound concentration (M)
Aß Total
Aß1-42
Aß11-40

h

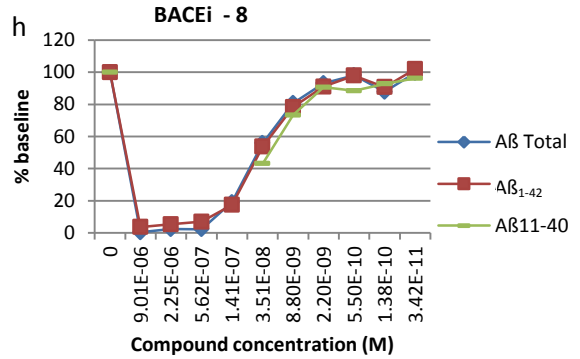
BACEi - 8
% baseline
0
20
40
60
80
100
120
0
9.01E-06
2.25E-06
5.62E-07
1.41E-07
3.51E-08
8.80E-09
2.20E-09
5.50E-10
1.38E-10
3.42E-11
Compound concentration (M)
Aß Total
Aß1-42
Aß11-40

i

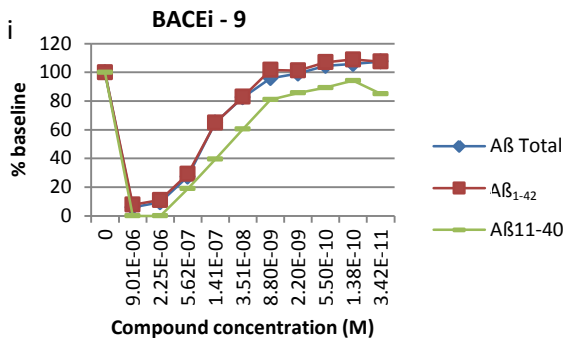
BACEi - 9
% baseline
120
100
80
60
40
20
0
0
9.01E-06
2.25E-06
5.62E-07
1.41E-07
3.51E-08
8.80E-09
2.20E-09
5.50E-10
1.38E-10
3.42E-11
Compound concentration (M)
Aß Total
Aß1-42
Aß11-40

j

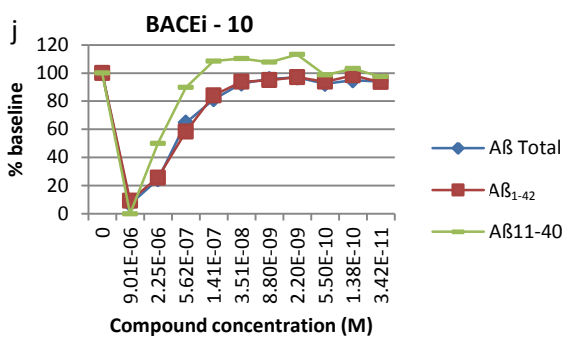
BACEi - 10
% baseline
120
100
80
60
40
20
0
0
9.01E-06
2.25E-06
5.62E-07
1.41E-07
3.51E-08
8.80E-09
2.20E-09
5.50E-10
1.38E-10
3.42E-11
Compound concentration (M)
Aß Total
Aß1-42
Aß11-40

k

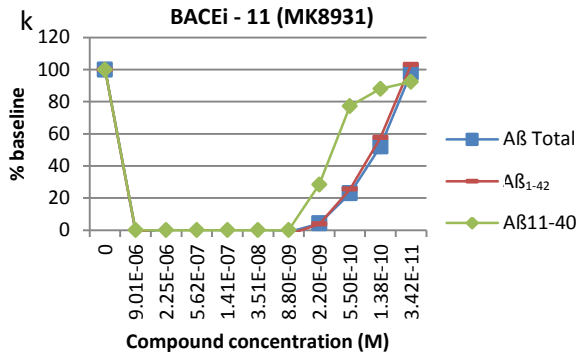
BACEi - 11 (MK8931)
% baseline
120
100
80
60
40
20
0
0
9.01E-06
2.25E-06
5.62E-07
1.41E-07
3.51E-08
8.80E-09
2.20E-09
5.50E-10
1.38E-10
3.42E-11
Compound concentration (M)
Aß Total
Aß1-42
Aß11-40

l

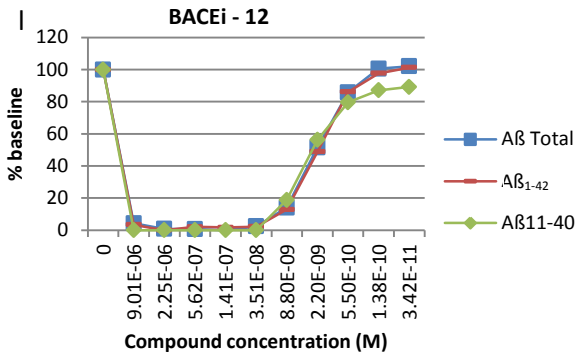
BACEi - 12
% baseline
120
100
80
60
40
20
0
0
9.01E-06
2.25E-06
5.62E-07
1.41E-07
3.51E-08
8.80E-09
2.20E-09
5.50E-10
1.38E-10
3.42E-11
Compound concentration (M)
Aß Total
Aß1-42
Aß11-40

m

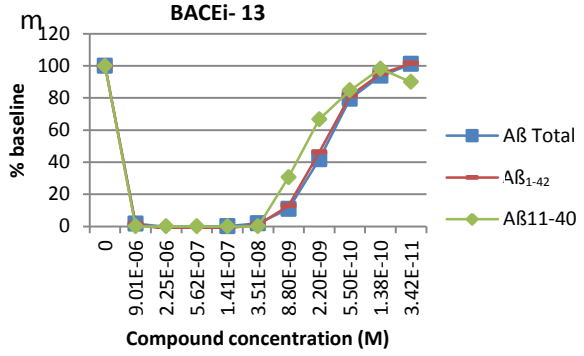
BACEi- 13
% baseline
120
100
80
60
40
20
0
0
9.01E-06
2.25E-06
5.62E-07
1.41E-07
3.51E-08
8.80E-09
2.20E-09
5.50E-10
1.38E-10
3.42E-11
Compound concentration (M)
Aß Total
Aß1-42
Aß11-40

n

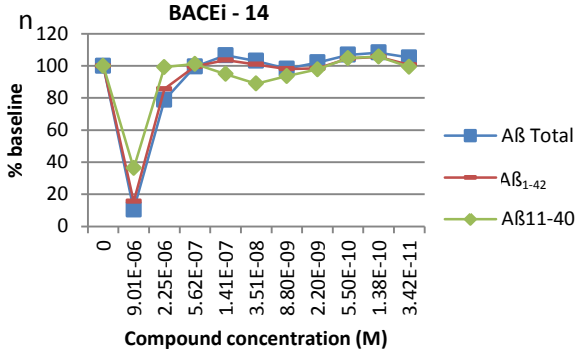
BACEi - 14
% baseline
120
100
80
60
40
20
0
0
9.01E-06
2.25E-06
5.62E-07
1.41E-07
3.51E-08
8.80E-09
2.20E-09
5.50E-10
1.38E-10
3.42E-11
Compound concentration (M)
Aß Total
Aß1-42
Aß11-40

o

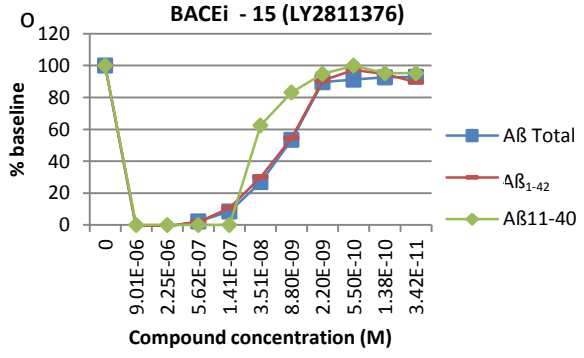
BACEi - 15 (LY2811376)
% baseline
120
100
80
60
40
20
0
0
9.01E-06
2.25E-06
5.62E-07
1.41E-07
3.51E-08
8.80E-09
2.20E-09
5.50E-10
1.38E-10
3.42E-11
Compound concentration (M)
Aß Total
Aß1-42
Aß11-40

p

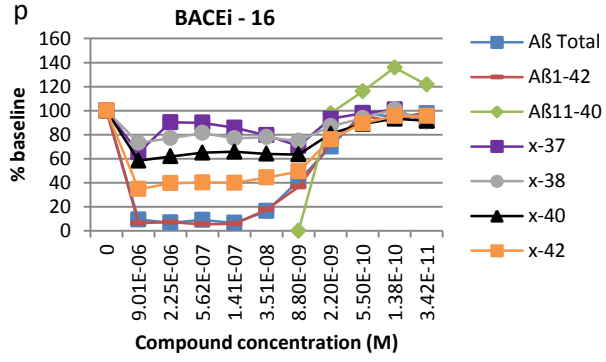
BACEi - 16
% baseline
160
140
120
100
80
60
40
20
0
0
9.01E-06
2.25E-06
5.62E-07
1.41E-07
3.51E-08
8.80E-09
2.20E-09
5.50E-10
1.38E-10
3.42E-11
Compound concentration (M)
Aß Total
Aß1-42
Aß11-40
x-37
x-38
x-40
x-42

q

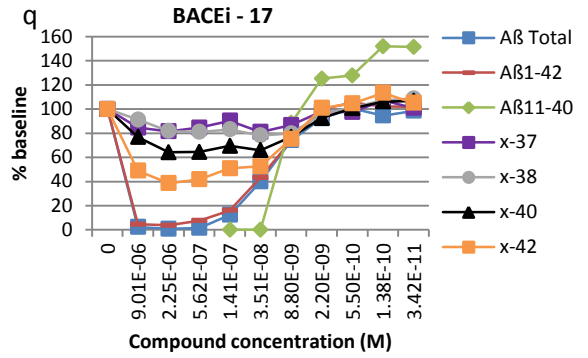
BACEi - 17
% baseline
Compound concentration (M)
Aß Total
Aß1-42
Aß11-40
x-37
x-38
x-40
x-42

r

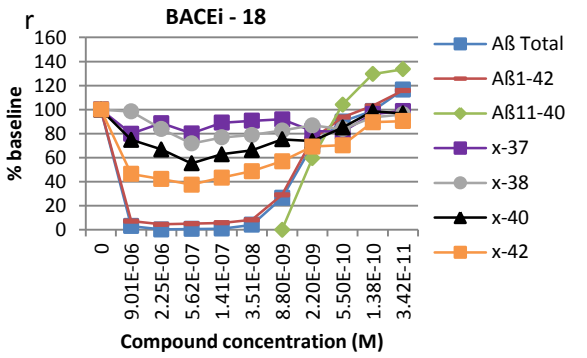
BACEi - 18
% baseline
Compound concentration (M)
Aß Total
Aß1-42
Aß11-40
x-37
x-38
x-40
x-42

s

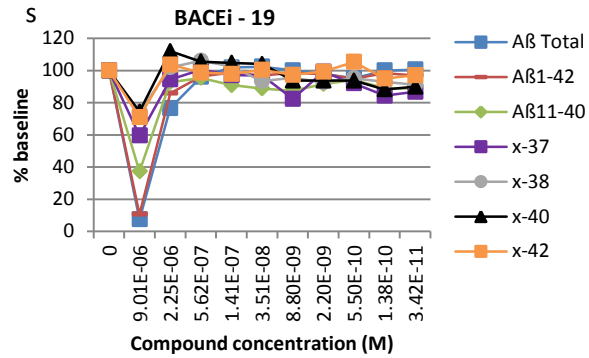
BACEi - 19
% baseline
Compound concentration (M)
Aß Total
Aß1-42
Aß11-40
x-37
x-38
x-40
x-42

t

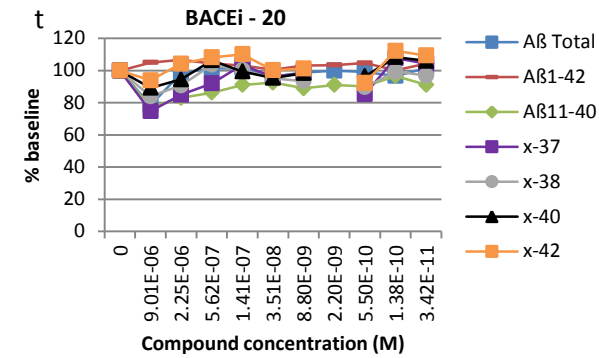
BACEi - 20
% baseline
Compound concentration (M)
Aß Total
Aß1-42
Aß11-40
x-37
x-38
x-40
x-42

u

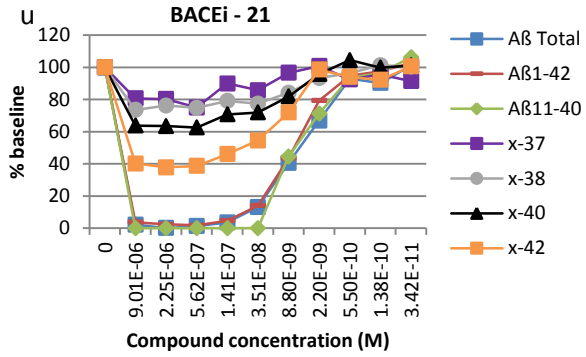
BACEi - 21
% baseline
Compound concentration (M)
Aß Total
Aß1-42
Aß11-40
x-37
x-38
x-40
x-42

v

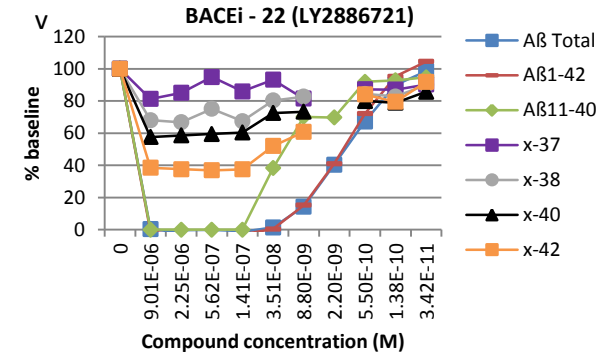
BACEi - 22 (LY2886721)
% baseline
Compound concentration (M)
Aß Total
Aß1-42
Aß11-40
x-37
x-38
x-40
x-42

w

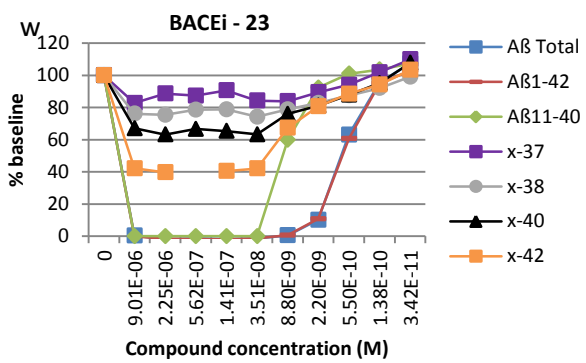
BACEi - 23
% baseline
Compound concentration (M)
Aß Total
Aß1-42
Aß11-40
x-37
x-38
x-40
x-42

x

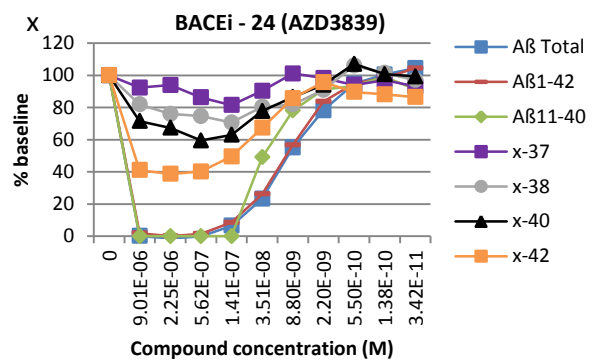
BACEi - 24 (AZD3839)
% baseline
Compound concentration (M)
Aß Total
Aß1-42
Aß11-40
x-37
x-38
x-40
x-42

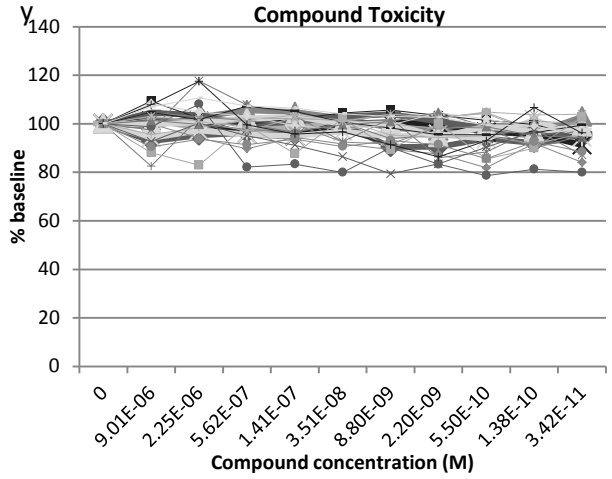

Figure 14 Effect of different BACEi (1 to 24) on Aß total, $Aß_{1-42}$, $Aß_{11-40}$, and for BACEi (16-24) on $Aß_{x-37/38/40/42}$ levels in cell supernatant of human neuroblastoma cells (SK-N-BE(2)), expressing human wild type APP. In all panels "0" in the x-axis corresponds to DMSO-treated cells, and this value was set to 100% baseline value. Cells were treated with different compound doses, and the effects were calculated as %baseline (DMSO-treated cells). Aß total and $Aß_{42}$ were determined by alpha-LISA, using the antibody pairs JRF/hAßN/25-4G8 and JRF/hAßN/25-JRF/cAß42/26, respectively. $Aß_{11-40}$ was determined by ELISA using the antibody pair J&JPRD/hAß11/1-JRF/cAß40/28. $Aß_{x-37/38/40/42}$ was determined by MSD 4-plex using 4G8-SULFO-TAG as detection antibody. The last panel (γ) represents compound toxicity which was determined using the Alamar Blue assay. Aß – amyloid-ß peptide, BACEi – ß-secretase inhibitor.

3 AMYLOID ß MEASUREMENTS IN DOG CSF

In the third part of this project we aimed at evaluating the Aß-reducing effect of different selected compounds in CSF of treated dogs. Using the developed ELISA assay, $Aß_{11-40}$ levels were measured after compound treatment, and further compared with $Aß_{1-37/38/40/42}$, to evaluate if any difference was present regarding the reduction patterns. Two classes of compounds were tested: γ-secretase modulators (GSM F) and BACE1 inhibitors (BACEi 25).

$Aß_{11-40}$ levels were measured by ELISA using J&JPRD/hAß11/1 as capture antibody and JRF/cAß40/28-HRPO as detection antibody. $Aß_{1-37/38/40/42}$ levels were measured by MSD-4Plex using JRF/hAßN/25-SULFO-TAG as detection antibody.

For all the assays, compound effect was measured following the underneath formula:

$$\%\, effect = \frac{Compound\ treated\ sample\ x\ concentration(pg/ml)}{Baseline\ sample\ x\ concentration(pg/ml)} * 100$$

% effect is calculated for each animal, and then averaged per treatment group.

3.1 COMPARISON BETWEEN CSF COLLECTION SITES – CISTERNA MAGNA AND LATERAL VENTRICLE

As observed in previous studies, the CSF collection site in the dog model can highly influence the amount of recovered Aß species. Collection of CSF in the cisterna magna was shown to yield up to two times more Aß as compared to CSF collected from the lateral ventricle (*Figure 15)*.[40]

To evaluate if a similar effect was observed for $A\beta_{11\text{-}40}$ concentrations, a group of 16 dogs was sampled two times to compare possible differences in Aß levels between collection sites. The first time, animals were sample awake in the lateral ventricle, and after a period of at least one week, animals were sampled a second time in cisterna magna under anaesthesia.

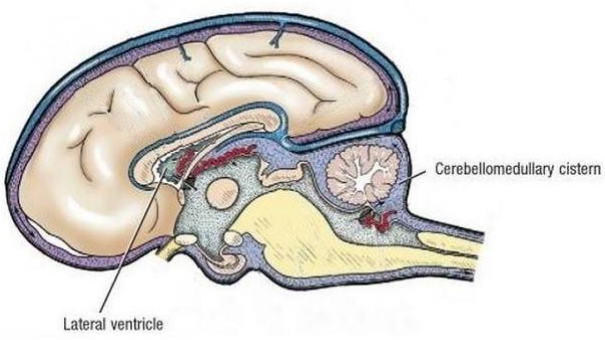

Figure 15 Schematic representation of the anatomy and location of lateral ventricle and cerebellomedullary cistern, also known as cisterna magna in the dog model. (Adapted from Evans HE, de Lahunta A (1974).[318]

Regarding $A\beta_{1\text{-}40}$ levels, 13 of the 16 dogs showed higher levels in cisterna magna than in lateral ventricle, with an average of 1,4 times higher Aß concentrations in cisterna magna *(Figure 16 (a))*, and there was a correlation of r=0.53 between cisterna magna and lateral ventricle. Of notice, $A\beta_{1\text{-}37/38/42}$ showed the same pattern as $A\beta_{1\text{-}40,}$ with higher levels in the cisterna magna then lateral ventricle.

$A\beta_{11\text{-}40}$ levels in lateral ventricle were bellow detection limit in 14 of the 16 samples. In contrast, for cisterna magna signal was detected for all samples with an average of 312pg/ml (SD=84). Therefore, it is clear that $A\beta_{11\text{-}40}$ levels are significantly higher in the cisterna magna then in the lateral ventricle *(Figure 16 (b)).* There was a correlation of r=0.62 between $A\beta_{11\text{-}40}$ and $A\beta_{1\text{-}40}$ levels in the cisterna magna.

The lack of a detectable signal in most of lateral ventricle CSF samples led to the need to select studies including only animals that were sampled from the cisterna magna for further evaluation of $A\beta_{11\text{-}40}$ levels upon compound-treatment.

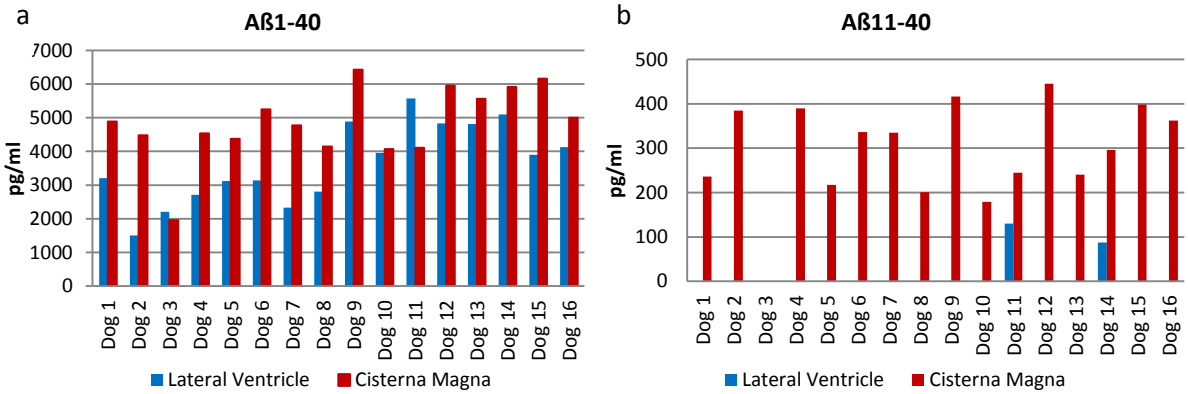

Figure 16 Evaluation of differences in Aß levels between CSF collection at cisterna magna and lateral ventricle. A goup of 16 dogs was sampled from the LV (awake), and after a period of at least 1 week, animals were sampled from the CM (under anesthesia) (a) Evaluation of $A\beta_{1\text{-}40}$ in both collection sites by MSD 4-plex using JRF/hAßN/25 as detection antibody, revealed higher levels of $A\beta_{1\text{-}40}$ in the cisterna magna. (b) Measurement of $A\beta_{11\text{-}40}$ by ELISA, using the antibody pair J&JPRD/hAß11/1 - JRF/cAß40/28-HRPO showed higher levels of $A\beta_{11\text{-}40}$ in the cisterna magna when compared with lateral ventricle. Sample from dog number 3 ($A\beta_{11\text{-}40}$) was excluded due to %CV >20. Aß – amyloid-ß peptide.

3.2 EVALUATION OF GSM Aß-REDUCING EFFECT IN DOG CSF

To evaluate the Aß lowering effect of a GSM compound (GSM F), a study using a group of 24 beagle dogs (12 males and 12 females in total) was performed, having the following subgroups:

- Vehicle group 0mg/kg: 6 beagle dogs (3 females, 3 males), 20% HP-ß-CD;
- Dosing 2.5mg/kg (low dose(L)): 6 beagle dogs (3 females, 3 males);
- Dosing 5mg/kg (medium dose(M)): 6 beagle dogs (3 females, 3 males);
- Dosing 20mg/kg (high dose(H)): 6 beagle dogs (3 females, 3 males).

CSF samples were collected from the cisterna magna after 1 day and after 7 days of repeated dosing. For all groups, samples were collected before dosing (Pre-dose), at day 1 (8h and 25h), and at day 7 (8h and 25h).

GSM F compound was shown to reduce the production of longer Aß species ($Aß_{1-40/42}$) in CSF *(Figure 17)*. For both Aß species a dose-dependent and time-dependent response was observed, with higher reductions at the highest dose (20mg/kg), and after repeated doses (day 7). Comparison of $Aß_{11-40}$, $Aß_{1-40}$ and $Aß_{1-42}$ revealed a similar reduction pattern, although $Aß_{1-42}$ is generally slightly more reduced than $Aß_{1-40}$ and $Aß_{11-40}$.

At day 7 – 8h in the low dose group, $Aß_{1-40}$ and $Aß_{11-40}$ was reduced to 82% and 78%, respectively, while $Aß_{1-42}$ was reduced to 63%. At the same time point, in the medium dose group, reductions to 69, 73 and 59% were observe for $Aß_{1-40}$, $Aß_{11-40}$ and $Aß_{1-42}$, respectively. In the high dose group reductions were very similar between the peptides, $Aß_{1-40}$ reduced to 48%, $Aß_{11-40}$ reduced to 53% and $Aß_{1-42}$ reduced to 56%.

Simultaneously to $Aß_{1-40/42}$ and $Aß_{11-40}$ reduction, shorter Aß species – $Aß_{1-37/38}$ – show a significant increase in their levels, which was most pronounced for $Aß_{1-37}$. Regarding shorter species, $Aß_{1-37}$ increases with an average of 167% and 234% compared to baseline in the low dose and medium dose groups (day 7 – 8h), reaching an increase of over 500% of baseline in the high dose group. $Aß_{1-38}$ shows an increase over 20% only in the highest dose group, increasing with an average of 55% (day 7 – 8h) *(Table 12)*.

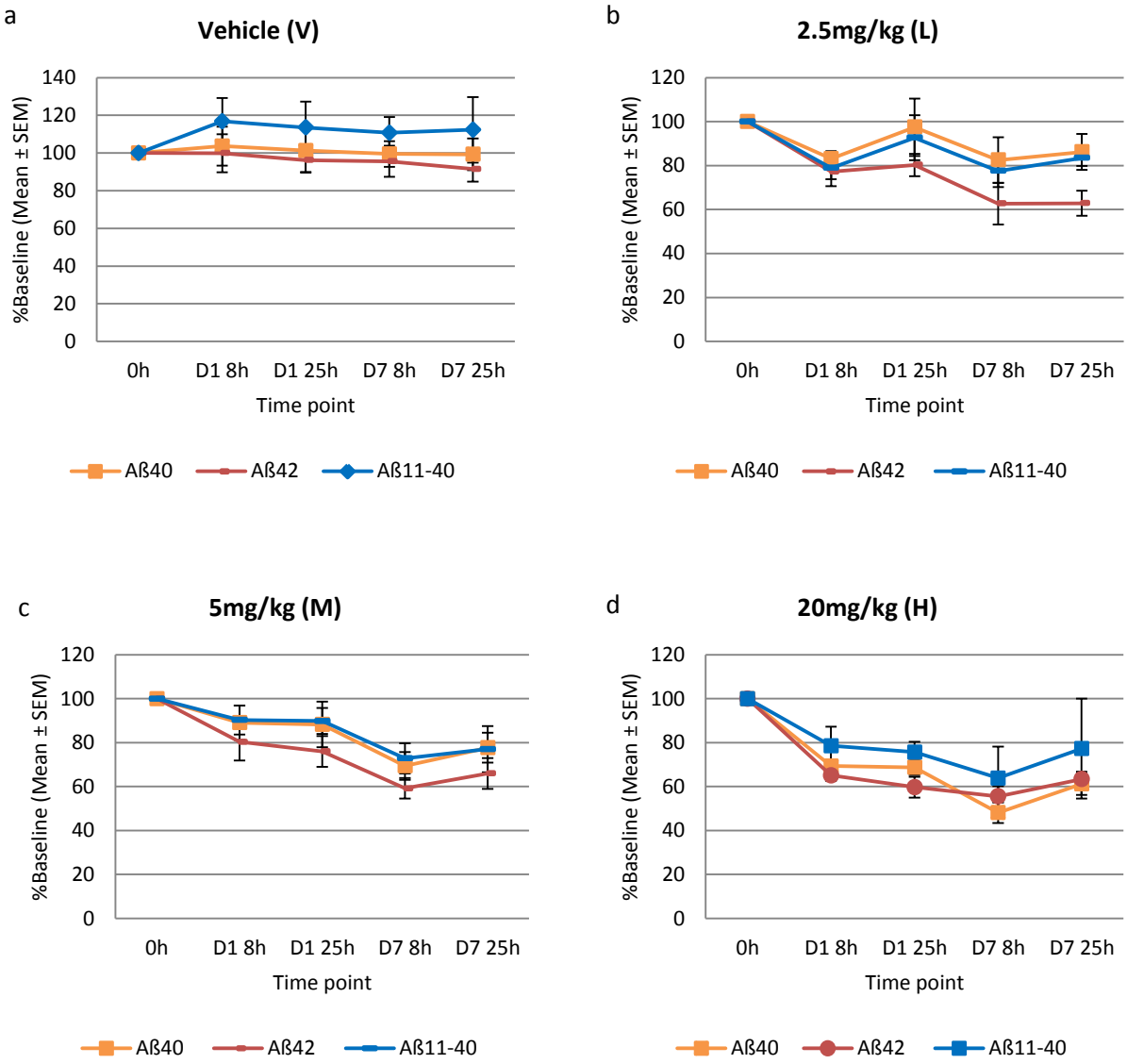

Figure 17 Evaluation of the Aß-reducing effect of GSM F in dog CSF. Each group consisted of 6 dogs (3males and 3 females). Treated groups received a repeated oral dosing throughout 7 days. All animals were sampled from the CM before dosing, at day 1 (8 and 25h), and at day 7 (8 and 25h). In each sample $Aß_{1\text{-}37/38/40/42}$ levels were measured using MSD 4-Plex assay, and $Aß1_{1\text{-}40}$ levels were measured using the developed ELISA assay. (a) Aß levels in vehicle group revealed almost no variation throughout the study. A dose-dependent reduction in Aß levels can be seen by comparison of the low dose group (2.5mg/kg) (b), medium- dose group (5mg/kg) (c) and the high-dose group (20mg/kg) (d). Aß – amyloid-ß peptide.

Table 12 Summary table of mean (and SD) $A\beta_{1-37/38/40/42}$ and $A\beta_{11-40}$ reduction in dog CSF after GSM F dosing, expressed as % of baseline (predose) levels. Each group consisted of 6 dogs (3males and 3 females). Treated groups received a repeated oral dosing throughout 7 days. All animals were sampled from the CM before dosing, at day 1 (8 and 25h), and at day 7 (8 and 25h). In each sample $A\beta_{1-37/38/40/42}$ levels were measured using MSD 4-Plex assay, and $A\beta_{11-40}$ levels were measured using the developed ELISA assay.

	VEHICLE 0 mg/kg									
	Mean					SD				
	$A\beta_{1-37}$	$A\beta_{1-38}$	$A\beta_{1-40}$	$A\beta_{1-42}$	$A\beta_{11-40}$	$A\beta_{1-37}$	$A\beta_{1-38}$	$A\beta_{1-40}$	$A\beta_{1-42}$	$A\beta_{11-40}$
0h (predose)	100	100	100	100	100	0	0	0	0	0
D1 8h	109	108	104	100	117	18	14	21	20	21
D1 25h	105	107	101	96	114	18	18	23	12	27
D7 8h	97	102	100	96	111	15	11	14	16	17
D7 25h	93	101	99	92	112	9	18	17	13	35
	2.5 mg/kg									
	Mean					SD				
	$A\beta_{1-37}$	$A\beta_{1-38}$	$A\beta_{1-40}$	$A\beta_{1-42}$	$A\beta_{11-40}$	$A\beta_{1-37}$	$A\beta_{1-38}$	$A\beta_{1-40}$	$A\beta_{1-42}$	$A\beta_{11-40}$
0h (predose)	100	100	100	100	100	0	0	0	0	0
D1 8h	154	100	83	77	79	19	12	7	13	10
D1 25h	166	106	97	80	93	24	12	26	10	20
D7 8h	267	110	82	63	78	46	15	21	19	15
D7 25h	236	113	86	63	83	49	10	16	11	7
	5 mg/kg									
	Mean					SD				
	$A\beta_{1-37}$	$A\beta_{1-38}$	$A\beta_{1-40}$	$A\beta_{1-42}$	$A\beta_{11-40}$	$A\beta_{1-37}$	$A\beta_{1-38}$	$A\beta_{1-40}$	$A\beta_{1-42}$	$A\beta_{11-40}$
0h (predose)	100	100	100	100	100	0	0	0	0	0
D1 8h	228	116	89	80	90	36	22	16	17	13
D1 25h	204	112	88	76	90	52	12	21	14	12
D7 8h	334	119	69	59	73	56	6	13	9	14
D7 25h	255	120	78	66	77	55	20	14	14	21
	20 mg/kg									
	Mean					SD				
	$A\beta_{1-37}$	$A\beta_{1-38}$	$A\beta_{1-40}$	$A\beta_{1-42}$	$A\beta_{11-40}$	$A\beta_{1-37}$	$A\beta_{1-38}$	$A\beta_{1-40}$	$A\beta_{1-42}$	$A\beta_{11-40}$
0h (predose)	100	100	100	100	100	0	0	0	0	0
D1 8h	373	130	69	65	79	72	20	3	5	17
D1 25h	377	128	69	60	76	54	15	7	10	9
D7 8h	569	155	48	56	53	76	22	9	9	29
D7 25h	655	180	61	63	52	149	38	10	7	45

Aß – amyloid-ß peptide, D – day.

3.3 EVALUATION OF BACEI Aß-REDUCING EFFECT IN DOG CSF

To evaluate the Aß-reducing effect of a BACE1 inhibitor (BACEi 25) in dog CSF, a group of 16 beagle dogs was treated with a single oral dose of the BACEi and then CSF was sampled from the cisterna magna at different time points: pre-dosing (0h; baseline), 8h and 25h.

The animals were distributed into four subgroups, each constituted of 4 dogs (2 males and 2 females):

- Vehicle group 0mg/kg (20% HP-ß-CD);
- Dosing 0.63mg/kg (low dose (L));
- Dosing 2.5 mg/kg (medium dose (M));
- Dosing 10 mg/kg (high dose (H)).

BACEi 25 was able to reduce Aß production *(Figure 18)*. For all the Aß species evaluated – $A\beta_{1-37/38/40/42}$ and $A\beta_{11-40}$ - there was a dose-dependent and time-dependent reduction in the levels,

where the highest Aß reduction was measured in the highest dose group (10mg/kg) and at the 8h time point for all the administered doses.

The vehicle group maintained stable Aß levels throughout the study (variation compared to baseline level inferior to 20%). For dosed groups, $Aß_{1\text{-}37/38/40/42}$ reduction was similar for each dose and time point *(Table 13)*. $Aß_{11\text{-}40}$ showed a slightly higher reduction than Aß1-x species, particularly at the 8h time point. In the low dose group, at the 8h time point, $Aß_{1\text{-}40}$ was reduced 17% and $Aß_{11\text{-}40}$ was reduced 46%. In the medium dose group, at the 8h time point, $Aß_{1\text{-}40}$ was reduced 54% and $Aß_{11\text{-}40}$ was reduced 78%. In the high dose group, at the 8h time point, $Aß_{1\text{-}40}$ was reduced 78% and $Aß_{11\text{-}40}$ was reduced 88%.

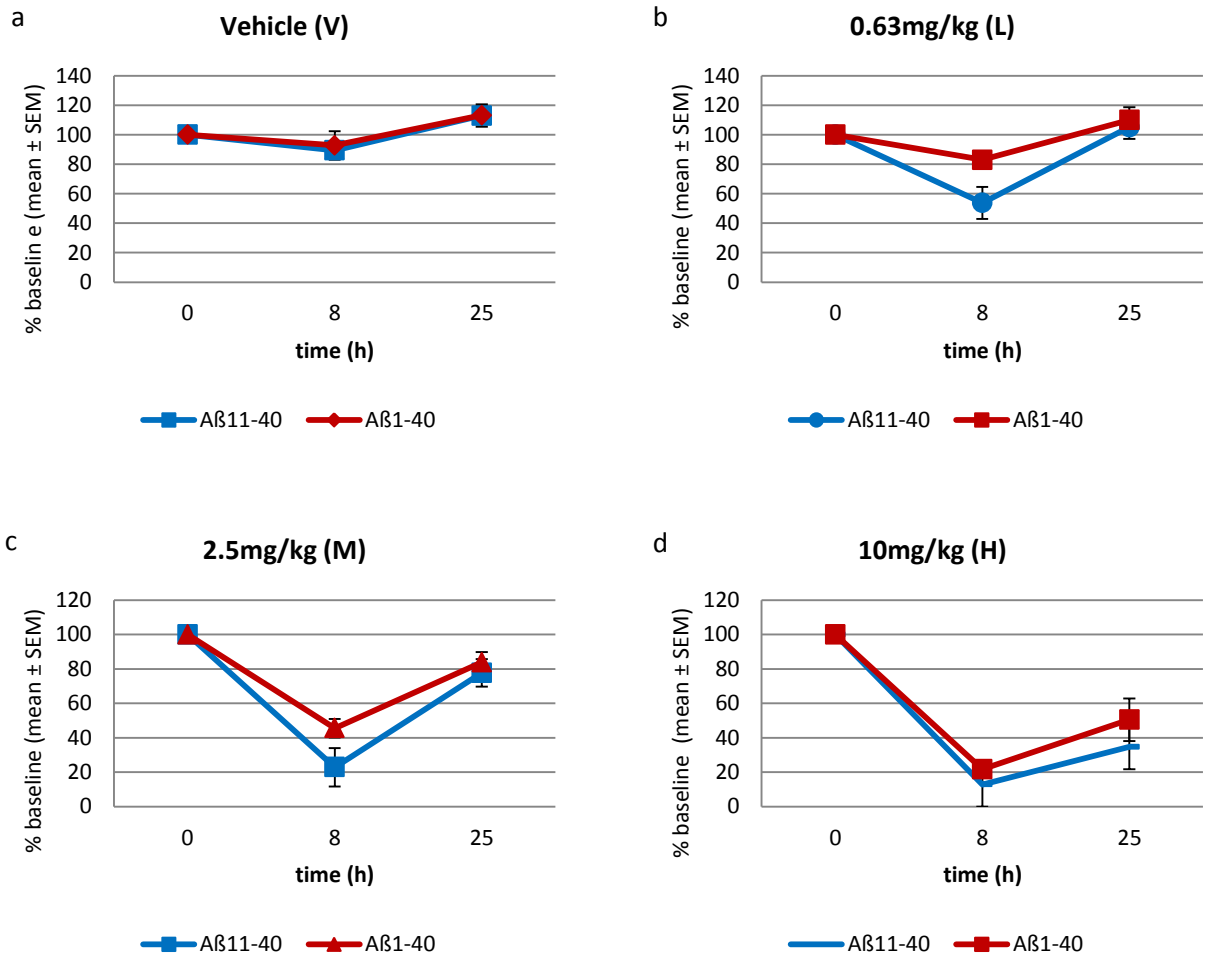

Figure 18 Evaluation of the Aß-reducing effect of BACEi 25 in dog CSF after treatment with single oral dose. Each group consisted of 4 animals (2 males and 2 females). Each animal was sampled from the CM before dosing, and at 8h and 25h after dosing. (a) Aß levels in vehicle group reveal almost no variation throughout the study. A dose-dependent reduction in Aß levels can be seen by comparison of the low dose group (0.63mg/kg) (b), medium-dose group (2.5mg/kg) (c) and the high-dose group (10mg/kg) (d). In each sample $Aß_{1\text{-}37/38/40/42}$ levels were measured using MSD 4-Plex assay, and $Aß_{11\text{-}40}$ levels were measured using the developed ELISA assay. L – low dose, M – medium dose – H – high dose, Aß – amyloid-ß peptide

Table 13 Summary table of mean (and SD) Aß$_{1-37/38/40/42}$ and Aß$_{11-40}$ reduction in dog CSF upon BACEi 25 dosing. Each group consisted of 4 animals (2 males and 2 females). Within each treatment group, animals received a single oral dose of BACEi 25. Each animal was sampled from the CM before dosing, and at 8h and 25h after dosing. In each sample Aß$_{1-37/38/40/42}$ levels were measured using MSD 4-Plex assay, and Aß$_{11-40}$ levels were measured using the developed ELISA assay.

	VEHICLE 0 mg/kg									
	Average % baseline					SD				
	Aß$_{1-37}$	***Aß$_{1-38}$***	***Aß$_{1-40}$***	***Aß$_{1-42}$***	***Aß$_{11-40}$***	***Aß$_{1-37}$***	***Aß$_{1-38}$***	***Aß$_{1-40}$***	***Aß$_{1-42}$***	***Aß$_{11-40}$***
0 h (predose)	100	100	100	100	100	0	0	0	0	0
8 h	92	91	93	92	89	14	14	19	21	11
25 h	119	116	113	117	113	9	12	13	14	15
	0.63 mg/kg									
	Average % baseline					SD				
	Aß$_{1-37}$	***Aß$_{1-38}$***	***Aß$_{1-40}$***	***Aß$_{1-42}$***	***Aß$_{11-40}$***	***Aß$_{1-37}$***	***Aß$_{1-38}$***	***Aß$_{1-40}$***	***Aß$_{1-42}$***	***Aß$_{11-40}$***
0h (predose)	100	100	100	100	100	0	0	0	0	0
8 h	75	81	83	80	54	13	11	12	10	22
25 h	105	108	110	110	105	9	12	17	23	16
	2.5 mg/kg									
	Average % baseline					SD				
	Aß$_{1-37}$	***Aß$_{1-38}$***	***Aß$_{1-40}$***	***Aß$_{1-42}$***	***Aß$_{11-40}$***	***Aß$_{1-37}$***	***Aß$_{1-38}$***	***Aß$_{1-40}$***	***Aß$_{1-42}$***	***Aß$_{11-40}$***
0 h (predose)	100	100	100	100	100	0	0	0	0	0
8 h	39	50	46	44	23	9	13	11	12	22
25 h	84	89	84	84	78	15	16	12	17	16
	10 mg/kg									
	Average % baseline					SD				
	Aß$_{1-37}$	***Aß$_{1-38}$***	***Aß$_{1-40}$***	***Aß$_{1-42}$***	***Aß$_{11-40}$***	***Aß$_{1-37}$***	***Aß$_{1-38}$***	***Aß$_{1-40}$***	***Aß$_{1-42}$***	***Aß$_{11-40}$***
0 h (predose)	100	100	100	100	100	0	0	0	0	0
8 h	23	28	22	27	13	4	5	7	4	26
25 h	61	64	50	58	35	22	20	25	16	26

Aß – amyloid-ß peptide, h – hours.

4 AMYLOID ß MEASUREMENTS IN HUMAN CSF

For the fourth part of this project, analysis of two sets of human CSF samples was performed. The first set of samples was used to evaluate:

- Influence of matrix components on Aß$_{1-42}$ measurements, by comparing crude CSF and HPLC-processed CSF samples;
- Possible differences between assays (MSD 4-plex and Innotest Aß$_{1-42}$) in Aß$_{1-42}$ measurement, and the effect of sample dilution on the detection of the AD CSF biosignature;
- Value of Aß$_{11-40}$ as a possible diagnostic marker for AD.

For the second set of human CSF samples, the Aß-reducing effect of a BACEi (BACEi 26) was evaluated, by measuring Aß$_{1-37/38/40/42}$, Aß$_{11-40}$, and N-truncated Aß$_{x-37/38/40/42}$ species in CSF after 14-day- treatment of healthy elderly subjects.

4.1 EVALUATION OF MATRIX-INTERFERENCE IN Aß MEASUREMENTS AND AD DIAGNOSTIC

Previous studies have shown that $Aß_{1-42}$ peptide levels could be under-estimated due to a fraction of peptide that is in a form that is not soluble or accessible to antibody binding, probably due to its interaction with other matrix components.[282,283] These data suggest that the often measured $Aß_{1-42}$ levels correspond to only a specific pool of the total $Aß_{1-42}$ present in the CSF. Therefore it becomes of interest to study how the different pools of $Aß_{1-42}$ can affect and contribute to the performance of $Aß_{1-42}$ "biosignature" for AD in CSF.

One possible approach into understanding how the different $Aß_{1-42}$ pools contribute to AD's diagnostic is to compare the measured $Aß_{1-42}$ pool to the total $Aß_{1-42}$ peptide levels. To evaluate total $Aß_{1-42}$ levels, the peptide can be extracted using a 6M GuHCL extraction protocol, and then enriched for $Aß_{1-42}$ by RP-HPLC, where only the peptide of interest will remain in the sample to be tested.

Besides comparing Aß levels in crude-unprocessed samples and in HPLC-enriched CSF samples, possible differences between immunoassays (MSD 4-plex and Innotest $Aß_{1-42}$) were also evaluated. Different assays can have different Aß detection capacities, and therefore some assays may detect a higher percentage of the total $Aß_{1-42}$ pool present.

CSF samples were collected from a group of 40 individuals, from which 20 were diagnosed with Alzheimer's disease (AD) and 20 were non-AD patients (NC). This classification was done according to CSF biomarker levels obtained in clinical routine analyses using Innotest ELISAs, and following the criteria in *Table 5.*

Each individual CSF sample was then subdivided into 3 different aliquots, each receiving a different treatment:

- Crude unprocessed CSF sample – containing the neat sample;
- HPLC40-purified sample – sample enriched for $Aß_{1-40}$;
- HPLC42-purified sample – sample enriched for $Aß_{1-42}$.

4.1.1 MSD 4-Plex assay

4.1.1.1 *Dilution Linearity*

Samples were diluted 4 and 8 times to test for dilution linearity of the assay, which is defined as concentration measurements between dilutions having a difference inferior to 20% (80-120% of reference dilution).

The 4-plex assay can detect the four Aß peptides simultaneously, but since there were only HPLC-purified samples for $Aß_{1-40}$ and $Aß_{1-42}$, comparison between crude and HPLC-samples was only done for those two peptides. $Aß_{1-37}$ and $Aß_{1-38}$ measures were further used for comparison with $Aß_{1-40/42}$ levels in crude CSF samples.

Dilution linearity between 1:4 and 1:8 dilution factors was observed in the majority for the samples for all the evaluated peptides – $Aß_{1-37/38/40/42}$ *(Figure 19)*. In crude CSF samples dilution linearity for $Aß_{1-37}$ was present in 36 of the 40 samples; for $Aß_{1-38}$ was present in 34 of the 40 samples; for $Aß_{1-40}$ was present in 39 of the 40 samples; and for $Aß_{1-42}$ was present in 34 of the 40 samples. In HPLC purified samples, dilution linearity was found in 39 of 40 samples for HPLC40, and in 35 of the 40 samples for HPLC42.

Since there is dilution linearity between 1:4 and 1:8 sample dilutions, further analysis of the obtained data will only be described for the 4 times diluted samples

4.1.1.2 *Diagnostic value of individual Aß peptides and peptide ratios*

Comparison of $Aß_{1-40}$ and $Aß_{1-42}$ concentrations measured in crude-unprocessed and HPLC-purified samples did not show any major difference overall *(Figure 20).*

For $Aß_{1-40}$, 8 of the 40 samples had a difference higher than 20% between crude and HPLC samples. For all these samples, variation was inferior to 40%. All samples had a higher value of $Aß_{1-40}$ in crude than in HPLC40. Correlation (calculated as r) between crude and HPLC sample concentrations was 0.97 for AD and 0.93 for NC individuals.

For $Aß_{1-42}$, 11 of the 40 individuals had a difference higher than 20% between crude and HPLC samples. From those 11, 3 had higher concentrations in HPLC-purified CSF, and the remaining 8 had higher concentrations in crude CSF than in HPLC-purified CSF, reaching a maximum of 77% higher concentration in sample 20, and a 107% higher concentration in crude in sample 35. Correlation between crude and HPLC samples was 0.96 for AD and 0.8 for NC individuals.

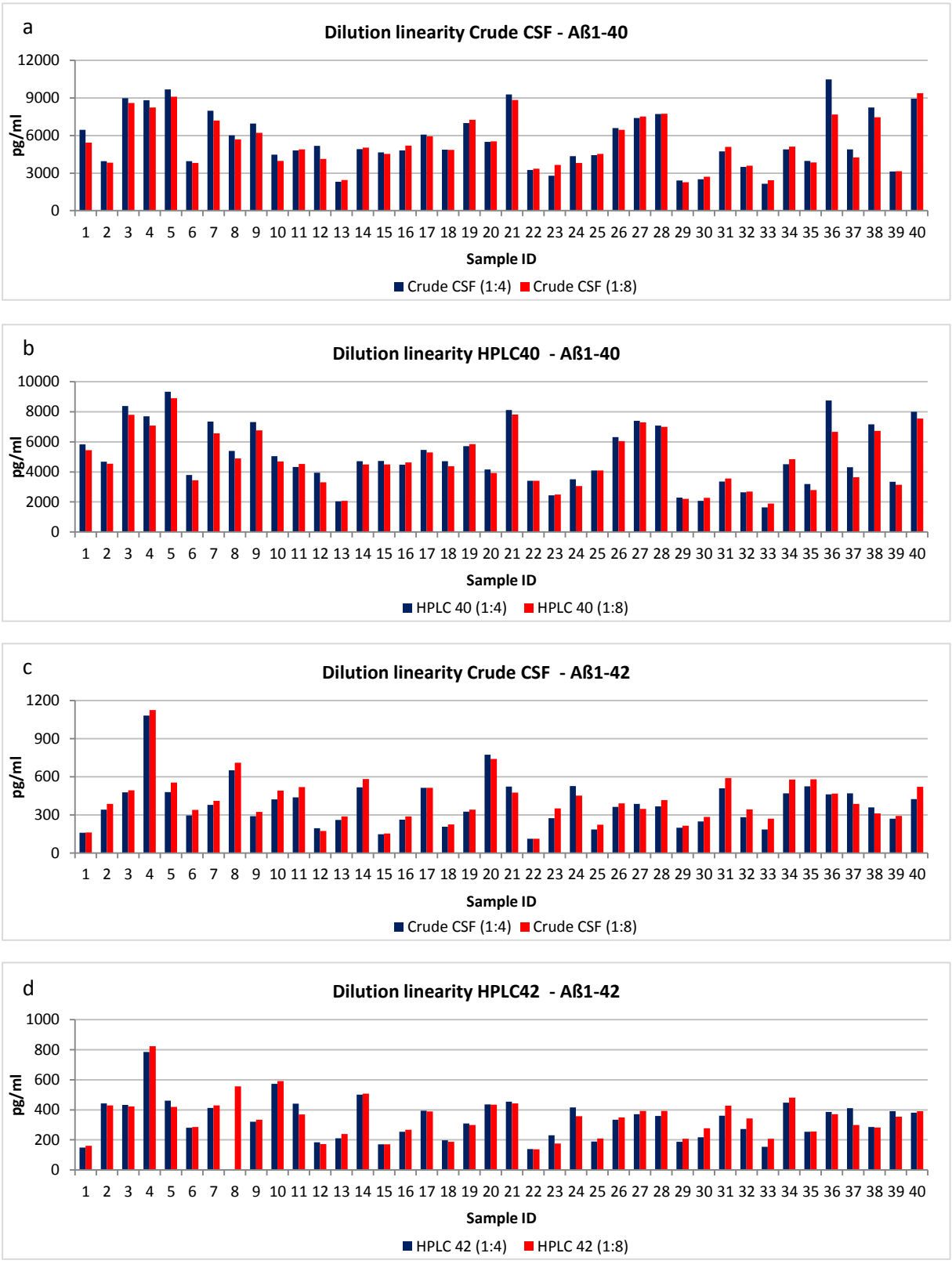

Figure 19 Dilution linearity between sample dilution factors 1:4 and 1:8 in crude-unprocessed and HPLC-purified samples. Dilution linearity was present for all Aß species measured ((a) and (b) - $Aß_{1-40}$; (c) and (d) - $Aß_{1-42}$) and in both types of samples ((a) and (c) – crude CSF; (b) and (d) – HPLC-purified CSF). Levels of $Aß_{1-37/38/40/42}$ were measured with MSD 4-plex using JRF/hAßN/25-SULFO-TAG as detection antibody. Aß – amyloid-ß peptide CSF – cerebrospinal fluid.

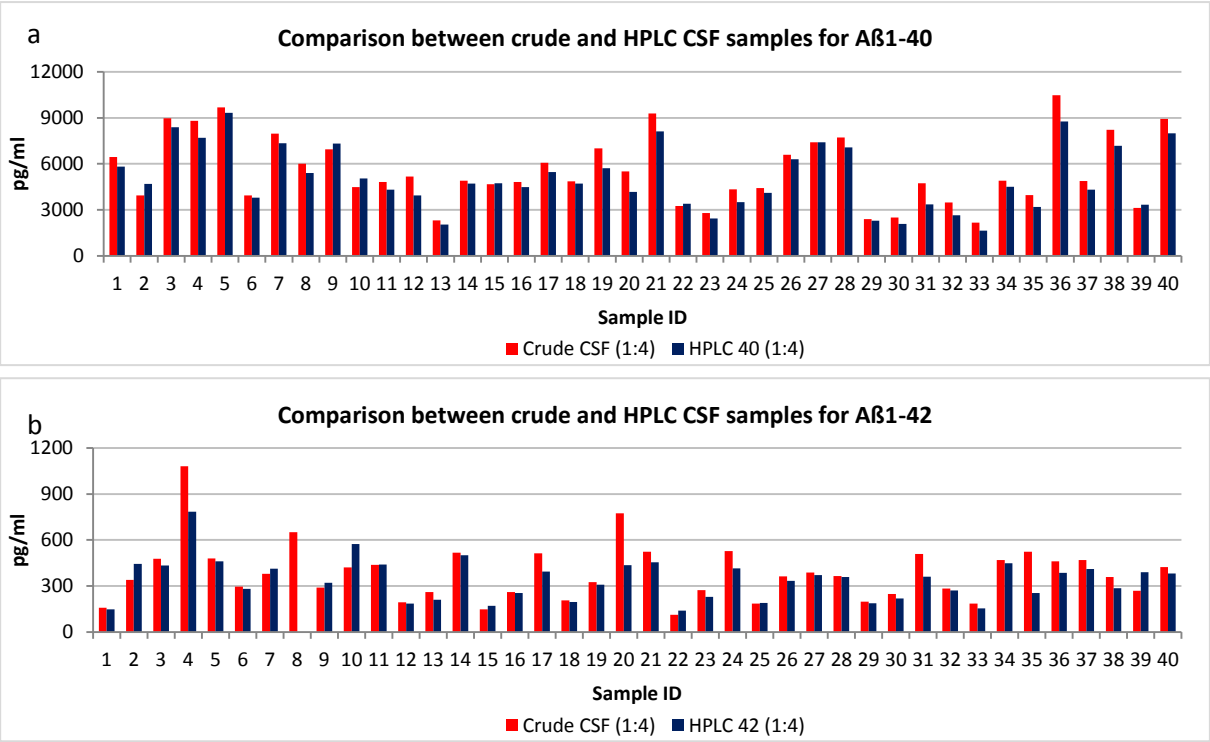

Figure 20 Comparison of $Aß_{1-40}$ and $Aß_{1-42}$ concentrations obtained in crude-unprocessed and HPLC-purified samples. (a) No major difference was observed between crude and HPLC $Aß_{1-40}$ concentrations. (b) Similarly, $Aß_{1-42}$ levels also did not change betwen crude and HPLC-purified for most of the samples. In 3 of the 40 individuals, crude CSF $Aß_{1-42}$ levels were higher than the levels in HPLC samples. Results of sample dilution 1:4 are shown. Aß – amyloid-ß peptide. Levels of $Aß_{1-37/38/40/42}$ were measured with MSD 4-plex using JRF/hAßN/25-SULFO-TAG as detection antibody. CSF – cerebrospinal fluid.

The next step was to evaluate possible differences in the diagnostic value of $Aß_{1-42}$ as well as the $Aß_{1-42}/Aß_{1-40}$ ratio in crude-unprocessed or HPLC-purified samples *(Figure 21)*. While $Aß_{1-42}$ shows no significant difference between AD and NC individuals, $Aß_{1-40}$ levels were significantly higher in AD individuals.

The use of $Aß_{1-42}/Aß_{1-40}$ ratio clearly increases the separation between the two groups, which is complete in HPLC-purified CSF, and is nearly complete in crude CSF. In crude CSF only one AD individual shows a high ratio overlapping with the NC group. $Aß_{1-40}$ levels of this individual (6063.7pg/ml), were in line with $Aß_{1-40}$ levels in AD subjects (mean 6944pg/ml (SD=1992)). $Aß_{1-42}$ levels in this subject (512.63pg/ml) were closer to the mean of NC individuals (mean 436.7pg/ml (SD=217.5)) than AD individuals (mean 330.4pg/ml (SD=129.9)).

To evaluate the diagnostic value, ROC curves were created, plotting the sensitivity (true positive rate) versus (1 – specificity) (false positive rate) of the AD diagnostic *(Figure 22)*. The area under the ROC curve, also known as AUC, was then used to compare the diagnostic value of the peptides, where an AUC=1 corresponds to a 100% sensitive and specific diagnostic.

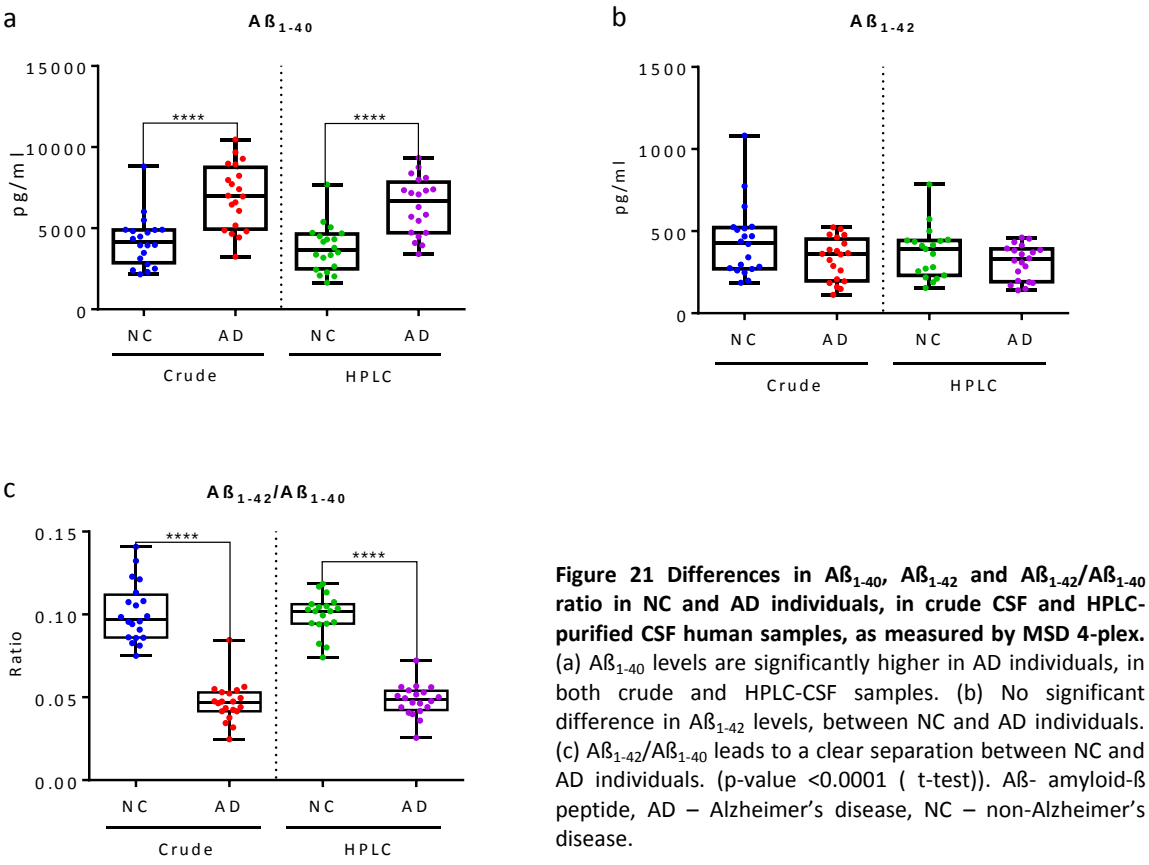

Figure 21 Differences in $Aß_{1-40}$, $Aß_{1-42}$ and $Aß_{1-42}/Aß_{1-40}$ ratio in NC and AD individuals, in crude CSF and HPLC-purified CSF human samples, as measured by MSD 4-plex. (a) $Aß_{1-40}$ levels are significantly higher in AD individuals, in both crude and HPLC-CSF samples. (b) No significant difference in $Aß_{1-42}$ levels, between NC and AD individuals. (c) $Aß_{1-42}/Aß_{1-40}$ leads to a clear separation between NC and AD individuals. (p-value <0.0001 (t-test)). Aß- amyloid-ß peptide, AD – Alzheimer's disease, NC – non-Alzheimer's disease.

ROC curves for $Aß_{1-42}$ alone showed no significant difference between crude and HPLC-purified samples, having an AUC of 0.643 for crude CSF and an AUC of 0.635 for HPLC-purified CSF samples.

The $Aß_{1-42}/Aß_{1-40}$ ratio significantly increased the diagnostic value of the assay, increasing the AUC to 1 in HPLC samples, and to 0.99 in crude samples.

Additionally, the ratios of $Aß_{1-42}$ with $Aß_{1-37}$ and $Aß_{1-38}$ peptides were also calculated in crude CSF samples. In the 4 times diluted samples the $Aß_{1-42}/Aß_{1-37}$ ratio had an AUC of 0.93, and the $Aß_{1-42}/Aß_{1-38}$ ratio, had an AUC of 0.98. Although the obtained AUC wee slightly lower than the ones obtained with the $Aß_{1-42}/Aß_{1-40}$ ratio, reflecting the best separation between the diagnostic groups for the latter ratio, these ratios also confirm an increased diagnostic value of the ratios over the $Aß_{1-42}$ concentration by itself. Individual sample analysis also showed that individuals with higher $Aß_{1-42}/Aß_{1-40}$ ratios also have in general, higher $Aß_{1-42}/Aß_{1-37}$ and $Aß_{1-42}/Aß_{1-38}$ ratios.

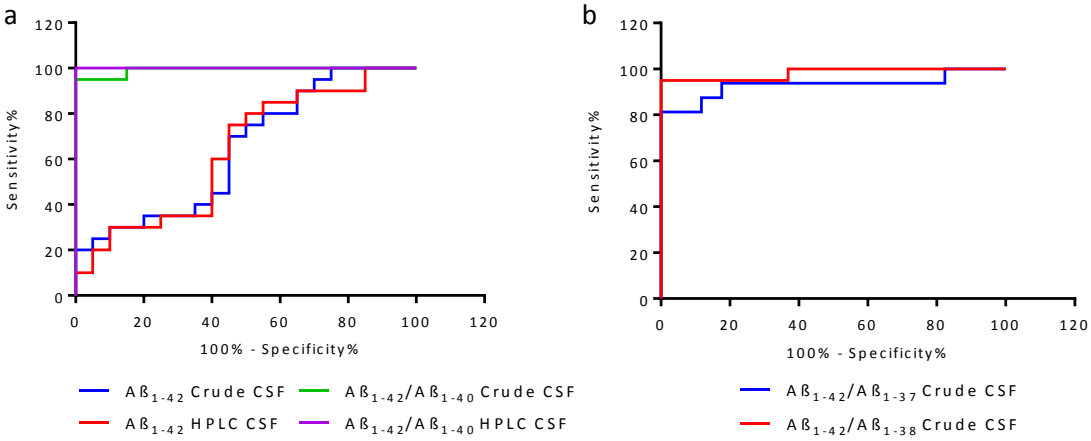

Peptide	Area under the curve (AUC)	Std. Error
Aß1-42 Crude CSF	0.643	0.088
Aß1-42 HPLC CSF	0.635	0.089
Aß1-42/ Aß1-40 Crude CSF	0.993	0.009
Aß1-42/ Aß1-40 HPLC CSF	1.000	0.000
Aß1-42/ Aß1-37 Crude CSF	0.930	0.053
Aß1-42/ Aß1-38 Crude CSF	0.982	0.020

Figure 23 Comparison of crude CSF and HPLC-purified CSF diagnostic value, as measured by MSD 4-plex. (a) Comparison between the use of $Aß_{1-42}$ or $Aß_{1-42}/Aß_{1-40}$ ratio shows that the use of the ratio strongly increases the diagnostic value. (b) Other ratios – $Aß_{1-42}/Aß_{1-37}$ or $Aß_{1-42}/Aß_{1-38}$ - also show a higher diagnostic value than $Aß_{1-42}$ by itself. Aß – amyloid-ß peptide, CSF – cerebrospinal fluid.

4.1.2 ELISA Assays

Levels of $Aß_{1-42}$ and $Aß_{1-40}$ were also measured on the same samples using the Innotest $Aß_{1-42}$ and Invitrogen ELISA Aß40, respectively.

To compare Crude and HPLC CSF samples, levels of $Aß_{1-40}$ were measured on 100 times (final dilution) diluted samples, and $Aß_{1-42}$ were measured on 4 times (final dilution) diluted samples *(Figure 23)*. Comparison between $Aß_{1-40}$ levels in crude-unprocessed and in HPLC-purified samples did not reveal significant differences between them. In 30 of the 40 individuals the difference between crude and HPLC was inferior to 20%, from the remaining 10, 4 had higher concentrations in HPLC and 6 had higher concentrations in crude CSF. For 39 of the 40 samples, variation between crude and HPLC concentrations was < 35%.

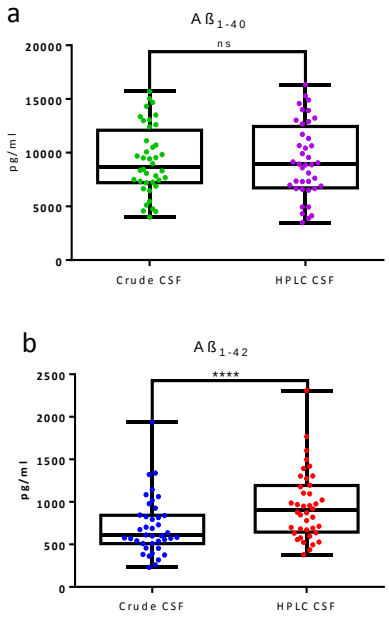

Figure 22 Difference in Aß concentrations in crude-unprocessed CSF samples and HPLC-purified CSF samples as measured by Innotest Aß(1-42) and Invitrogen Aß40. (a) Comparison of $Aß_{1-40}$ levels revealed no significant difference between crude and HPLC CSF samples. (b) Comparison of $Aß_{1-42}$ revealed significantly higher $Aß_{1-42}$ levels in HPLC-samples than in crude CSF samples. (p value <0.0001 (paired t-test). Aß – amyloid-ß peptide.

On the other hand, comparison of $A\beta_{1-42}$ levels in crude CSF and HPLC-purified CSF revealed a significant difference, showing a higher concentration in HPLC samples than in crude CSF samples on a group level. From the 40 individuals analyzed, 14 had a variation < 20%, the remaining 26 individuals had a higher (more than 20% compared to crude) concentration of $A\beta_{1-42}$ in HPLC-purified samples than in crude-unprocessed CSF samples.

Comparison of crude-unprocessed or HPLC-purified samples *(Figure 24)*, showed that $A\beta_{1-42}$ levels were significantly lower in AD individuals, while $A\beta_{1-40}$ levels were significantly higher in AD individuals.

The use of $A\beta_{1-42}/A\beta_{1-40}$ ratio increased the separation between the two groups, which is complete in HPLC-purified CSF, and is nearly complete in crude CSF. In crude CSF only two individuals shows a high ratio overlapping with the AD group. Of notice, the individual showing the higher ratio in MSD 4-plex was not the one showing the higher ratio in the Innotest $A\beta_{1-42}$. These individuals had particularly high $A\beta_{1-42}$ levels (1538.9pg/ml and 1116.9pg/ml) when compared with both the average of NC individuals (mean 865.6pg/ml (SD=406.1)) and the average of AD individuals (mean 629.3pg/ml (SD=305.6)).

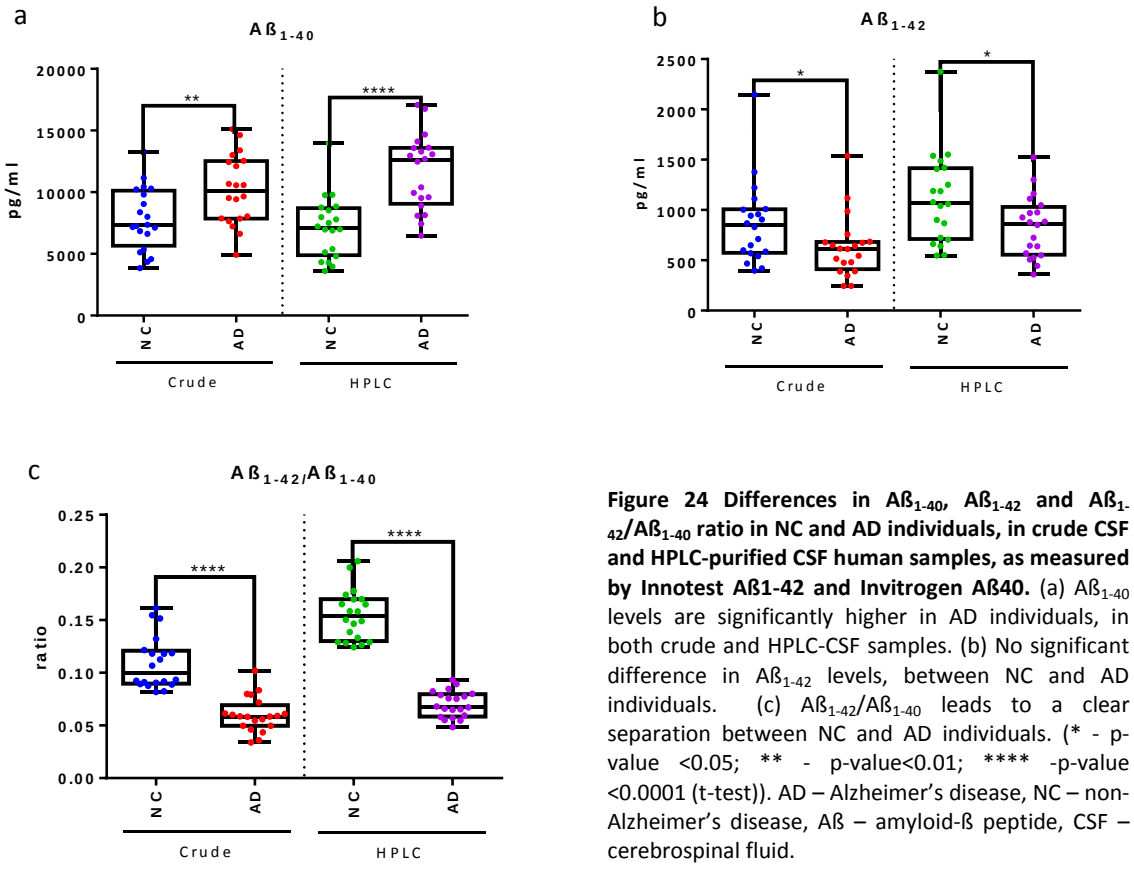

Figure 24 Differences in $A\beta_{1-40}$, $A\beta_{1-42}$ and $A\beta_{1-42}/A\beta_{1-40}$ ratio in NC and AD individuals, in crude CSF and HPLC-purified CSF human samples, as measured by Innotest Aß1-42 and Invitrogen Aß40. (a) $A\beta_{1-40}$ levels are significantly higher in AD individuals, in both crude and HPLC-CSF samples. (b) No significant difference in $A\beta_{1-42}$ levels, between NC and AD individuals. (c) $A\beta_{1-42}/A\beta_{1-40}$ leads to a clear separation between NC and AD individuals. (* - p-value <0.05; ** - p-value<0.01; **** -p-value <0.0001 (t-test)). AD – Alzheimer's disease, NC – non-Alzheimer's disease, Aß – amyloid-ß peptide, CSF – cerebrospinal fluid.

Despite the increase in Aß$_{1-42}$ levels upon HPLC-purification, no significant difference was observed regarding the diagnostic power between crude and HPLC samples *(Figure 25)*. Plotting of the ROC curves and calculation of the respective AUC, showed an AUC of 0.69 for Aß$_{1-42}$ in crude CSF and an AUC of 0.678 in HPLC-purified CSF samples. When the ratio Aß$_{1-42}$/Aß$_{1-40}$ was calculated, the diagnostic power increased to 0.975 in crude CSF samples, and to 1.00 in HPLC-purified CSF samples.

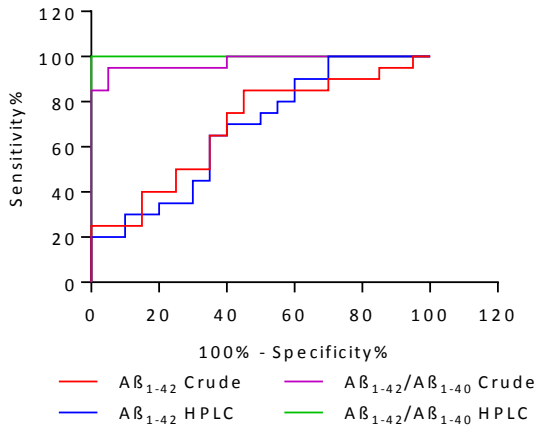

Peptide	Area	Std. Error
Aß1-42 Crude CSF	0.690	0.085
Aß1-42 HPLC CSF	0.678	0.085
Aß1-42/ Aß1-40 Crude CSF	0.975	0.022
Aß1-42/ Aß1-40 HPLC CSF	1.000	0.000

Figure 25 Comparison of crude CSF and HPLC-purified CSF diagnostic value, using Innotest Aß$_{1-42}$ assays and Invitrogen Aß40. The use of Aß$_{1-42}$/ Aß$_{1-40}$ ratio has a higher diagnostic value than Aß$_{1-42}$ by itself. Aß – amyloid-ß peptide, CSF – cerebrospinal fluid.

4.1.2.1 *Effect of the dilution factor on Aß measurements using Innotest Aß$_{1-42}$ assay*

The increase in Aß$_{1-42}$ concentrations in HPLC-purified samples was only registered when using the Innotest Aß$_{1-42}$ assay, and not in the MSD 4-plex assay. Although in both assays final sample dilution was 1:4, in the Innotest Aß$_{1-42}$ samples working dilution was undiluted. To assess if the difference between assays was related with the dilution factor of the samples, a subset of samples was selected and tested undiluted, diluted 4, 8, and 16 times (corresponding to final dilutions of 4, 8, 16 and 32). From the original 40 individual samples, 4 AD samples and 4 NC samples were selected, based on the fact that they demonstrated a clear difference between crude-CSF and HPLC-CSF concentrations of Aß$_{1-42}$ in the previous experiment.

Due to the high dilution factor most of the samples diluted 16 times, and some of the samples diluted 8 times had concentrations below the detection limit of the assay and values were thus excluded from further analysis.

Analysis of the crude CSF samples at different dilutions revealed that there is no dilution linearity between undiluted and further diluted samples, with higher dilutions of the sample resulting in a

higher Aß$_{1-42}$ concentration *(Figure 26)*. In 6 of the 8 samples, dilution of the samples up to 8 times, resulted in an increase over 35% in Aß$_{1-42}$ concentrations compared to undiluted samples.

In HPLC-purified CSF samples, dilution linearity is present for all the samples, showing a difference between concentrations at various dilutions of < 20%, with the exception of sample 1 which as a variation of 30%.

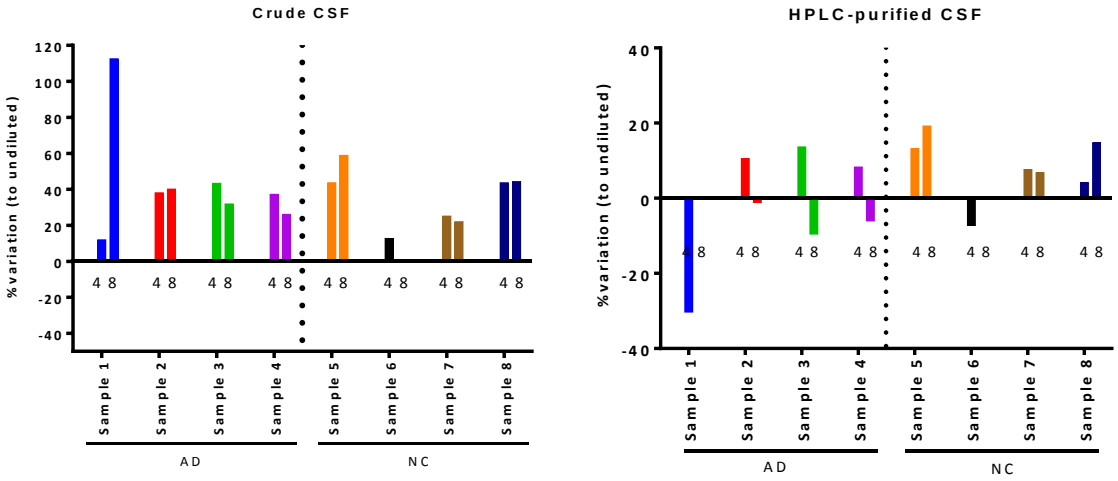

Figure 26 Evaluation of dilution linearity of crude-unprocessed and HPLC-purified CSF samples in the Innotest Aß$_{1-42}$ assay. (a) % variation (100-(diluted/undiluted concentration*100) between undiluted crude CSF samples, and 4 or 8 times diluted samples. An increase in Aß$_{1-42}$ concentrations is seen across dilutions, particularly between the undiluted and the 4 times diluted samples. (b) % variation between undiluted HPLC CSF samples, and 4 or 8 times diluted samples. No significant (i.e. >20%) variation is seen between sample dilutions, except for sample 1. In both (a) and (b) the 16 times dilution was not included, since for most of the samples the values were below the limit of quantification. AD – Alzheimer's disease, NC – non-Alzheimer's disease, Aß – amyloid-ß peptide.

Of note, comparison with the previous results *(Figure 24)* for the undiluted samples showed that the differences between crude and HPLC samples were not completely replicated between the Innotest Aß$_{1-42}$ assays. While for AD samples the increase in Aß$_{1-42}$ in HPLC-purified CSF remained, for NC samples that increase disappeared almost completely, reaching a maximum of 13% for sample 3 (green) *(Figure 27)*.

Further dilution of the samples led to an increase in crude CSF Aß$_{1-42}$ levels in Innotest Aß$_{1-42}$ assay, but no significant change in HPLC CSF concentrations. This alteration led to smaller differences between crude and HPLC CSF upon sample dilution. For most samples, differences between crude and HPLC CSF remained lower than 20% for 1:4 and 1:8 sample dilutions.

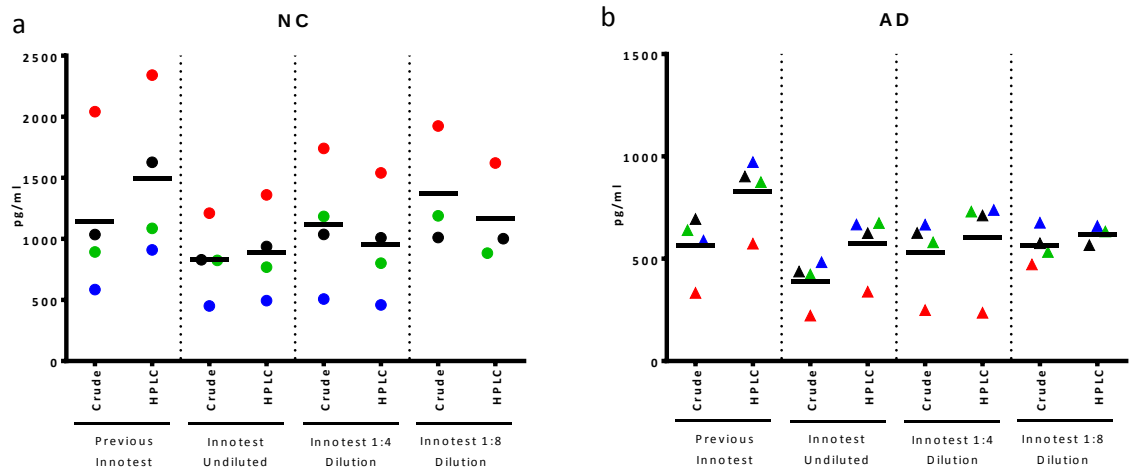

Figure 27 Difference between crude-CSF and HPLC-CSF Aß$_{1-42}$ levels throughout the performed Innotest Aß$_{1-42}$ assays. (a) In NC individuals, the re-evaluation of the same samples undiluted did not fully replicate the increase in HPLC concentrations seen in the previous Innotest Aß$_{1-42}$ (Figure 24). Further sample dilution 4 and 8 times, resulted in the reverse effect, with higher concentrations of Aß$_{1-42}$ in crude CSF than in HPLC- CSF. (b) In AD individuals, the increase in HPLC Aß$_{1-42}$ concentrations was replicated, although the concentrations were lower than in the previous assay (Figure 24). Further dilution of the samples 4 and 8 times resulted in a loss of that difference, due to an increase in crude CSF concentrations. Measures from the same individual are represented by the same color. Aß – amyloid-ß peptide, CSF – cerebrospinal fluid, AD – Alzheimer's disease, NC – non-Alzheimer's disease.

4.1.3 Comparison of MSD 4-Plex and Innotest Aß$_{1-42}$ results

Comparison between the two assays reveals an important difference: while in MSD 4-plex the concentration of Aß$_{1-42}$ remains relatively constant between crude CSF and HPLC-purified CSF, in the Innotest Aß$_{1-42}$ there is an increase in Aß$_{1-42}$ concentrations in HPLC-purified samples. Additionally, the analysis of crude CSF samples by Innotest Aß$_{1-42}$ appears to be highly affected by the dilution factor in which the samples are tested.

Comparing the Aß peptide concentrations, levels of Aß$_{1-40}$ and Aß$_{1-42}$ were in general lower in the MSD 4-plex assay than in the ELISA assays.

For Aß$_{1-40}$, levels between assays shows a good correlation (r) in both crude CSF (0.90 in NC, and 0.96 in AD), and in HPLC CSF (0.91 in NC, and 0.92 in AD). In both assays Aß$_{1-40}$ shows significantly higher levels in AD than in NC individuals. Additionally, no significant difference is seen between crude and HPLC-purified CSF samples, although in the Invitrogen Aß40 assay there is less overlap between NC and AD groups in HPLC-purified CSF *(Figure 28 (a)).*

Regarding Aß$_{1-42}$, there is also a good correlation (r) between assays, although it is slightly lower for AD samples. In crude CSF there was a 0.97 correlation for NC and 0.76 for AD, while in HPLC CSF the correlation was 0.95 for NC and 0.88 in AD samples. Nonetheless, while MSD shows no increase in Aß$_{1-42}$ in HPLC samples, in the Innotest Aß$_{1-42}$ there is a significant increase in HPLC CSF compared to crude CSF concentrations.

Moreover, while in MSD 4-plex assay $Aß_{1-42}$ levels did not differentiate between NC and AD, in the Innotest $Aß_{1-42}$ assay a significant difference ($p<0.05$) was observed, in crude and HPLC CSF *(Figure 28 (b))*.

However, when $Aß_{1-42}/Aß_{1-40}$ ratio is taken into consideration the correlation (r) between assays is highly affected. For crude CSF samples, there is a correlation of 0.82 for NC samples, and a correlation of 0.54 for AD samples. In HPLC-purified CSF samples there is no correlation (r=-0.032) for NC samples, and for AD samples there is a correlation of 0.62. Nonetheless, the use of $Aß_{1-42}/Aß_{1-40}$ ratio increases the separation between NC and AD individuals in both assays. In the MSD 4-plex separation between groups is similar for crude and HPLC-CSF. In the Innotest $Aß_{1-42}$ assay the separation between AD and NC groups in HPLC CSF is higher (no overlap) than in crude CSF *(Figure 28 (c))*.

To compare the differences in $Aß_{1-42}$ concentrations in crude and HPLC CSF, the % difference between HPLC and crude was calculated. Crude $Aß_{1-42}$ concentration was considered baseline, and HPLC CSF concentration was determined as %variation from that baseline (formula below). In this manner a direct comparison between assays can be performed. For this comparison, only the subset of 8 samples *(Figure 27)* was used, so the dilution factor effect in the Innotest $Aß_{1-42}$ assay could also be investigated *(Figure 29)*.

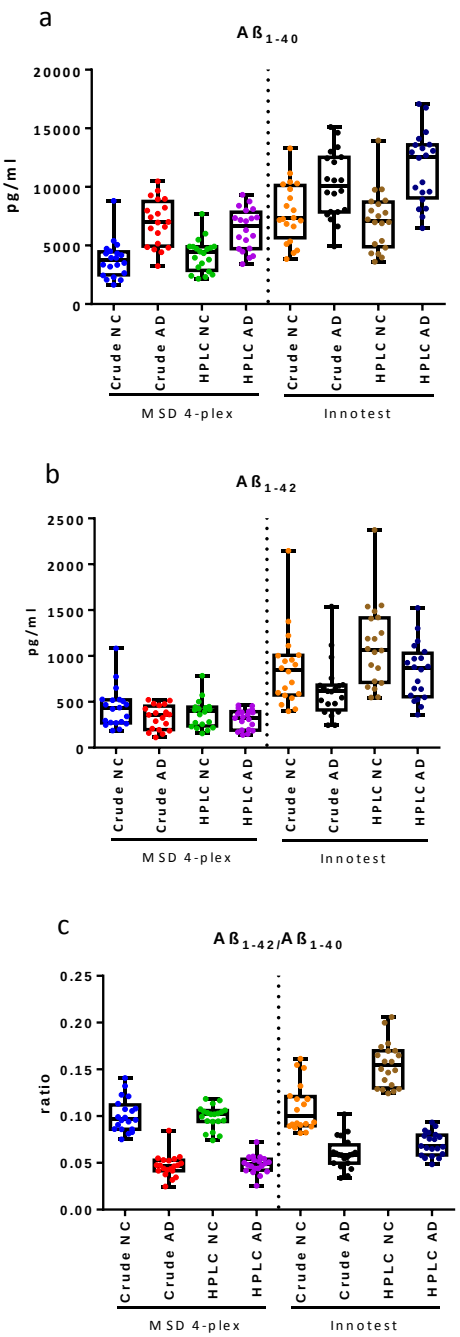

Figure 28 Comparison of $Aß_{1-40}$, $Aß_{1-42}$ and $Aß_{1-42}/Aß_{1-40}$ ratio in MSD 4-plex, Invitrogen Aß40 and Innotest $Aß_{1-42}$ assays. (a) For $Aß_{1-40}$, the higher levels of the peptide in AD samples were replicated in both assays (MSD 4-plex and Invitrogen Aß40). (b) Regarding $Aß_{1-42}$, no significant difference was observed in the MSD 4-plex assay, while for the Innotest $Aß_{1-42}$ assay $Aß_{1-42}$ levels are significantly lower in AD individuals (c) The use of $Aß_{1-42}/Aß_{1-40}$ ratio increases the separation between NC and AD individuals. Aß – amyloid-ß peptide, AD – Alzheimer's disease, NC – non-Alzheimer's disease.

$$\%variation = 100 - \left(\frac{HPLC\ A\beta 1-42\ Concentration\ (pg/ml)}{Crude\ A\beta 1-42\ Concentration\ (pg/ml)}\right) * 100$$

On MSD 4-plex, the 4 AD samples tested had on average 24% more (SD=12.9) $A\beta_{1\text{-}42}$ in crude CSF than in HPLC CSF samples. For the 4 NC samples, on average 10% (SD= 8.6) more $A\beta_{1\text{-}42}$ was also measured in crude versus HPLC CSF.

When tested by the Innotest $A\beta_{1\text{-}42}$ assay, the undiluted samples showed a different pattern. For the first assay, NC samples had on average 37% (SD=22) more $A\beta_{1\text{-}42}$ in HPLC-purified CSF, while AD samples had on average 51% (SD=21) more in HPLC-purified than in crude CSF.

We next compared these results with the data obtained in the second experiment. The same NC samples when re-tested using the Innotest $A\beta_{1\text{-}42}$ assay undiluted, showed a lower increase, with only an average increase of 7% (SD=9) in $A\beta_{1\text{-}42}$ levels in HPLC-purified samples. For AD samples, the increase in HPLC concentrations remained similar to the first experiment, having an average of 48% (SD=9) more $A\beta_{1\text{-}42}$ in HPLC-CSF compared to crude CSF.

Further dilution of the samples led to an increase in crude CSF $A\beta_{1\text{-}42}$ levels in Innotest $A\beta_{1\text{-}42}$ assay, but no significant change in HPLC CSF concentrations. This alteration led to smaller differences between crude and HPLC CSF upon sample dilution. For most samples, differences between crude and HPLC CSF remained lower than 20% for 1/4 and 1/8 sample dilutions.

Despite the differences between crude CSF and HPLC CSF concentrations of $A\beta_{1\text{-}42}$ in MSD 4-plex and Innotest $A\beta_{1\text{-}42}$ assay *(Figure 30)*, in both assays the use of $A\beta_{1\text{-}42}/A\beta_{1\text{-}40}$ ratio increases the diagnostic value when compared with the use of $A\beta_{1\text{-}42}$ by itself. In crude CSF, AUC increased from 0.643 when using $A\beta_{1\text{-}42}$, to 0.993 when using $A\beta_{1\text{-}42}/A\beta_{1\text{-}40}$ ratio in the MSD 4-plex assay. In the Innotest $A\beta_{1\text{-}42}$ assay a similar increase from 0.69 ($A\beta_{1\text{-}42}$) to 0.97 ($A\beta_{1\text{-}42}/A\beta_{1\text{-}40}$) was seen.

In HPLC CSF, AUC increased from 0.635 for $A\beta_{1\text{-}42}$, to 0.95 for $A\beta_{1\text{-}42}/A\beta_{1\text{-}40}$ ratio, in the MSD4-plex assay. Again, the Innotest $A\beta_{1\text{-}42}$ showed a similar increase from 0.7 ($A\beta_{1\text{-}42}$) to 1.0 ($A\beta_{1\text{-}42}/A\beta_{1\text{-}40}$).

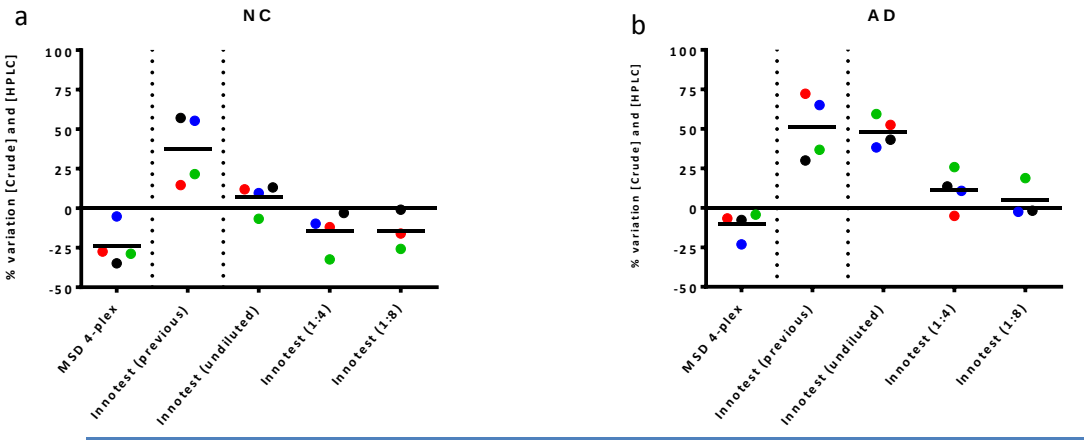

NC

	MSD 4-plex	Innotest (Previous)	Innotest (Undiluted)	Innotest (1:4)	Innotest (1:8)
Sample1	-27%	15%	12%	-12%	-16%
Sample2	-5%	55%	10%	-10%	
Sample3	-35%	57%	13%	-3%	-1%
Sample4	-29%	22%	-7%	-32%	-26%

AD

	MSD 4-plex	Innotest (Previous)	Innotest (Undiluted)	Innotest (1:4)	Innotest (1:8)
Sample5	-7%	72%	53%	-5%	
Sample6	-23%	65%	38%	11%	-2%
Sample7	-8%	30%	43%	13%	-2%
Sample8	-4%	37%	59%	26%	19%

Figure 29 Comparison of % difference (100-([HPLC]/[Crude]*100)) of Aß$_{1-42}$ concentrations between HPLC-purified CSF and crude CSF, measured by MSD-4plex and Innotest Aß$_{1-42}$ assay. For this comparison a subset of 8 samples (4 NC and 4 AD) was selected and their %variation further compared. In both NC (a) and AD (b) groups, the MSD 4plex shows higher levels of Aß$_{1-42}$ in crude than in HPLC CSF. For the Innotest Aß$_{1-42}$ assay, the increase in Aß$_{1-42}$ in HPLC observed in the first assay was only replicated in the AD samples, and in both groups further dilution of the samples leads to a reduction in the %variation between HPLC and crude CSF. AD – Alzheimer's disease, NC – non-Alzheimer's disease. Aß – amyloid-ß peptide.

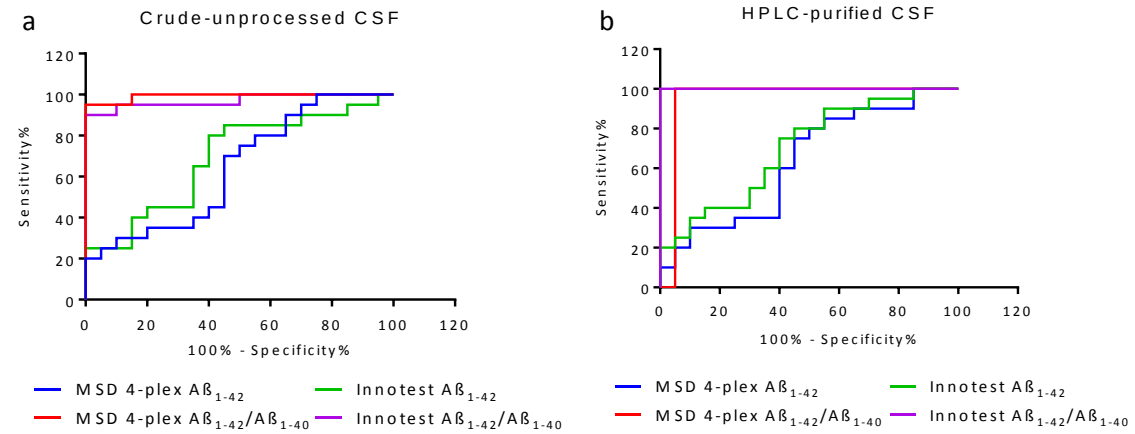

Peptide	Area	Standard Error
Aß1-42 – MSD 4-Plex	0.643	0.088
Aß1-42 – Innotest	0.690	0.085
Aß1-42/Aß1-40 – MSD 4-Plex	0.993	0.009
Aß1-42/Aß1-40 – Innotest	0.970	0.026

Peptide	Area	Standard Error
Aß1-42 – MSD 4-Plex	0.635	0.089
Aß1-42 – Innotest	0.700	0.083
Aß1-42/Aß1-40 – MSD 4-Plex	0.950	0.049
Aß1-42/Aß1-40 – Innotest	1.000	0.000

Figure 30 Evaluation of the diagnostic value of Aß$_{1-42}$ and Aß$_{1-42}$/Aß$_{1-40}$ ratio in crude-CSF and HPLC-purified CSF, as measured by MSD 4-plex and Innotest Aß$_{1-42}$ assay. Results for crude CSF (a) and HPLC CSF (b) did not show a major difference between both sample types, and in both assays the use of the ratio increases the diagnostic value compared to single-peptide measurement. ROC curves correspond to 4 times diluted samples. Aß – Amyloid-ß peptide.

4.1.4 Evaluation of Aß$_{11-40}$ as a diagnostic tool for AD

Additionally, the levels of Aß$_{11-40}$ peptide were measured on the sample set described above.

Due to assay sensitivity, 19 of the 40 samples had levels below the detection limit of the assay.

For the remaining samples, an average of 143.8 pg/ml (SD = 57.76) was detected in AD individuals, and an average of 123.4 pg/ml (SD= 23.23) was detected in NC samples *(Figure 31).*

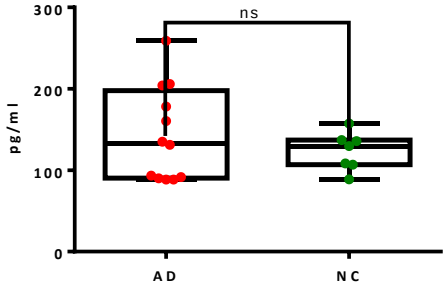

Figure 29 Comparison of Aß$_{11-40}$ levels in AD and NC individuals. No significant difference was observed between the two groups, suggesting a lack of diagnostic value for Aß$_{11-40}$ peptide. ns – non-significant (t-test), Aß – amyloid-ß peptide, AD – Alzheimer's disease, NC – non-Alzheimer's disease.

4.2 EVALUATION OF A BACEI EFFECTS IN HUMAN CSF

In a second set of human CSF samples the Aß-reducing effects of BACEi 26 were evaluated. CSF samples were selected from a double-blind, placebo-controlled, randomized multiple ascending dose study in healthy elderly subjects. Different species of Aß were measured in CSF samples collected at different time points post dosing, followed by a comparison between the reduction profiles of the various species.

CSF samples from subjects from 3 cohorts were analyzed:

- Cohort 1: 6 individuals, dosed with 5mg of BACEi;
- Cohort 2: 5 individuals, dosed with 50mg of BACEi;
- Cohort 3: 6 individuals, dosed with 90mg BACEi.

For each individual subject, 4 time points were evaluated: pre-dose, day 14 at 2h, day 14 at 10h, and day 15 at 24h.

To measure full length Aß species – Aß$_{1-37}$, Aß$_{1-38}$, Aß$_{1-40}$, Aß$_{1-42}$ - the MSD 4-plex assay was employed with JRF/hAßN/25 was used as detection antibody, which recognizes an end-specific epitope in the Aß peptide that is generated after cleavage at residue 1 by BACE1.[289]

For the measurement of Aß$_{11-40}$, the developed ELISA assay was employed, with the J&JPRD/hAß11/1 - JRF/cAß40/28-HRPO antibody pair. J&JPRD/hAß11/1 is also targeted against an end-specific epitope that is generated after cleavage at residue 11 by BACE1.[288]

To measure N-truncated Aß species – $Aß_{x-37}$, $Aß_{x-38}$, $Aß_{x-40}$, $Aß_{x-42}$ - the MSD 4-plex assay was employed using two different detection antibodies: 6E10-SULFO-TAG, which targets the 3rd to 8th residue of the Aß peptide, detecting any species that are truncated before the 3rd residue as well as full-length Aß; 4G8-SULFO-TAG, which targets the 17th to 23rd residue of the Aß peptide, detecting species that are truncated before the 17th residues of the peptide as well as full-length Aß (*Figure 32)*.

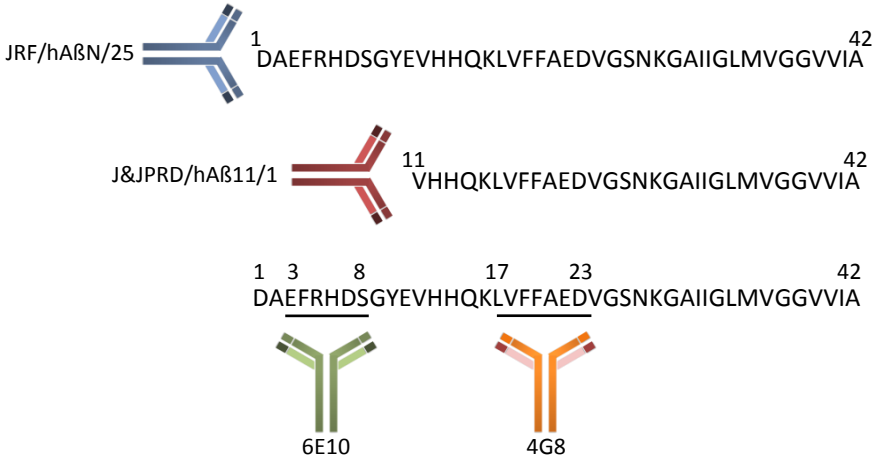

Figure 30 Schematic representation of the detection antibodies used for full length (JRF/hAßN/25) and N-truncated (J&JPRD/hAß11/1, 4G8 and 6E10) Aß measurements, and their respective binding sites on the Aß peptide sequence. Aß – amyloid-ß peptide.

4.2.1 Comparison of BACEi effects on full-length and N-truncated Aß species

A dose-dependent response was observed for all the peptides measured. A significant reduction is already seen at the 5mg dose, increasing further from 5mg to 50 mg and 90mg. All cohorts show a stable reduction pattern after repeated dosing for 14 days.

A similar reduction pattern was seen for all Aß species measured, within each cohort *(Figure 33)*. The $Aß_{11-40}$ showed stronger reduction that the other peptides in the 5 mg cohort, while levels were below detection limit after 50 and 90 mg dosing.

Comparison between the reduction pattern of full length and N-truncated Aß species showed no major differences. Differences between % baseline measures were in general below 5-10% for most assay comparisons. The highest difference was seen for the cohort 1 (5mg), where a maximum reduction to 50% was observed for $Aß_{1-40}$, while for $Aß_{x-40}$ a maximum reduction to 58% of baseline was observed, with 4G8 detection antibody, and to 62% of baseline, with 6E10 detection antibody. This variability is considered to be within the expected limits of inter-assay variability *(Table 14)*.

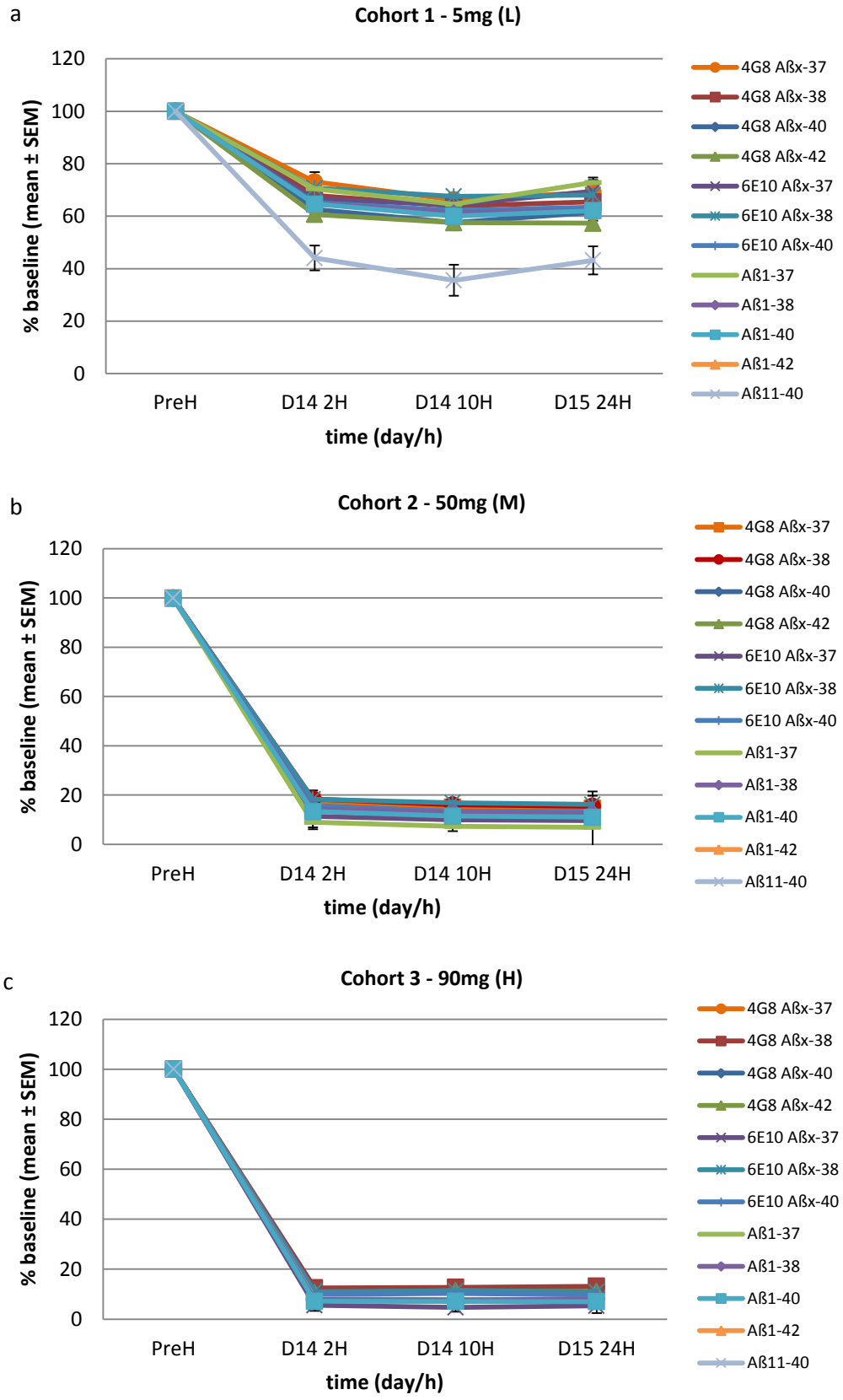

Figure 31 Evaluation of the Aß-reducing effect of BACEi 26 in Human CSF. A dose-dependent reduction in Aß levels can be seen by comparison of the cohort 1 (5mg) (a), cohort 2 (50mg) (b), and cohort 3 (90mg) (c). For N-truncated measurements using 6E10 detection antibody, the $Aß_{x-42}$ results were rejected due to rejected standard curve, and therefore cannot be compared with the other species. $Aß_{11-40}$ levels in Cohort 2 and 3 were below detection limit and therefore are not represented in the graph. Aß – amyloid-ß peptide. L – low dose, M – medium dose, H – high dose.

Table 14 Summary table of mean (and SD) Aß$_{1-37/38/40/42}$, Aß$_{x-37/38/40/42}$ and Aß$_{11-40}$ reduction in Human CSF upon BACEi 26 dosing (5mg, 50mg, and 90mg). Aß$_{x-42}$ levels measured by 6E10 detection antibody, were excluded due to rejection of standard curve, and therefore cannot be compared with the other species. Aß$_{11-40}$ levels in Cohort 2 and 3 were below detection limit and therefore were also excluded.

	5mg (L)												
	4G8				**6E10**				**JRF/hAßN/25**				**J&JPRD/hAß1 1/1**
	Aßx-37	Aßx-38	Aß$_{x-40}$	Aß$_{x-42}$	Aßx-37	Aßx-38	Aß$_{x-40}$	Aß$_{x-42}$	Aß$_{1-37}$	Aß$_{1-38}$	Aß$_{1-40}$	Aß$_{1-42}$	Aß$_{11-40}$
PreH	100	100	100	100	100	100	100	-	100	100	100	100	100
D14 2H	73	68	63	61	67	71	65	-	75	64	63	65	44
D14 10H	66	64	58	58	64	68	62	-	58	60	50	56	36
D15 24H	69	65	61	57	70	68	63	-	55	60	50	50	43
	50mg (M)												
	4G8				**6E10**				**JRF/hAßN/25**				**J&JPRD/hAß1 1/1**
	Aßx-37	Aßx-38	Aß$_{x-40}$	Aß$_{x-42}$	Aßx-37	Aßx-38	Aß$_{x-40}$	Aß$_{x-42}$	Aß$_{1-37}$	Aß$_{1-38}$	Aß$_{1-40}$	Aß$_{1-42}$	Aß$_{11-40}$
PreH	100	100	100	100	100	100	100	-	100	100	100	100	100
D14 2H	17	18	16	16	11	18	15	-	3	-	9	17	-
D14 10H	15	16	13	13	10	17	13	-	6	10	10	18	-
D15 24H	15	15	13	12	10	16	13	-	5	9	10	20	-
	90mg (H)												
	4G8				**6E10**				**JRF/hAßN/25**				**J&JPRD/hAß1 1/1**
	Aßx-37	Aßx-38	Aß$_{x-40}$	Aß$_{x-42}$	Aßx-37	Aßx-38	Aß$_{x-40}$	Aß$_{x-42}$	Aß$_{1-37}$	Aß$_{1-38}$	Aß$_{1-40}$	Aß$_{1-42}$	Aß$_{11-40}$
PreH	100	100	100	100	100	100	100	-	100	100	100	100	100
D14 2H	12	12	11	11	6	11	10	-	9	8	8	9	-
D14 10H	12	13	10	11	5	11	10	-	8	7	7	9	-
D15 24H	13	13	10	11	5	11	10	-	8	5	7	8	-

Aß – amyloid-ß peptide. L – low dose, M – medium dose, H – high dose.

5 COMPARISON OF BACEI EFFECT ON FULL-LENGTH AND N-TRUNCATED Aß SPECIES IN CELL SUPERNATANT AND HUMAN CSF

Comparison of BACEi Aß-reducing effect registered in cell supernatant (*Figure 14* (BACEi 16 to 24)) and in human CSF (*Figure 33*), showed a clear difference in the reduction levels of full-length and n-truncated species between the models.

In cell supernatant N-truncated species levels (Aß$_{x-37/38/40/42}$), were less reduced than full-length Aß. Additionally there also appears to be a size- dependent effect with regard to the N-truncated species, where inhibition is stronger for the longer Aß species: Aß$_{x-42}$ > Aß$_{x-40}$ > Aß$_{x-38}$ > Aß$_{x-37}$.

On the other hand, in human CSF the BACEi resulted in very similar reductions for full-length and N-truncated Aß species, with no significant difference between the different C-terminal truncated species ($Aß_{x-37/38/40/42}$).

To assess if this difference was related with different full-length/N-truncated levels in the two models, comparison of Aß levels detected by the different antibodies - JRF/hAßN/25 (Aß1-x), 6E10 (N-truncated up to 3rd residue), and 4G8 (N-truncated up to 17th residue) - was done. Aß total was defined as 4G8 detected levels, as this antibody was capable of detecting a larger pool of Aß species.

$$\%\ Aß\ detected = \frac{Aß\ levels\ detected\ by\ antibody}{Aß\ Total\ levels} * 100$$

In cell supernatant, Aß levels detected by 4G8 were higher than Aß levels measured by 6E10 or JRF/hAßN/25 for all the species measured, with no significant difference between $Aß_{x-37/38/40/42}$. For all species JRF/hAßN/25 and 6E10 measurements account for 30% (±5%) of the total Aß pool. In human CSF, similar levels of $Aß_{1-37/38/40}$ and $Aß_{x-37/38/40}$ were detected by all antibodies (*Figure 34)*.

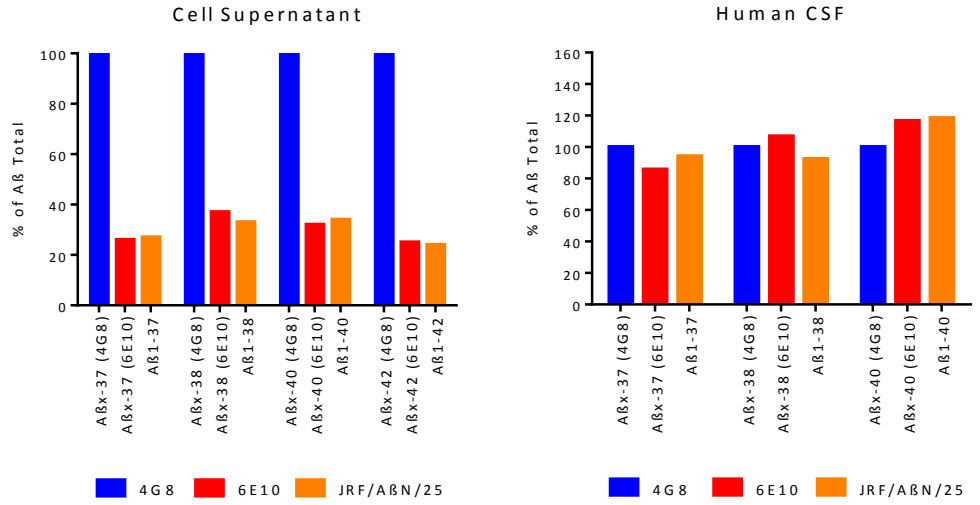

Cell supernatant	4G8				6E10				JRF/AßN/25			
	Aßx-37	Aßx-38	Aßx-40	Aßx-42	Aßx-37	Aßx-38	Aßx-40	Aßx-42	Aß1-37	Aß1-38	Aß1-40	Aß1-42
Average	100	100	100	100	26	37	32	25	27	33	34	24

Human CSF	4G8				6E10				JRF/AßN/25			
	Aßx-37	Aßx-38	Aßx-40	Aßx-42	Aßx-37	Aßx-38	Aßx-40	Aßx-42	Aß1-37	Aß1-38	Aß1-40	Aß1-42
Average	100	100	100	100	86	107	117	-	94	92	118	-
SD	0	0	0	0	8	8	13	-	10	5	16	-

Figure 32 Comparison of Aß levels detected by JRF/AßN/25, 4G8, and 6E10 in cell supernatant and in Human CSF. All Aß measurements were performed on MSD 4-plex. Cell supernatant was collected from DMSO-treated SK-N-BE(2) cells. Human CSF levels were calculated as an average from 17 healthy individuals. Aß total (100%) levels were defined as 4G8 measurements, as this antibody was able to detect a larger Aß pool. % of Aß total was calculated as (Aßx level measured by antibody/ Aß total (4G8)*100). (-) $Aß_{x-42}$ levels as measured by 6E10 and JRF/AßN/25 were not considered due to exclusion of the standard curve. Aß – amyloid-ß peptide, CSF – cerebrospinal fluid.

Chapter V. Discussion

Development of a sensitive immunoassay for Aß$_{11-x}$ measurement for application in in vitro and in vivo models.

Changes in CSF Aß have been recognized as being reflective of the changes in brain Aß upon a therapeutic treatment.[290] Besides the classically investigated Aß$_{1-40}$ and Aß$_{1-42}$ species, several other Aß species, such as N-terminally and C-terminally truncated Aß species, have been identified in human CSF, and are being investigated as possible biomarkers of compound target engagement and to monitor secondary outcomes of compound treatment.[46,47,244]

One N-terminally truncated Aß species of interest is Aß$_{11-x}$, which is generated through the cleavage of BACE1 at the ß' site of APP instead of the ß site, which generates full-length Aß (Aß$_{1-x}$). Upon BACE1 inhibition it is assumed that both Aß$_{1-x}$ and Aß$_{11-x}$ are affected by BACE1 inhibitors. However, kinetic data indicate that BACE1 has a higher enzymatic efficiency for the ß-site than for the ß'-site[291], suggesting that a BACE1 inhibitor might have different effects on the two sites depending on the concentrations used. Therefore studies are warranted to evaluate BACE1 inhibitor effects on the Aß$_{11-x}$ as well as the effects on the Aß $_{1-x}$ peptide levels.[68]

Availability of a J&J proprietary antibody that is able to specifically detect Aß$_{11-x}$ (i.e. J&JPRD/hAß11/1) allowed the development of an assay for the measurement of this species.[288] The assay was developed with the goal to obtain a maximum sensitivity and accuracy in measurements in various sample types. Testing of different platforms, assays and conditions, resulted in the selection of a sandwich ELISA assay using the J&JPRD/hAß11/1 antibody as the capture antibody and JRF/cAß40/48 or JRF/cAß42/26 as detection antibodies for Aß$_{11-40}$ or Aß$_{11-42}$, respectively. The use of an ultra-sensitive TMB substrate added to the assay sensitivity and resulted in a limit of detection of 6.86pg/ml for Aß$_{11-40}$ and 15.63pg/ml for Aß$_{11-42}$.

Aß$_{11-x}$ is reduced in parallel with Aß$_{1-x}$ upon GSI, GSM and BACEi treatment in various model systems

Levels of Aß$_{11-x}$ were measured in cell supernatant, dog and human CSF after treatment with a variety of compounds, and results were further compared with reductions of Aß$_{1-x}$ levels caused by treatment with the same compounds.

Of notice, Aß$_{11-42}$ was only detectable in cell supernatant, but due to assay sensitivity only reductions up to 50% were able to be detected, while for Aß$_{11-40}$ an average reduction of 15% of baseline was detectable by the assay.

A human neuroblastoma cell line (SK-N-BE(2)) expressing human wild-type APP695 was used to investigate the effect of various γ-secretase inhibitors (GSI), γ-secretase modulators (GSM) and BACE1 inhibitors (BACEi).

GSIs inhibit γ-secretase activity thus blocking APP proteolytic processing at the Aß C-terminus, and are expected to reduce the production of several Aß species. However, due to their role in processing multiple substrates, including Notch, GSIs have been found to be associated with the development of severe adverse effects.[206,207] GSMs on the other hand, selectively block the production of longer Aß forms, such as $Aß_{1-42}$, without affecting the cleavage of other substrates, including Notch. In general, this type of compounds do not change total Aß levels, as shorter isoforms like $Aß_{37}$ and $Aß_{38}$ are upregulated simultaneously with downregulation of longer species.[209] BACE1 is the enzyme responsible for the first and rate-limiting APP cleavage of the amyloidogenic pathway. BACEi block BACE1 activity, preventing APP proteolytic processing, and generation of Aß peptide.[138]

GSI A (Semagacestat) and GSI B (Begacestat) dose-dependently reduced the levels of all measured Aß species ($Aß_{1-x}$, $Aß_{1-42}$, and $Aß_{11-40/42}$). Remarkably, at compound concentrations of 8.8E-09M an increase in $Aß_{11-x}$ was observed, which was more pronounced for $Aß_{11-42}$ (reaching 50% more than baseline) and this effect was observed in two independent experiments. This rebound effect after a transient reduction in Aß levels is commonly found for GSIs, possibly due to the accumulation of ß-CTFs upon γ-secretase inhibition. [292] It is not clear why this effect is present for $Aß_{11-x}$ and not $Aß_{1-x}$. It may be related to the BACE1 levels present in the cell: when BACE1 is present in higher levels $Aß_{11-x}$ is a preferential cleavage, while when BACE1 is reduced $Aß_{1-x}$ is the preferred cleavage site.[116] Semagacestat and Begacestat results were in line with literature results, where $Aß_{1-40/42}$ were similarly reduced.[206,293]

GSM C, D (JNJ-42601572), and E (E2012) dose-dependently reduced $Aß_{1-42}$ levels while Aß total levels remained relatively stable upon compound administration, supporting the selective effect for reduction of longer Aß species. For GSM C, $Aß_{11-40}$ showed only a partial reduction (to 53% of baseline) as compared to 16% of baseline reduction of $Aß_{1-42}$. This could be related to the particular chemical class of the compound, with specific targeting $Aß_{x-42}$ species.[294] For GSM D and E $Aß_{11-40}$ was reduced to a similar extent as $Aß_{1-42}$, consistently with literature results on these compounds.[295,296] The lack of an Aß-rebound effect upon GSM treatment is likely related to the fact that GSMs do not induce accumulation of ß-CTFs. [292]

BACE1 inhibitors (1-24) were also tested in the cellular assay. BACEi inhibit BACE1 activity, preventing APP proteolytic processing at the 1st and 11th residue of the Aß peptide, and the

consequent generation of $Aß_{1-x}$ and $Aß_{11-x}$ species. Results indeed showed a dose-dependent response for all the compounds and in general a very similar reduction pattern for $Aß_{1-x}$, $Aß_{1-42}$, and $Aß_{11-40}$. These results corroborate literature reports in SH-SY5Y (APP*wt*) cell culture and in dog CSF, indicating a similar reduction in both BACE1 proteolytic products ($Aß_{1-x}$ and $Aß_{11-x}$) upon BACEi exposure.[247,248,297] Of note, for 3 of the 24 BACEi, an increase in $Aß_{11-40}$ levels was seen at concentrations lower than 2.2E-09M, reaching a maximum of 36%, 52% and 33% of baseline for BACEi 16, 17, and 18, respectively, while no such increase was registered for $Aß_{1-x}$ species. Currently the reason for this increase remains unclear, and this effect was not observed in any of the other measured Aß species ($Aß_{1-x}$, $Aß_{1-42}$, $Aß_{x-40}$, $Aß_{x-42}$). Further studies are warranted to further investigate this effect. For BACEi 11 (MK8931)[298], 15 (LY2811376)[224], 20 (LY2886721)[215,251,299], and 24 (AZD3839)[300] our results were concordant with literature findings showing a dose-dependent Aß reduction for the compounds throughout preclinical studies and clinical trials.

Prior to evaluating $Aß_{11-40}$ levels in CSF of a dog model, an assessment of potential differences in Aß levels between different CSF collection sites was performed. The site of CSF collection is already known to affect CSF biomarkers levels, and specifically in dogs, CSF sampling from the cisterna magna can result in two times higher Aß levels than lateral ventricle sampling.[40] Collection of cisterna magna CSF may therefore allow an easier detection of low abundant fragments. Indeed, evaluation of $Aß_{11-x}$ levels in CSF sampled from the cisterna magna revealed significantly higher levels of the peptide in comparison with CSF sampled from the lateral ventricle. CSF samples for all the 16 dogs showed a detectable signal in cisterna magna, while only 2 of the 16 dogs showed any signal in the lateral ventricle CSF. A possible explanation for differences in Aß levels between collection sites could be deduced from Aß metabolism at the various sites. CSF flows from the lateral ventricles towards the third ventricle, followed by the fourth ventricle, and from there into the cisterna magna and subarachnoid space. The choroid plexus in the ventricles has a major role in Aß clearance by its metabolism, and efflux from CSF to blood. A combination of fast uptake of Aß from CSF by the choroid plexus in the lateral ventricle and/or a higher excretion of brain Aß at the subarachnoid side than the ventricular side could provide a potential explanation for the observed differences. [40]

We next selected dog studies that include cisterna magna sampling of CSF for evaluation of treatment effects. A dose-dependent response was observed for GSM F, as well as an increased response upon repetitive dosing of the compound. As expected, the selectivity of the GSM F for longer Aß species was observed, as $Aß_{1-42}$ was in general the most reduced species, with a

maximum reduction to 56% of baseline at the highest dose (20mg/kg). $Aß_{1-40}$ and $Aß_{11-40}$ had a very similar reduction pattern for all the doses, though less reduced than $Aß_{1-42}$. Simultaneously to the reduction of longer Aß species, an increase in the shorter species – $Aß_{1-37}$ and $Aß_{1-38}$ – was observed. For $Aß_{1-37}$ this increase was already clear for the low dose group, reaching an increase of 167% (D7 8h), which in the high dose group reached 469% (D7 8h). For $Aß_{1-38}$ the maximum increase was observed in the highest dose group, reaching more than 80% compared to baseline. The increase in shorter Aß species combined with reduction of longer forms has been described for GSM treatment, and highlights the selectivity of this type of compounds for reduction of longer, more amyloidogenic forms. [301,302]

Treatment of dogs with BACEi 25 resulted in reduction of all $Aß_{1-x}$ species in CSF to a similar extent. This is in line with the mechanism of action of this type of compounds, as BACE is responsible for the N-terminal cleavage of the Aß peptide. A dose- and time-dependent response was observed for all Aß species measured.

In a clinical study, repeated administration of BACEi (BACEi 26) to 17 elderly healthy volunteers during 14 days, resulted in a dose-dependent response of Aß reduction in CSF. Similar to the results obtained in the dog study, comparison of full length Aß with $Aß_{11-40}$ levels showed that $Aß_{11-40}$ levels were slightly more reduced than $Aß_{1-x}$ species in the low dose-group (5mg), where $Aß_{1-40}$ reached a maximum reduction of 50% and $Aß_{11-40}$ reached a maximum reduction of 64% of baseline levels. For the 50mg and 90mg dose group, $Aß_{11-40}$ levels fall below the assay detection limit after dosing. It was estimated that a reduction up until 80% could be quantified for $Aß_{11-40}$ in human CSF, indicating that for 50 and 90mg doses the reduction is probably superior to 80%. $Aß_{1-37/38/40/42}$ species all demonstrated very similar reduction patterns within each dose group, in line with the BACEi mechanism of action. [143]

In summary, these results from preclinical and clinical studies indicate that $Aß_{11-x}$ levels are reduced to a similar extent as full-length Aß species after GSI, GSM and BACEi treatment. Measurement of $Aß_{11-x}$ levels after BACEi treatment confirmed BACE1 inhibitor target engagement.

$Aß_{11-40}$ has low diagnostic value for AD

Some studies suggested that $Aß_{11-x}$ peptides might have some diagnostic value, although contradictory data was found on different studies. In one study lower $Aß_{11-40/42}$ levels were found in MCI than control subjects.[303] In another study, $Aß_{11-40}$ levels were higher in AD than in individuals with other types of dementias that not AD.[297] In the current study and with a limited

sample set, evaluation of $A\beta_{11-40}$ levels in human CSF did not show any significant difference between AD and NC individuals. It is important to note that from the initial 40 individual samples set (20 AD samples and 20 NC samples), only 21 of the samples (14 AD versus only 7 NC) had levels above the detection limit of the assay, which had an important impact on the sample size and thus conclusions have to be made taking this limitation into account.

Depending on the model system, full-length and N-truncated Aß species are reduced differentially upon BACE1 inhibition

Published studies comparing reduction of full length Aß to N-terminally truncated Aß have suggested that these two pools can behave differently upon treatment with Aß-targeted therapies. For example, BACE1 inhibitors have been shown to have a higher effect on $A\beta_{1-40}$ than on $A\beta_{X-40}$ concentrations in neuroblastoma and primary neuronal cultures.[245,246] Research on specific N-truncated species, revealed differential effects upon BACE1 inhibition, where $A\beta_{1-x}$ was decreased, but $A\beta_{2-x}$ and $A\beta_{5-x}$ species were increased in neuroblastoma cell cultures.[247] Similarly, an increase in $A\beta_{1-34}$ with a simultaneous decrease in $A\beta_{5-x}$ and $A\beta_{5-40}$ was found in preclinical models (APP-transfected cells and dog CSF)[226] and in CSF of healthy individuals upon treatment.[252] Additionally it has also been shown that between *in vivo* models, such as rodents and dogs, the $A\beta_{1-40}/A\beta_{X-40}$ ratio may vary.[279] Therefore it is important to investigate if besides full-length Aß, various N-truncated Aß-species are also reduced after BACEi treatment. Especially as a higher tendency to aggregate has been demonstrated for some N-truncated forms.[149,172,227]

Comparison of BACEi effects on $A\beta_{x-37/38/40/42}$ (N-truncated) and $A\beta_{1-x}$ (full-length) concentrations revealed variable effects in different models. In human CSF, BACEi treatment resulted in a very similar reduction for both N-truncated and full-length Aß species. These results allowed us to conclude that in human CSF samples we do not observe a detectable shift towards N-terminal variants after BACEi treatment. However, it cannot be excluded that small shifts have occurred for specific peptides (e.g. $A\beta_{5-40}$ peptide)[252] that do not result in a detectable difference after BACE inhibition in the assays utilized in the current study. On the other hand, when a similar measurement was performed in the cellular assay, BACEi treatment resulted in significantly higher reduction of $A\beta_{1-x}$ species than N-truncated species. While $A\beta_{1-x}$ species were completely reduced at the highest dose of compound in most BACEi evaluated, N-terminally truncated Aß species were in general reduced only 60% at the same compound doses. Additionally, different C-terminal truncated species were differentially affected: $A\beta_{x-42}$ was the more reduced species, followed by $A\beta_{x-40}$ while $A\beta_{x-37}$ and $A\beta_{x-38}$ were only slightly reduced.

Several factors can contribute to this differential response to BACEi treatment in neuroblastoma cells and human CSF. First, it is important to consider that this cellular model overexpresses human APP695, which by itself may already affect the production rate of different Aß pools. Secondly, different models might have different ratios of full-length versus N-truncated species.[279] Therefore, if these truncated species are generated by a BACE1 independent pathway, BACEi inhibition would reduce only $Aß_{1-x}$/$Aß_{11-x}$ species.[304–308]

If in the cellular model full-length Aß species account for a lower percentage of the total Aß pool, different effects in full-length and N-truncated species would be observed upon BACE inhibition. In human CSF, as $Aß_{1-x}$ species are relatively more abundant, the total Aß pool would be affected in a similar manner as the full-length pool.[215,224] As mentioned above, potential increases of some N-truncated species in human CSF cannot be excluded and may not be observed due to relatively higher levels of the $Aß_{1-x}$ pool compared to N-truncated species.[226,252]

Indeed comparison between the detected Aß pools showed that the full-length peptides correspond to different percentages of total Aß in cell supernatant and in human CSF. In human CSF, measurements of full length or N-truncated Aß give similar results for $Aß_{37/38/40}$, suggesting that full-length Aß accounts for the higher portion of total Aß. Although no data is available in human CSF for $Aß_{42}$ levels, the results from $Aß_{37/38/40}$ suggest that similar results are likely to be present this specie. On the other hand, in the cellular supernatant full length Aß appears to account for a smaller percentage of the total Aß pool. Suggesting that in cells, most of the total Aß pool is composed of N-truncated Aß species.

Although these results give a plausible explanation to why there is a differential reduction between cells and human CSF upon BACE inhibition, it does supply an answer to why there were different degrees of reduction between $Aß_{x-37}$, $Aß_{x-38}$, $Aß_{x-40}$ and $Aß_{x-42}$, and further research is required to study this effect.

This difference across models highlights that translation between preclinical and clinical studies needs to be done with caution, and underscores the importance of investigating compound effects across a variety of preclinical models.

Ratio of $Aß_{1-42}$ levels to other Aß peptides increases diagnostic value in both crude and HPLC-enriched CSF samples

Shorter Aß species, like $Aß_{1-40}$, may have protective function as compared to $Aß_{1-42}$, as these forms are less amyloidgenic.[166] As these shorter species are deposited to a lesser extent in human AD brain, they could potentially provide a way for normalizing $Aß_{1-42}$ levels to the

individual's baseline Aß concentrations. Therefore, it becomes relevant to compare the levels of $Aß_{1-42}$ to $Aß_{1-40}$, or to the levels of other non-amyloidogenic species, like $Aß_{1-37}$ or $Aß_{1-38}$. This is particularly important given the large inter-individual variability in Aß concentrations between individuals. This variability results in difficulties in establishing the diagnostic cut-off values for a single peptide, which could be facilitated by the use of a peptide ratio. [46–49]

Studies have shown that $Aß_{1-42}$ peptide levels as measured with immunoassays could be under-estimated due to a fraction of peptide that is in a form that is not soluble or accessible to antibody binding. These data suggest that the often measured $Aß_{1-42}$ levels correspond to only a specific fraction of the total $Aß_{1-42}$ pool present in the CSF.[282] One possible approach into understanding how the different $Aß_{1-42}$ pools contribute to AD diagnostic value is to define the ratio of the measured $Aß_{1-42}$ pool to the total $Aß_{1-42}$ peptide levels for various assays.

Recovery of this "hidden" fraction has given different results in different studies. In one study by Slemmon J. R. *et al.* (2012)[282], to evaluate total $Aß_{1-42}$ levels, the samples were enriched for $Aß_{1-42}$ using a 6M GuHCL extraction protocol and HPLC enrichment, followed by an immunoassay for $Aß_{1-42}$ measurements. The enrichment resulted in an approximately 3-fold increase in $Aß_{1-42}$ levels, suggesting that only 1 third of the total $Aß_{1-42}$ is available in the crude sample. Moreover, upon sample enrichment the separation between AD and controls was reduced. In another study by Pannee J. et al. (2013)[283], $Aß_{1-42}$ was enriched using a 2M GuHCl at acidic pH, followed by mass spectrometry process for $Aß_{1-42}$ measurement. In this case, the enrichment resulted in a 2-fold increase of $Aß_{1-42}$ levels compared with the ELISA of the crude sample, suggesting through mass spectrometry about half the total pool was being measured. However, in this study sample enrichment did not affect the diagnostic power of $Aß_{1-42}$.

When $Aß_{1-42}/Aß_{1-40}$ ratio was taken into consideration, diagnostic power was significantly increased in both studies, and independent of whether crude of extracted CSF was being analyzed. These results highlight that further studies are required to understand how the different pools of $Aß_{1-42}$ can affect and contribute to the performance of $Aß_{1-42}$ "biosignature" for AD in CSF.[282,283]

In this project, a set of 40 samples (20 AD and 20 NC, classified based on $Aß_{1-42}$, p-tau and t-tau measures) was analyzed, and the levels of $Aß_{1-42}$ and $Aß_{1-40}$ were compared in crude samples and in HPLC enriched samples. Additionally the diagnostic value of the $Aß_{1-42}$ peptide when used by itself or as a ratio with $Aß_{1-40}$ levels was evaluated. The HPLC protocol followed was the same as in Slemmon J. R. *et al*. (2012).[282] Furthermore, the samples were analyzed using two different

immunoassays for Aß$_{1-42}$ detection: Innotest® Aß$_{1-42}$ ELISA (Fujirebio Europe, Belgium) and an internally developed Meso Scale Discovery (MSD) 4-plex assay.[286,287]

Comparison of the two assays shows that for Aß$_{1-40}$ results are very similar, and there is a very good correlation between the assays. For Aß$_{1-40}$, HPLC-enrichment did not affect the amount of peptide detected in either assay as compared to the crude samples. When Aß$_{1-42}$ is analysed the results become different between assays. HPLC-enrichment does not affect the amount of peptide detected in the MSD 4–plex, and in some samples Aß$_{1-42}$ levels are even higher in crude CSF. In contrast, using the Innotest Aß$_{1-42}$ assay, HPLC-enrichment resulted in higher Aß$_{1-42}$ levels. Nonetheless, the assays still have a very high correlation for Aß$_{1-42}$ as well. The differential result may arise from the MSD 4-plex assay having the capacity of detect the total Aß$_{1-42}$ pool, while Innotest Aß$_{1-42}$ is measuring only a fraction. Moreover, we show that the dilution factor of the samples is crucial in the peptide detection by the Innotest Aß$_{1-42}$ assay.

Lack of dilution linearity is usually associated with matrix-effects, due to the presence of proteins or other components in CSF that interfere with analyte detection.[281] A possible solution for the non-linearity is the denaturation of the sample in high concentrations of guanidine hydrochloride and reverse-phase HPLC (RP-HPLC), as this process would purify the sample for the desired analyte and allow a measurement without matrix interference.[309] Indeed, in this study HPLC-enriched samples showed dilution linearity between 1:4 and 1:8 dilution for MSD 4-plex, and between undiluted, 1:4, and 1:8 dilution for Innotest Aß$_{1-42}$. In contrast, crude CSF samples showed dilution linearity between 1:4 and 1:8 dilutions for MSD 4-plex, but in general no dilution linearity between undiluted, 1:4 and 1:8 dilutions using the Innotest Aß$_{1-42}$ assay. In the Innotest Aß$_{1-42}$ assay further dilution of the samples resulted in increased Aß$_{1-42}$ levels in the crude CSF, which in turn resulted in lower differences between HPLC and crude CSF Aß$_{1-42}$ levels.

It must be taken into consideration that the re-evaluation of the sub-group of samples at different dilutions for the Innotest Aß$_{1-42}$ did not replicate the initial results completely, more specifically, while for AD samples an increase in Aß$_{1-42}$ was seen upon HPLC-enrichment, no increase was observed in the NC samples. Interestingly, further sample dilution in the Innotest Aß$_{1-42}$, lead to similar results to the ones obtained in MSD 4-plex regarding % variation between HPLC and crude. This lack of replication of differences between crude and HPLC values for NC samples may be related with the extra freeze-thaw cycle that the samples were subjected or to the use of a newer version of the Innotest Aß$_{1-42}$ kit. Nonetheless, it is clear that dilution factor is an important player in biomarker measurements in crude CSF samples, and that careful optimization of this parameter must be done prior to sample analysis.

Despite the differences between the assays, when the diagnostic value of the $Aß_{1-42}$ peptide was calculated, it resulted in highly similar results between assays, and between HPLC and crude CSF samples. While in the Innotest $Aß_{1-42}$, AUC for $Aß_{1-42}$ was 0.69 in crude CSF and 0.7 in HPLC CSF, in the MSD 4-plex this value was slightly decreased to 0.64 in crude CSF and HPLC CSF. The use of $Aß_{1-42}/Aß_{1-40}$ ratio strongly increased the diagnostic value in the Innotest $Aß_{1-42}$ to 0.97 in crude CSF and to 1.0 in HPLC CSF, and also in the MSD 4-plex to 0.99 in crude CSF and 0.95 in HPLC CSF. It is important to take into account that $Aß_{1-40}$ levels were significantly higher in AD than in NC samples in this sample set, which clearly contributes to the diagnostic value.[310,311]

By using the MSD 4-plex, $Aß_{1-37}$ and $Aß_{1-38}$ were measured simultaneously with $Aß_{1-42}$ and $Aß_{1-40}$. Similarly to $Aß_{1-40}$, ratios using these peptides increased the diagnostic value of $Aß_{1-42}$ to an AUC of 0.93 for $Aß_{1-42}/Aß_{1-37}$ ratio and to 0.98 for $Aß_{1-42}/Aß_{1-38}$ ratio. Although ratios with $Aß_{1-37}$ and $Aß_{1-38}$ had slightly higher overlap between AD and NC than the ratio with Aß1-42. Additionally, individuals with high $Aß_{1-42}/Aß_{1-40}$ ratios also had high $Aß_{1-42}/Aß_{1-37}$ and $Aß_{1-42}/Aß_{1-38}$ ratios.

In conclusion, these results indicate that measurement of the total $Aß_{1-42}$ pool, as defined by the extraction procedure using HPLC, did not change the diagnostic value of the peptide when compared with $Aß_{1-42}$ in the crude CSF sample. The increase in diagnostic value after application of the ratio $Aß_{1-42}/Aß_{1-40}$ is in line with several published studies.[312–315] Comparison of the two assays used, indicate that MSD 4-plex is measuring total or close to total $Aß_{1-42}$ levels, as no difference is observed in Aß concentrations between crude and HPLC-enriched samples. On other hand, Innotest $Aß_{1-42}$ assay appears to be detecting only a fraction of the total $Aß_{1-42}$ pool, as an increase in $Aß_{1-42}$ is observed between crude and HPLC-enriched samples. Dilution linearity is an important factor that could contribute to this observation.

Final remarks and Conclusions

Inhibiting APP processing by targeting the enzymes responsible for Aß generation has the theoretical advantage of preventing Aß production before aggregation can take place. Following the lack of significant clinical results from GSIs and GSMs, BACE has become one of the main targets for AD's-modifying therapies.[316] Several orally bioavailable BACEi are currently undergoing clinical trials, and so far positive outcomes have been described.[216,298,316] Nonetheless several important questions remain unanswered: how much inhibition of BACE1 is required to achieve efficacy? At what AD stages would BACEi be useful? Will there be side-effects regarding BACE1 additional substrates?[317] Even though the answers to these questions may still be far away, development of BACE inhibitors will for sure continue, and CSF biomarkers will most certainly play an important role in their progress.

In this project, evaluation of the Aß-reducing effect of GSIs, GSMs, and BACEi in several preclinical models and human CSF samples showed that $Aß_{11-x}$ levels were in general reduced to a similar extent as $Aß_{1-x}$ species. Moreover, the $Aß_{11-40}$ peptide did not have diagnostic value in the analysed sample set.

Comparison of the reduction profiles upon BACEi administration of full-length ($Aß_{1-x}$) and n-truncated Aß species ($Aß_{x-37/38/40/42}$) in a human neuroblastoma cell line and in human CSF, revealed that while in human CSF full-length and n-truncated species are reduced to a similar extent, in cell supernatant full-length species are reduced to a larger extent than N-truncated species. This difference is likely the result of different full-length/N-truncated ratios in the studied models. This difference highlights the need for careful evaluation of preclinical results and testing in variety of preclinical models to allow translation to the clinical situation.

Regarding the diagnostic value of $Aß_{1-42}$, it was shown that it was independent of the sample type (crude CSF or HPLC-enriched CSF). Additionally, use of the ratio with other peptides such as $Aß_{1-37}$, $Aß_{1-38}$ or $Aß_{1-40}$, significantly increases the diagnostic power when compared to use of the peptide by itself.

Overall this project provides some interesting insights into how several amyloid-biomarkers respond to disease-modifying therapies, and may be useful for the future development of amyloid-targeted therapies.

Chapter VI. Bibliography

1. Selkoe, D. J. Alzheimer's disease. *Cold Spring Harb. Perspect. Biol.* **3,** (2011).

2. Aminoff, M. J. & Daroff, R. B. *Encyclopedia of the Neurological Sciences, Fourth Volume*. (Academic Press, 2003).

3. Jalbert, J. J., Daiello, L. a & Lapane, K. L. Dementia of the Alzheimer type. *Epidemiol. Rev.* **30,** 15–34 (2008).

4. Alzheimer's Disease International. *World Alzheimer Report 2013 - Journey of Caring, An analysis of long-term care for dementia*. (2013).

5. Thies, W. & Bleiler, L. 2013 Alzheimer's disease facts and figures. *Alzheimers. Dement.* **9,** 208–45 (2013).

6. Cummings, J. L., Ringman, J. & Vinters, H. V. Neuropathologic correlates of trial-related instruments for Alzheimer's disease. *Am. J. Neurodegener. Dis.* **3,** 45–9 (2014).

7. Reitz, C. & Mayeux, R. Alzheimer disease: epidemiology, diagnostic criteria, risk factors and biomarkers. *Biochem. Pharmacol.* **88,** 640–51 (2014).

8. Rosenthal, S. L. & Kamboh, M. I. Late-Onset Alzheimer's Disease Genes and the Potentially Implicated Pathways. *Curr. Genet. Med. Rep.* **2,** 85–101 (2014).

9. Parent, M. J. *et al.* Cholinergic Depletion in Alzheimer's Disease Shown by [(18) F]FEOBV Autoradiography. *Int. J. Mol. Imaging* **2013,** 205045 (2013).

10. Crimins, J. L., Pooler, A., Polydoro, M., Luebke, J. I. & Spires-Jones, T. L. The intersection of amyloid β and tau in glutamatergic synaptic dysfunction and collapse in Alzheimer's disease. *Ageing Res. Rev.* **12,** 757–63 (2013).

11. Mendez, M. & Cummings, J. *Dementia: A Clinical Approach*. (Philadelphia, PA: Butterworth Heinemann, 2003).

12. Aguzzi, A. & O'Connor, T. Protein aggregation diseases: pathogenicity and therapeutic perspectives. *Nat. Rev. Drug Discov.* **9,** 237–48 (2010).

13. Himmelstein, D. S., Ward, S. M., Lancia, J. K., Patterson, K. R. & Binder, L. I. Tau as a therapeutic target in neurodegenerative disease. *Pharmacol. Ther.* **136,** 8–22 (2012).

14. Medina, M. & Avila, J. The role of extracellular Tau in the spreading of neurofibrillary pathology. *Front. Cell. Neurosci.* **8,** 113 (2014).

15. Medina, M. & Avila, J. New perspectives on the role of tau in Alzheimer's disease. Implications for therapy. *Biochem. Pharmacol.* **88,** 540–7 (2014).

16. Desikan, R. S. *et al.* Genetic overlap between Alzheimer's disease and Parkinson's disease at the MAPT locus. *Mol. Psychiatry* (2015).

17. Kuret, J. *et al.* Pathways of tau fibrillization. *Biochim. Biophys. Acta* **1739,** 167–78 (2005).

18. Haass, C. *Molecular Biology of Alzheimer's Disease: Genes and Mechanisms Involved in Amyloid Generation*. (Taylor & Francis e-Library, 2005).

19. Patterson, K. R. *et al.* Characterization of prefibrillar Tau oligomers in vitro and in Alzheimer disease. *J. Biol. Chem.* **286,** 23063–76 (2011).

20. Nussbaum, J. M., Seward, M. E. & Bloom, G. S. Alzheimer disease: a tale of two prions. *Prion* **7,** 14–9 (2013).

21. Arriagada, P. V, Growdon, J. H., Hedley-Whyte, E. T. & Hyman, B. T. Neurofibrillary tangles but not senile plaques parallel duration and severity of Alzheimer's disease. *Neurology* **42,** 631–639 (1992).

22. Bierer, L. M. *et al.* Neocortical neurofibrillary tangles correlate with dementia severity in Alzheimer's disease. *Arch. Neurol.* **52,** 81–88 (1995).

23. Rapoport, M., Dawson, H. N., Binder, L. I., Vitek, M. P. & Ferreira, A. Tau is essential to beta -amyloid-induced neurotoxicity. *Proc. Natl. Acad. Sci. U. S. A.* **99,** 6364–9 (2002).

24. Roberson, E. D. *et al.* Reducing endogenous tau ameliorates amyloid beta-induced deficits in an Alzheimer's disease mouse model. *Science* **316,** 750–4 (2007).

25. D'Andrea, M. R. & Nagele, R. G. Morphologically distinct types of amyloid plaques point the way to a better understanding of Alzheimer's disease pathogenesis. *Biotech. Histochem.* **85,** 133–47 (2010).

26. Carrillo-Mora, P., Luna, R. & Colín-Barenque, L. Amyloid beta: Multiple mechanisms of toxicity and only some protective effects? *Oxid. Med. Cell. Longev.* **2014,** (2014).

27. Tiiman, A., Palumaa, P. & Tõugu, V. The missing link in the amyloid cascade of Alzheimer's disease - metal ions. *Neurochem. Int.* **62,** 367–78 (2013).

28. De Strooper, B. Proteases and proteolysis in Alzheimer disease: a multifactorial view on the disease process. *Physiol. Rev.* **90,** 465–94 (2010).

29. Kim, D. H. *et al.* Genetic markers for diagnosis and pathogenesis of Alzheimer's disease. *Gene* (2014).

30. Dubois, B. *et al.* Advancing research diagnostic criteria for Alzheimer's disease: the IWG-2 criteria. *Lancet Neurol.* **13,** 614–629 (2014).

31. Jack, C. R. *et al.* Introduction to the recommendations from the National Institute on Aging-Alzheimer's Association workgroups on diagnostic guidelines for Alzheimer's disease. *Alzheimers. Dement.* **7,** 257–62 (2011).

32. Croisile, B., Auriacombe, S., Etcharry-Bouyx, F. & Vercelletto, M. [The new 2011 recommendations of the National Institute on Aging and the Alzheimer's Association on diagnostic guidelines for Alzheimer's disease: Preclinal stages, mild cognitive impairment, and dementia]. *Rev. Neurol. (Paris).* **168,** 471–82 (2012).

33. Sperling, R., Mormino, E. & Johnson, K. Perspective The Evolution of Preclinical Alzheimer ' s Disease : Implications for Prevention Trials. *Neuron* (2014).

34. Lopez, O. L. *et al.* Prevalence and classification of mild cognitive impairment in the Cardiovascular Health Study Cognition Study: part 1. *Arch. Neurol.* **60,** 1385–9 (2003).

35. Biomarkers Definitions Working Group. Biomarkers and surrogate endpoints: preferred definitions and conceptual framework. *Clin. Pharmacol. Ther.* **69,** 89–95 (2001).

36. Zetterberg, H. Is plasma amyloid-beta a reliable biomarker for Alzheimer's disease? *Recent Pat. CNS Drug Discov.* **3,** 109–11 (2008).

37. Blennow, K., Hampel, H., Weiner, M. & Zetterberg, H. Cerebrospinal fluid and plasma biomarkers in Alzheimer disease. *Nat. Rev. Neurol.* **6,** 131–44 (2010).

38. Kiddle, S. J. *et al.* Candidate blood proteome markers of Alzheimer's disease onset and progression: A systematic review and replication study. *Journal of Alzheimer's Disease* **38,** 515–531 (2014).

39. Lahunta, A. de & Glass, E. N. in *Veterinary Neuroanatomy and Clinical Neurology* 54–76 (2009).

40. Borghys, H. *et al.* Comparison of two different methods for measurement of amyloid-β peptides in cerebrospinal fluid after BACE1 inhibition in a dog model. *J. Alzheimers. Dis.* **38,** 39–48 (2014).

41. Höglund, K. *et al.* Prediction of Alzheimer's disease using a cerebrospinal fluid pattern of C-terminally truncated beta-amyloid peptides. *Neurodegener. Dis.* **5,** 268–76 (2008).

42. Augustinack, J. C., Schneider, A., Mandelkow, E.-M. & Hyman, B. T. Specific tau phosphorylation sites correlate with severity of neuronal cytopathology in Alzheimer's disease. *Acta Neuropathol.* **103,** 26–35 (2002).

43. Blennow, K. Cerebrospinal fluid protein biomarkers for Alzheimer's disease. *NeuroRx* **1,** 213–25 (2004).

44. Blennow, K. *et al.* Clinical utility of cerebrospinal fluid biomarkers in the diagnosis of early Alzheimer's disease. *Alzheimers. Dement.* 1–12 (2014).

45. Sämgård, K. *et al.* Cerebrospinal fluid total tau as a marker of Alzheimer's disease intensity. *Int. J. Geriatr. Psychiatry* **25,** 403–10 (2010).

46. Höglund, K. *et al.* Alzheimer's disease — Recent biomarker developments in relation to updated diagnostic criteria. *Clin. Chim. Acta* (2015).

47. Blennow, K., Mattsson, N., Schöll, M., Hansson, O. & Zetterberg, H. Amyloid biomarkers in Alzheimer's disease. *Trends Pharmacol. Sci.* (2015).

48. Spies, P. E. *et al.* The cerebrospinal fluid amyloid beta42/40 ratio in the differentiation of Alzheimer's disease from non-Alzheimer's dementia. *Curr. Alzheimer Res.* **7,** 470–476 (2010).

49. Dumurgier, J. *et al.* Cerebrospinal fluid amyloid-β 42/40 ratio in clinical setting of memory centers: a multicentric study. *Alzheimers. Res. Ther.* **7,** (2015).

50. Fiandaca, M. S., Mapstone, M. E., Cheema, A. K. & Federoff, H. J. The critical need for defining preclinical biomarkers in Alzheimer's disease. *Alzheimers. Dement.* **10,** S196–212 (2014).

51. Jack, C. R. *et al.* Tracking pathophysiological processes in Alzheimer's disease: an updated hypothetical model of dynamic biomarkers. *Lancet Neurol.* **12,** 207–16 (2013).

52. Frisoni, G. B., Fox, N. C., Jack, C. R., Scheltens, P. & Thompson, P. M. The clinical use of structural MRI in Alzheimer disease. *Nat. Rev. Neurol.* **6,** 67–77 (2010).

53. Rowe, C. C. *et al.* Imaging beta-amyloid burden in aging and dementia. *Neurology* **68,** 1718–1725 (2007).

54. Edison, P. *et al.* Microglia, amyloid, and cognition in Alzheimer's disease: An [11C](R)PK11195-PET and [11C]PIB-PET study. *Neurobiol. Dis.* **32,** 412–419 (2008).

55. Klunk, W. E. *et al.* Imaging Brain Amyloid in Alzheimer's Disease with Pittsburgh Compound-B. *Ann. Neurol.* **55,** 306–319 (2004).

56. Cohen, A. D. & Klunk, W. E. Early detection of Alzheimer's disease using PiB and FDG PET. *Neurobiol. Dis.* 1–6 (2014).

57. Herholz, K. & Ebmeier, K. Clinical amyloid imaging in Alzheimer's disease. *The Lancet Neurology* **10,** 667–670 (2011).

58. Vallabhajosula, S. Positron emission tomography radiopharmaceuticals for imaging brain beta-amyloid. *Seminars in Nuclear Medicine* **41,** 283–299 (2011).

59. Tapiola, T. *et al.* Cerebrospinal fluid {beta}-amyloid 42 and tau proteins as biomarkers of Alzheimer-type pathologic changes in the brain. *Arch. Neurol.* **66,** 382–389 (2009).

60. Fagan, A. M. *et al.* Cerebrospinal fluid tau and ptau181 increase with cortical amyloid deposition in cognitively normal individuals: Implications for future clinical trials of Alzheimer's disease. *EMBO Mol. Med.* **1,** 371–380 (2009).

61. Fagan, A. M. CSF Biomarkers of Alzheimer's Disease: Impact on Disease Concept, Diagnosis, and Clinical Trial Design. *Adv. Geriatr.* **2014,** 1–14 (2014).

62. Ryan, N. S. & Rossor, M. N. Correlating familial Alzheimer's disease gene mutations with clinical phenotype. *Biomark. Med.* **4,** 99–112 (2010).

63. Thinakaran, G. & Koo, E. H. Amyloid precursor protein trafficking, processing, and function. *J. Biol. Chem.* **283,** 29615–9 (2008).

64. Cruts, M., Theuns, J. & Van Broeckhoven, C. Locus-specific mutation databases for neurodegenerative brain diseases. *Hum. Mutat.* **33,** 1340–4 (2012).

65. Vassar, R. *et al.* Function, therapeutic potential and cell biology of BACE proteases: current status and future prospects. *J. Neurochem.* (2014).

66. Jonsson, T. *et al.* A mutation in APP protects against Alzheimer's disease and age-related cognitive decline. *Nature* **488,** 96–9 (2012).

67. Hardy, J. & Selkoe, D. J. The amyloid hypothesis of Alzheimer's disease: progress and problems on the road to therapeutics. *Science* **297,** 353–6 (2002).

68. Zhou, L. *et al.* Amyloid precursor protein mutation E682K at the alternative β-secretase cleavage β'-site increases Aβ generation. *EMBO Mol. Med.* **3,** 291–302 (2011).

69. De Strooper, B. Loss-of-function presenilin mutations in Alzheimer disease. Talking Point on the role of presenilin mutations in Alzheimer disease. *EMBO Rep.* **8,** 141–6 (2007).

70. Cruts, M. *et al.* Estimation of the genetic contribution of presenilin-1 and -2 mutations in a population-based study of presenile Alzheimer disease. *Hum. Mol. Genet.* **7,** 43–51 (1998).

71. Park, M. H. *et al.* Mutant presenilin 2 increases β-secretase activity through reactive oxygen species-dependent activation of extracellular signal-regulated kinase. *J. Neuropathol. Exp. Neurol.* **71,** 130–9 (2012).

72. Liu, C.-C., Liu, C.-C., Kanekiyo, T., Xu, H. & Bu, G. Apolipoprotein E and Alzheimer disease: risk, mechanisms and therapy. *Nat. Rev. Neurol.* **9,** 106–18 (2013).

73. Karch, C. M. & Goate, A. M. Alzheimer's disease risk genes and mechanisms of disease pathogenesis. *Biol. Psychiatry* (2014).

74. Nelson, P. T. *et al.* APOE-ε2 and APOE-ε4 correlate with increased amyloid accumulation in cerebral vasculature. *J. Neuropathol. Exp. Neurol.* **72,** 708–15 (2013).

75. Bu, G. Apolipoprotein E and its receptors in Alzheimer's disease: pathways, pathogenesis and therapy. *Nat. Rev. Neurosci.* **10,** 333–44 (2009).

76. Kim, J., Basak, J. M. & Holtzman, D. M. The role of apolipoprotein E in Alzheimer's disease. *Neuron* **63,** 287–303 (2009).

77. Cruchaga, C. *et al.* Rare variants in APP, PSEN1 and PSEN2 increase risk for AD in late-onset Alzheimer's disease families. *PLoS One* **7,** (2012).

78. Hardy, J. A. & Higgins, G. A. Alzheimer's disease: the amyloid cascade hypothesis. *Science* **256,** 184–5 (1992).

79. Karran, E., Mercken, M. & De Strooper, B. The amyloid cascade hypothesis for Alzheimer's disease: an appraisal for the development of therapeutics. *Nat. Rev. Drug Discov.* **10,** 698–712 (2011).

80. Reitz, C. Alzheimer's disease and the amyloid cascade hypothesis: a critical review. *Int. J. Alzheimers. Dis.* **2012,** 369808 (2012).

81. Roberson, E. D. *et al.* Amyloid-β/Fyn-induced synaptic, network, and cognitive impairments depend on tau levels in multiple mouse models of Alzheimer's disease. *J. Neurosci.* **31,** 700–11 (2011).

82. Bloom, G. S. Amyloid-β and tau: the trigger and bullet in Alzheimer disease pathogenesis. *JAMA Neurol.* **71,** 505–8 (2014).

83. Johnson, V. E., Stewart, W. & Smith, D. H. Traumatic brain injury and amyloid-β pathology: a link to Alzheimer's disease? *Nat. Rev. Neurosci.* **11,** 361–370 (2010).

84. Gentleman, S. M., Nash, M. J., Sweeting, C. J., Graham, D. I. & Roberts, G. W. Beta-amyloid precursor protein (beta APP) as a marker for axonal injury after head injury. *Neurosci. Lett.* **160,** 139–144 (1993).

85. Lannfelt, L., Relkin, N. R. & Siemers, E. R. Amyloid-ß-directed immunotherapy for Alzheimer's disease. *J. Intern. Med.* **275,** 284–95 (2014).

86. Giannakopoulos, P. *et al.* Tangle and neuron numbers, but not amyloid load, predict cognitive status in Alzheimer's disease. *Neurology* **60,** 1495–500 (2003).

87. Golde, T. E., Schneider, L. S. & Koo, E. H. Anti-aβ therapeutics in Alzheimer's disease: the need for a paradigm shift. *Neuron* **69,** 203–13 (2011).

88. Mullane, K. & Williams, M. Alzheimer's therapeutics: continued clinical failures question the validity of the amyloid hypothesis-but what lies beyond? *Biochem. Pharmacol.* **85,** 289–305 (2013).

89. Biogen. *Single Ascending Dose Study of BIIB037 in Participants With Alzheimer's Disease*. (2015). at <https://clinicaltrials.gov/ct2/show/NCT01397539?term=BIIB037&rank=1>

90. Giacobini, E. & Gold, G. Alzheimer disease therapy--moving from amyloid-β to tau. *Nat. Rev. Neurol.* **9,** 677–86 (2013).

91. Shankar, G. M. *et al.* Amyloid-beta protein dimers isolated directly from Alzheimer's brains impair synaptic plasticity and memory. *Nat. Med.* **14,** 837–42 (2008).

92. Lesné, S. *et al.* A specific amyloid-beta protein assembly in the brain impairs memory. *Nature* **440,** 352–7 (2006).

93. Nimmrich, V. *et al.* Amyloid beta oligomers (A beta(1-42) globulomer) suppress spontaneous synaptic activity by inhibition of P/Q-type calcium currents. *J. Neurosci.* **28,** 788–97 (2008).

94. Resende, R. *et al.* Brain oxidative stress in a triple-transgenic mouse model of Alzheimer disease. *Free Radic. Biol. Med.* **44,** 2051–7 (2008).

95. Eckert, A. *et al.* Soluble beta-amyloid leads to mitochondrial defects in amyloid precursor protein and tau transgenic mice. *Neurodegener. Dis.* **5,** 157–9 (2008).

96. Klyubin, I. *et al.* Amyloid beta protein dimer-containing human CSF disrupts synaptic plasticity: prevention by systemic passive immunization. *J. Neurosci.* **28,** 4231–7 (2008).

97. Barry, A. E. *et al.* Alzheimer's disease brain-derived amyloid-β-mediated inhibition of LTP in vivo is prevented by immunotargeting cellular prion protein. *J. Neurosci.* **31,** 7259–63 (2011).

98. Shankar, G. M. *et al.* Natural oligomers of the Alzheimer amyloid-beta protein induce reversible synapse loss by modulating an NMDA-type glutamate receptor-dependent signaling pathway. *J. Neurosci.* **27,** 2866–75 (2007).

99. De Felice, F. G. *et al.* Abeta oligomers induce neuronal oxidative stress through an N-methyl-D-aspartate receptor-dependent mechanism that is blocked by the Alzheimer drug memantine. *J. Biol. Chem.* **282,** 11590–601 (2007).

100. Lacor, P. N. *et al.* Abeta oligomer-induced aberrations in synapse composition, shape, and density provide a molecular basis for loss of connectivity in Alzheimer's disease. *J. Neurosci.* **27,** 796–807 (2007).

101. King, M. E. *et al.* Tau-dependent microtubule disassembly initiated by prefibrillar beta-amyloid. *J. Cell Biol.* **175,** 541–6 (2006).

102. LaFerla, F. M., Green, K. N. & Oddo, S. Intracellular amyloid-beta in Alzheimer's disease. *Nat. Rev. Neurosci.* **8,** 499–509 (2007).

103. Wirths, O., Multhaup, G. & Bayer, T. A. A modified beta-amyloid hypothesis: intraneuronal accumulation of the beta-amyloid peptide--the first step of a fatal cascade. *J. Neurochem.* **91,** 513–20 (2004).

104. Cabrejo, L. *et al.* Phenotype associated with APP duplication in five families. *Brain* **129,** 2966–76 (2006).

105. Oakley, H. *et al.* Intraneuronal beta-amyloid aggregates, neurodegeneration, and neuron loss in transgenic mice with five familial Alzheimer's disease mutations: potential factors in amyloid plaque formation. *J. Neurosci.* **26,** 10129–40 (2006).

106. Knobloch, M., Konietzko, U., Krebs, D. C. & Nitsch, R. M. Intracellular Abeta and cognitive deficits precede beta-amyloid deposition in transgenic arcAbeta mice. *Neurobiol. Aging* **28,** 1297–306 (2007).

107. Rogers, J. *et al.* Complement activation by beta-amyloid in Alzheimer disease. *Proc. Natl. Acad. Sci. U. S. A.* **89,** 10016–20 (1992).

108. McGeer, P. L. & McGeer, E. G. The amyloid cascade-inflammatory hypothesis of Alzheimer disease: implications for therapy. *Acta Neuropathol.* **126,** 479–97 (2013).

109. Stoltenberg, M. *et al.* Amyloid plaques arise from zinc-enriched cortical layers in APP/PS1 transgenic mice and are paradoxically enlarged with dietary zinc deficiency. *Neuroscience* **150,** 357–69 (2007).

110. Nicolakakis, N. & Hamel, E. Neurovascular function in Alzheimer's disease patients and experimental models. *J. Cereb. Blood Flow Metab.* **31,** 1354–70 (2011).

111. Kaden, D., Munter, L. M., Reif, B. & Multhaup, G. The amyloid precursor protein and its homologues: structural and functional aspects of native and pathogenic oligomerization. *Eur. J. Cell Biol.* **91,** 234–9 (2012).

112. Schmechel, D. E. *et al.* Cellular localization of messenger RNA encoding amyloid-beta-protein in normal tissue and in Alzheimer disease. *Alzheimer Dis. Assoc. Disord.* **2,** 96–111 (1988).

113. Turner, P. R., O'Connor, K., Tate, W. P. & Abraham, W. C. *Roles of amyloid precursor protein and its fragments in regulating neural activity, plasticity and memory*. *Progress in Neurobiology* **70,** (2003).

114. O'Brien, R. J. & Wong, P. C. Amyloid precursor protein processing and Alzheimer's disease. *Annu. Rev. Neurosci.* **34,** 185–204 (2011).

115. Capell, A. *et al.* Maturation and pro-peptide cleavage of beta-secretase. *J. Biol. Chem.* **275,** 30849–54 (2000).

116. Zhang, X. & Song, W. The role of APP and BACE1 trafficking in APP processing and amyloid-β generation. *Alzheimers. Res. Ther.* **5,** 46 (2013).

117. Zhang, H., Ma, Q., Zhang, Y. & Xu, H. Proteolytic processing of Alzheimer's β-amyloid precursor protein. *J. Neurochem.* **120 Suppl ,** 9–21 (2012).

118. Edbauer, D., Willem, M., Lammich, S., Steiner, H. & Haass, C. Insulin-degrading enzyme rapidly removes the β-amyloid precursor protein intracellular domain (AICD). *J. Biol. Chem.* **277,** 13389–13393 (2002).

119. Nalivaeva, N. N. & Turner, A. J. The amyloid precursor protein: a biochemical enigma in brain development, function and disease. *FEBS Lett.* **587,** 2046–54 (2013).

120. Vassar, R. *et al.* Beta-Secretase Cleavage of Alzheimer's Amyloid Precursor Protein by the Transmembrane Aspartic Protease BACE. *Science (80-.).* **286,** 735–741 (1999).

121. Parvathy, S., Hussain, I., Karran, E. H., Turner, A. J. & Hooper, N. M. Cleavage of Alzheimer's amyloid precursor protein by alpha-secretase occurs at the surface of neuronal cells. *Biochemistry* **38,** 9728–34 (1999).

122. Daugherty, B. L. & Green, S. A. Endosomal sorting of amyloid precursor protein-P-selectin chimeras influences secretase processing. *Traffic* **2,** 908–16 (2001).

123. Allinson, T. M. J., Parkin, E. T., Turner, A. J. & Hooper, N. M. ADAMs family members as amyloid precursor protein alpha-secretases. *J. Neurosci. Res.* **74,** 342–52 (2003).

124. Hartmann, D. *et al.* The disintegrin/metalloprotease ADAM 10 is essential for Notch signalling but not for alpha-secretase activity in fibroblasts. *Hum. Mol. Genet.* **11,** 2615–24 (2002).

125. Black, R. A. *et al.* A metalloproteinase disintegrin that releases tumour-necrosis factor-alpha from cells. *Nature* **385,** 729–33 (1997).

126. Lee, D. C. *et al.* TACE/ADAM17 processing of EGFR ligands indicates a role as a physiological convertase. *Ann. N. Y. Acad. Sci.* **995,** 22–38 (2003).

127. Lammich, S. *et al.* Constitutive and regulated alpha-secretase cleavage of Alzheimer's amyloid precursor protein by a disintegrin metalloprotease. *Proc. Natl. Acad. Sci. U. S. A.* **96,** 3922–7 (1999).

128. Haass, C., Kaether, C., Thinakaran, G. & Sisodia, S. Trafficking and proteolytic processing of APP. *Cold Spring Harb. Perspect. Med.* **2,** a006270 (2012).

129. Sinha, S. *et al.* Purification and cloning of amyloid precursor protein beta-secretase from human brain. *Nature* **402,** 537–40 (1999).

130. Tan, J. & Evin, G. B-site APP-cleaving enzyme 1 trafficking and Alzheimer's disease pathogenesis. *J. Neurochem.* **120,** 869–80 (2012).

131. Shi, X. P. *et al.* The pro domain of beta-secretase does not confer strict zymogen-like properties but does assist proper folding of the protease domain. *J. Biol. Chem.* **276,** 10366–73 (2001).

132. Charlwood, J. *et al.* Characterization of the glycosylation profiles of Alzheimer's beta -secretase protein Asp-2 expressed in a variety of cell lines. *J. Biol. Chem.* **276,** 16739–48 (2001).

133. Benjannet, S. *et al.* Post-translational processing of beta-secretase (beta-amyloid-converting enzyme) and its ectodomain shedding. The pro- and transmembrane/cytosolic domains affect its cellular activity and amyloid-beta production. *J. Biol. Chem.* **276,** 10879–87 (2001).

134. Kang, E. L., Cameron, A. N., Piazza, F., Walker, K. R. & Tesco, G. Ubiquitin regulates GGA3-mediated degradation of BACE1. *J. Biol. Chem.* **285,** 24108–19 (2010).

135. Westmeyer, G. G. *et al.* Dimerization of beta-site beta-amyloid precursor protein-cleaving enzyme. *J. Biol. Chem.* **279,** 53205–12 (2004).

136. Ehehalt, R. *et al.* Splice variants of the beta-site APP-cleaving enzyme BACE1 in human brain and pancreas. *Biochem. Biophys. Res. Commun.* **293,** 30–7 (2002).

137. Rossner, S., Apelt, J., Schliebs, R., Perez-Polo, J. R. & Bigl, V. Neuronal and glial beta-secretase (BACE) protein expression in transgenic Tg2576 mice with amyloid plaque pathology. *J. Neurosci. Res.* **64,** 437–46 (2001).

138. Yan, R. & Vassar, R. Targeting the β secretase BACE1 for Alzheimer's disease therapy. *Lancet Neurol.* **13,** 319–29 (2014).

139. Yang, L.-B. *et al.* Elevated beta-secretase expression and enzymatic activity detected in sporadic Alzheimer disease. *Nat. Med.* **9,** 3–4 (2003).

140. Fukumoto, H., Cheung, B. S., Hyman, B. T. & Irizarry, M. C. Beta-secretase protein and activity are increased in the neocortex in Alzheimer disease. *Arch. Neurol.* **59,** 1381–9 (2002).

141. Holsinger, R. M. D., McLean, C. A., Beyreuther, K., Masters, C. L. & Evin, G. Increased expression of the amyloid precursor beta-secretase in Alzheimer's disease. *Ann. Neurol.* **51,** 783–6 (2002).

142. Luo, Y. *et al.* BACE1 (beta-secretase) knockout mice do not acquire compensatory gene expression changes or develop neural lesions over time. *Neurobiol. Dis.* **14,** 81–8 (2003).

143. Willem, M., Lammich, S. & Haass, C. Function, regulation and therapeutic properties of beta-secretase (BACE1). *Semin. Cell Dev. Biol.* **20,** 175–82 (2009).

144. Schroeter, E. H., Kisslinger, J. A. & Kopan, R. Notch-1 signalling requires ligand-induced proteolytic release of intracellular domain. *Nature* **393,** 382–6 (1998).

145. Saito, T. *et al.* Potent amyloidogenicity and pathogenicity of Aβ43. *Nat. Neurosci.* **14,** 1023–32 (2011).

146. Xu, X. Gamma-secretase catalyzes sequential cleavages of the AbetaPP transmembrane domain. *J. Alzheimers. Dis.* **16,** 211–24 (2009).

147. Lu, D. C., Soriano, S., Bredesen, D. E. & Koo, E. H. Caspase cleavage of the amyloid precursor protein modulates amyloid β-protein toxicity. *J. Neurochem.* **87,** 733–741 (2003).

148. Lu, D. C. *et al.* A second cytotoxic proteolytic peptide derived from amyloid beta-protein precursor. *Nat. Med.* **6,** 397–404 (2000).

149. Bayer, T. A. & Wirths, O. Focusing the amyloid cascade hypothesis on N-truncated Abeta peptides as drug targets against Alzheimer's disease. *Acta Neuropathologica* **127,** 787–801 (2014).

150. Soldano, A. & Hassan, B. a. Beyond pathology: APP, brain development and Alzheimer's disease. *Curr. Opin. Neurobiol.* **27C,** 61–67 (2014).

151. Wang, P. *et al.* Defective neuromuscular synapses in mice lacking amyloid precursor protein (APP) and APP-Like protein 2. *J. Neurosci.* **25,** 1219–25 (2005).

152. Tyan, S.-H. *et al.* Amyloid precursor protein (APP) regulates synaptic structure and function. *Mol. Cell. Neurosci.* **51,** 43–52 (2012).

153. Bell, K. F. S., Zheng, L., Fahrenholz, F. & Cuello, A. C. ADAM-10 over-expression increases cortical synaptogenesis. *Neurobiol. Aging* **29,** 554–65 (2008).

154. Senechal, Y., Kelly, P. H. & Dev, K. K. Amyloid precursor protein knockout mice show age-dependent deficits in passive avoidance learning. *Behav. Brain Res.* **186,** 126–32 (2008).

155. Goguel, V. *et al.* Drosophila amyloid precursor protein-like is required for long-term memory. *J. Neurosci.* **31,** 1032–7 (2011).

156. Magdesian, M. H. *et al.* Secreted human amyloid precursor protein binds semaphorin 3a and prevents semaphorin-induced growth cone collapse. *PLoS One* **6,** e22857 (2011).

157. Meziane, H. *et al.* Memory-enhancing effects of secreted forms of the beta-amyloid precursor protein in normal and amnestic mice. *Proc. Natl. Acad. Sci. U. S. A.* **95,** 12683–8 (1998).

158. Taylor, C. J. *et al.* Endogenous secreted amyloid precursor protein-alpha regulates hippocampal NMDA receptor function, long-term potentiation and spatial memory. *Neurobiol. Dis.* **31,** 250–60 (2008).

159. Nikolaev, A., McLaughlin, T., O'Leary, D. D. M. & Tessier-Lavigne, M. APP binds DR6 to trigger axon pruning and neuron death via distinct caspases. *Nature* **457,** 981–9 (2009).

160. Chang, K.-A. & Suh, Y.-H. Pathophysiological roles of amyloidogenic carboxy-terminal fragments of the beta-amyloid precursor protein in Alzheimer's disease. *J. Pharmacol. Sci.* **97,** 461–71 (2005).

161. Kim, H. S. *et al.* Carboxyl-terminal fragment of Alzheimer's APP destabilizes calcium homeostasis and renders neuronal cells vulnerable to excitotoxicity. *FASEB J.* **14,** 1508–17 (2000).

162. Nakaya, T. & Suzuki, T. Role of APP phosphorylation in FE65-dependent gene transactivation mediated by AICD. *Genes Cells* **11,** 633–45 (2006).

163. Taru, H., Kirino, Y. & Suzuki, T. Differential roles of JIP scaffold proteins in the modulation of amyloid precursor protein metabolism. *J. Biol. Chem.* **277,** 27567–74 (2002).

164. Ozaki, T. *et al.* The intracellular domain of the amyloid precursor protein (AICD) enhances the p53-mediated apoptosis. *Biochem. Biophys. Res. Commun.* **351,** 57–63 (2006).

165. Guzmán, E. A. *et al.* Abundance of $A\beta_5$-x like immunoreactivity in transgenic 5XFAD, APP/PS1KI and 3xTG mice, sporadic and familial Alzheimer's disease. *Mol. Neurodegener.* **9,** 13 (2014).

166. Zou, K. *et al.* Amyloid beta-protein (Abeta)1-40 protects neurons from damage induced by Abeta1-42 in culture and in rat brain. *J. Neurochem.* **87,** 609–19 (2003).

167. Plant, L. D., Boyle, J. P., Smith, I. F., Peers, C. & Pearson, H. A. The production of amyloid beta peptide is a critical requirement for the viability of central neurons. *J. Neurosci.* **23,** 5531–5 (2003).

168. Murphy, M. P. & LeVine, H. Alzheimer's disease and the amyloid-beta peptide. *J. Alzheimers. Dis.* **19,** 311–23 (2010).

169. Hampel, H. *et al.* Biological markers of amyloid beta-related mechanisms in Alzheimer's disease. *Exp. Neurol.* **223,** 334–46 (2010).

170. Kuo, Y. M., Emmerling, M. R., Woods, A. S., Cotter, R. J. & Roher, A. E. Isolation, chemical characterization, and quantitation of A beta 3-pyroglutamyl peptide from neuritic plaques and vascular amyloid deposits. *Biochem. Biophys. Res. Commun.* **237,** 188–191 (1997).

171. Lewis, H. *et al.* Quantification of Alzheimer pathology in ageing and dementia: Age-related accumulation of amyloid-β(42) peptide in vascular dementia. *Neuropathol. Appl. Neurobiol.* **32,** 103–118 (2006).

172. Liu, K. *et al.* Characterization of Abeta11-40/42 peptide deposition in Alzheimer's disease and young Down's syndrome brains: implication of N-terminally truncated Abeta species in the pathogenesis of Alzheimer's disease. *Acta Neuropathol.* **112,** 163–74 (2006).

173. Murayama, K. S., Kametani, F., Tabira, T. & Araki, W. A novel monoclonal antibody specific for the amino-truncated beta-amyloid Abeta5-40/42 produced from caspase-cleaved amyloid precursor protein. *J. Neurosci. Methods* **161,** 244–9 (2007).

174. Nath, S. *et al.* Spreading of neurodegenerative pathology via neuron-to-neuron transmission of β-amyloid. *J. Neurosci.* **32,** 8767–77 (2012).

175. Lee, J.-E. & Han, P.-L. An update of animal models of Alzheimer disease with a reevaluation of plaque depositions. *Exp. Neurobiol.* **22,** 84–95 (2013).

176. Chen, M., Kretzschmar, D., Verdile, G. & Lardelli, M. *Models of Alzheimer ' s Disease*. (Academic Press, 2013).

177. Laurijssens, B., Aujard, F. & Rahman, A. Animal models of Alzheimer's disease and drug development. *Drug Discov. Today. Technol.* **10,** e319–27 (2013).

178. Van Dam, D. & De Deyn, P. P. Animal models in the drug discovery pipeline for Alzheimer's disease. *Br. J. Pharmacol.* **164,** 1285–300 (2011).

179. Fraser, P. E. *et al.* Fibril formation by primate, rodent, and Dutch-hemorrhagic analogues of Alzheimer amyloid beta-protein. *Biochemistry* **31,** 10716–23 (1992).

180. Spires, T. L. & Hyman, B. T. Transgenic models of Alzheimer's disease: learning from animals. *NeuroRx* **2,** 423–37 (2005).

181. Götz, J. *et al.* Transgenic animal models of Alzheimer's disease and related disorders: histopathology, behavior and therapy. *Mol. Psychiatry* **9,** 664–83 (2004).

182. Duff, K. & Suleman, F. Transgenic mouse models of Alzheimer's disease: how useful have they been for therapeutic development? *Brief. Funct. Genomic. Proteomic.* **3,** 47–59 (2004).

183. Bilkei-Gorzo, A. Genetic mouse models of brain ageing and Alzheimer's disease. *Pharmacol. Ther.* **142,** 244–57 (2014).

184. Holcomb, L. *et al.* Accelerated Alzheimer-type phenotype in transgenic mice carrying both mutant amyloid precursor protein and presenilin 1 transgenes. *Nat. Med.* **4,** 97–100 (1998).

185. Cohen, R. M. *et al.* A transgenic Alzheimer rat with plaques, tau pathology, behavioral impairment, oligomeric aβ, and frank neuronal loss. *J. Neurosci.* **33,** 6245–56 (2013).

186. Teng, E. *et al.* [F-18]FDDNP microPET imaging correlates with brain Aβ burden in a transgenic rat model of Alzheimer disease: effects of aging, in vivo blockade, and anti-Aβ antibody treatment. *Neurobiol. Dis.* **43,** 565–75 (2011).

187. O'Hare, E., Ardis, T., Page, D., Scopes, D. I. C. & Kim, E.-M. AβPP-overexpressing transgenic rat model of Alzheimer's disease utilizing the Tg2576 mouse protocol. *J. Alzheimers. Dis.* **37,** 77–88 (2013).

188. Charreau, B., Tesson, L., Soulillou, J. P., Pourcel, C. & Anegon, I. Transgenesis in rats: technical aspects and models. *Transgenic Res.* **5,** 223–234 (1996).

189. Tesson, L. *et al.* Transgenic modifications of the rat genome. *Transgenic Research* **14,** 531–546 (2005).

190. Cavanaugh, S. E., Pippin, J. J. & Barnard, N. D. Animal models of Alzheimer disease: historical pitfalls and a path forward. *ALTEX* **65,** 1–26 (2014).

191. Kaushal, A., Wani, W. Y., Anand, R. & Gill, K. D. Spontaneous and induced nontransgenic animal models of AD: modeling AD using combinatorial approach. *Am. J. Alzheimers. Dis. Other Demen.* **28,** 318–26 (2013).

192. Languille, S. *et al.* The grey mouse lemur: a non-human primate model for ageing studies. *Ageing Res. Rev.* **11,** 150–62 (2012).

193. Picq, J.-L. Aging affects executive functions and memory in mouse lemur primates. *Exp. Gerontol.* **42,** 223–32 (2007).

194. Kraska, A. *et al.* Age-associated cerebral atrophy in mouse lemur primates. *Neurobiol. Aging* **32,** 894–906 (2011).

195. Giannakopoulos, P. *et al.* Quantitative analysis of tau protein-immunoreactive accumulations and β amyloid protein deposits in the cerebral cortex of the mouse lemur, Microcebus murinus. *Acta Neuropathol.* **94,** 131–139 (1997).

196. Johnstone, E. M., Chaney, M. O., Norris, F. H., Pascual, R. & Little, S. P. Conservation of the sequence of the Alzheimer's disease amyloid peptide in dog, polar bear and five other mammals by cross-species polymerase chain reaction analysis. *Brain Res. Mol. Brain Res.* **10,** 299–305 (1991).

197. Portelius, E. *et al.* Acute effect on the Aβ isoform pattern in CSF in response to γ-secretase modulator and inhibitor treatment in dogs. *J. Alzheimers. Dis.* **21,** 1005–12 (2010).

198. Head, E. A canine model of human aging and Alzheimer's disease. *Biochim. Biophys. Acta* **1832,** 1384–9 (2013).

199. Inestrosa, N. C. *et al.* Human-like rodent amyloid-beta-peptide determines Alzheimer pathology in aged wild-type Octodon degu. *Neurobiol. Aging* **26,** 1023–8 (2005).

200. Anand, R., Gill, K. D. & Mahdi, A. A. Therapeutics of Alzheimer's disease: Past, present and future. *Neuropharmacology* **76 Pt A,** 27–50 (2014).

201. Hampel, H. *et al.* Advances in the therapy of Alzheimer's disease: targeting amyloid beta and tau and perspectives for the future. *Expert Rev. Neurother.* **15,** 83–105 (2015).

202. Citron, M. Alzheimer's disease: strategies for disease modification. *Nat. Rev. Drug Discov.* **9,** 387–98 (2010).

203. Golde, T. E., Petrucelli, L. & Lewis, J. Targeting Abeta and tau in Alzheimer's disease, an early interim report. *Exp. Neurol.* **223,** 252–66 (2010).

204. Nie, Q., Du, X. & Geng, M. Small molecule inhibitors of amyloid β peptide aggregation as a potential therapeutic strategy for Alzheimer's disease. *Acta Pharmacol. Sin.* **32,** 545–551 (2011).

205. Jia, Q., Deng, Y. & Qing, H. Potential Therapeutic Strategies for Alzheimer's Disease Targeting or Beyond β -Amyloid: Insights from Clinical Trials. *Biomed Res. Int.* **2014,** 837157 (2014).

206. Mitani, Y. *et al.* Differential Effects between -Secretase Inhibitors and Modulators on Cognitive Function in Amyloid Precursor Protein-Transgenic and Nontransgenic Mice. *Journal of Neuroscience* **32,** 2037–2050 (2012).

207. Alzforum. Semagacestat. at <http://www.alzforum.org/therapeutics/semagacestat>

208. Alzforum. Avagacestat. at <http://www.alzforum.org/therapeutics/avagacestat>

209. Czirr, E. *et al.* Independent generation of Aß42 and Aß38 peptide species by ß-secretase. *J. Biol. Chem.* **283,** 17049–17054 (2008).

210. Alzforum. Flurizan. at <http://www.alzforum.org/therapeutics/flurizantm>

211. Crump, C. J., Johnson, D. S. & Li, Y. M. Development and mechanism of ??-secretase modulators for Alzheimer's disease. *Biochemistry* **52,** 3197–3216 (2013).

212. Evin, G., Lessene, G. & Wilkins, S. BACE inhibitors as potential drugs for the treatment of Alzheimer's disease: focus on bioactivity. *Recent Pat. CNS Drug Discov.* **6,** 91–106 (2011).

213. Probst, G. & Xu, Y. Small-molecule BACE1 inhibitors: a patent literature review (2006 - 2011). *Expert Opin. Ther. Pat.* **22,** 511–40 (2012).

214. clinicaltrials.gov. at <clinicaltrials.gov>

215. May, P. C. *et al.* The Potent BACE1 Inhibitor LY2886721 Elicits Robust Central A Pharmacodynamic Responses in Mice, Dogs, and Humans. *J. Neurosci.* **35,** 1199–1210 (2015).

216. Janssen Pharmaceutica. *JNJ-54861911*. at <https://clinicaltrials.gov/ct2/results?term=JNJ+54861911&Search=Search>

217. Atwal, J. K. *et al.* A therapeutic antibody targeting BACE1 inhibits amyloid-β production in vivo. *Sci. Transl. Med.* **3,** 84ra43 (2011).

218. Yu, Y. J. *et al.* Boosting brain uptake of a therapeutic antibody by reducing its affinity for a transcytosis target. *Sci. Transl. Med.* **3,** 84ra44 (2011).

219. Couch, J. A. *et al.* Addressing safety liabilities of TfR bispecific antibodies that cross the blood-brain barrier. *Sci. Transl. Med.* **5,** 183ra57, 1–12 (2013).

220. Yu, Y. J. *et al.* Therapeutic bispecific antibodies cross the blood-brain barrier in nonhuman primates. *Sci. Transl. Med.* (2014).

221. Cheret, C. *et al.* Bace1 and Neuregulin-1 cooperate to control formation and maintenance of muscle spindles. *EMBO J.* **32,** 2015–28 (2013).

222. Wang, H., Megill, A., Wong, P. C., Kirkwood, A. & Lee, H.-K. Postsynaptic target specific synaptic dysfunctions in the CA3 area of BACE1 knockout mice. *PLoS One* **9,** e92279 (2014).

223. Filser, S. *et al.* Pharmacological Inhibition of BACE1 Impairs Synaptic Plasticity and Cognitive Functions. *Biol. Psychiatry* (2014).

224. May, P. C. *et al.* Robust Central Reduction of Amyloid- in Humans with an Orally Available, Non-Peptidic -Secretase Inhibitor. *Journal of Neuroscience* **31,** 16507–16516 (2011).

225. Blennow, K., Hampel, H. & Zetterberg, H. Biomarkers in amyloid-β immunotherapy trials in Alzheimer's disease. *Neuropsychopharmacology* **39,** 189–201 (2014).

226. Mattsson, N. *et al.* BACE1 inhibition induces a specific cerebrospinal fluid β-amyloid pattern that identifies drug effects in the central nervous system. *PLoS One* **7,** e31084 (2012).

227. Portelius, E. *et al.* β-site amyloid precursor protein-cleaving enzyme 1(BACE1) inhibitor treatment induces Aβ5-X peptides through alternative amyloid precursor protein cleavage. *Alzheimers. Res. Ther.* **6,** 75 (2014).

228. Deane, R. *et al.* A multimodal RAGE-specific inhibitor reduces amyloid ß-mediated brain disorder in a mouse model of Alzheimer disease. *J. Clin. Invest.* **122,** 1377–1392 (2012).

229. Gilman, S. *et al.* Clinical effects of Abeta immunization (AN1792) in patients with AD in an interrupted trial. *Neurology* **64,** 1553–62 (2005).

230. Alzforum. Vanutide cridificar. at <http://www.alzforum.org/therapeutics/vanutide-cridificar>

231. Wiessner, C. *et al.* The second-generation active Aβ immunotherapy CAD106 reduces amyloid accumulation in APP transgenic mice while minimizing potential side effects. *J. Neurosci.* **31,** 9323–31 (2011).

232. Alzforum. CAD106. at <http://www.alzforum.org/therapeutics/cad106>

233. Alzforum. Affitope AD02. at <http://www.alzforum.org/therapeutics/affitope-ad02>

234. Ostrowitzki, S. *et al.* Mechanism of amyloid removal in patients with Alzheimer disease treated with gantenerumab. *Arch. Neurol.* **69,** 198–207 (2012).

235. Alzforum. Aβ Antibody Gantenerumab Clears Plaques. (2011). at <http://www.alzforum.org/news/research-news/av-antibody-gantenerumab-clears-plaques>

236. Szabo, P., Relkin, N. & Weksler, M. E. Natural human antibodies to amyloid beta peptide. *Autoimmun. Rev.* **7,** 415–20 (2008).

237. O'Nuallain, B., Hrncic, R., Wall, J. S., Weiss, D. T. & Solomon, A. Diagnostic and therapeutic potential of amyloid-reactive IgG antibodies contained in human sera. *J. Immunol.* **176,** 7071–8 (2006).

238. Weksler, M. E. *et al.* Patients with Alzheimer disease have lower levels of serum anti-amyloid peptide antibodies than healthy elderly individuals. *Exp. Gerontol.* **37,** 943–8 (2002).

239. Alzforum. Gammagard™. at <http://www.alzforum.org/therapeutics/gammagardtm>

240. Farlow, M. *et al.* Safety and biomarker effects of solanezumab in patients with Alzheimer's disease. *Alzheimers. Dement.* **8,** 261–71 (2012).

241. Alzforum. Aducanumab. at <http://www.alzforum.org/therapeutics/aducanumab>

242. Alzforum. From Shared CAP, Secondary Prevention Trials Are Off and Running. at <http://www.alzforum.org/news/conference-coverage/shared-cap-secondary-prevention-trials-are-and-running>

243. Cummings, J. & Zhong, K. Biomarker-driven therapeutic management of Alzheimer's disease: establishing the foundations. *Clin. Pharmacol. Ther.* **95,** 67–77 (2014).

244. Lleó, A. *et al.* Cerebrospinal fluid biomarkers in trials for Alzheimer and Parkinson diseases. *Nat. Rev. Neurol.* **11,** 41–55 (2014).

245. Nishitomi, K. *et al.* BACE1 inhibition reduces endogenous Abeta and alters APP processing in wild-type mice2. *J. Neurochem.* **99,** 1555–1563 (2006).

246. Atchison, K. *et al.* Inhibition of BACE1 reduces beta-amyloid 1-40 but not N-terminal-truncated beta-amyloid. *Alzheimer's Dement.* **9,** P190 (2013).

247. Haußmann, U. *et al.* Analysis of amino-terminal variants of amyloid-β peptides by capillary isoelectric focusing immunoassay. *Anal. Chem.* **85,** 8142–8149 (2013).

248. Mattsson, N. *et al.* BACE1 inhibition induces a specific cerebrospinal fluid β-amyloid pattern that identifies drug effects in the central nervous system. *PLoS One* **7,** (2012).

249. Maccecchini, M. L. *et al.* Posiphen as a candidate drug to lower CSF amyloid precursor protein, amyloid-β peptide and τ levels: target engagement, tolerability and pharmacokinetics in humans. *J. Neurol. Neurosurg. Psychiatry* **83,** 894–902 (2012).

250. Lai, R. *et al.* First-in-human study of E2609, a novel BACE1 inhibitor, demonstrates prolonged reductions in plasma beta-amyloid levels after single dosing. *Alzheimer's Dement.* **8,** P96 (2012).

251. May, P. *et al.* Preclinical characterization of LY2886721: A BACE1 inhibitor in clinical development for early Alzheimer's disease. *Alzheimer's & Dementia* **8,** P95 (2012).

252. Portelius, E. *et al.* β-site amyloid precursor protein-cleaving enzyme 1(BACE1) inhibitor treatment induces Aβ5-X peptides through alternative amyloid precursor protein cleavage. *Alzheimers. Res. Ther.* **6,** 75 (2014).

253. Bell, J. *et al.* A novel BACE inhibitor (PF-05297909): : A two-part adaptive design to evaluate safety, pharmacokinetics and pharmacodynamics for modifying beta-amyloid in a first-in-human study. *Alzheimer's & Dementia* **9,** P287 (2013).

254. Doody, R. S. *et al.* A phase 3 trial of semagacestat for treatment of Alzheimer's disease. *N. Engl. J. Med.* **369,** 341–50 (2013).

255. Fleisher, A. S. *et al.* Phase 2 safety trial targeting amyloid beta production with a gamma-secretase inhibitor in Alzheimer disease. *Arch. Neurol.* **65,** 1031–8 (2008).

256. Siemers, E. R. *et al.* Effects of a -secretase inhibitor in a randomized study of patients with Alzheimer disease. *Neurology* **66,** 602–604 (2006).

257. Portelius, E. *et al.* Amyloid-β(1-15/16) as a marker for γ-secretase inhibition in Alzheimer's disease. *J. Alzheimers. Dis.* **31,** 335–41 (2012).

258. Bateman, R. J. *et al.* A gamma-secretase inhibitor decreases amyloid-beta production in the central nervous system. *Ann. Neurol.* **66,** 48–54 (2009).

259. Tong, G. *et al.* Effects of single doses of avagacestat (BMS-708163) on cerebrospinal fluid Aβ levels in healthy young men. *Clin. Drug Investig.* **32,** 761–9 (2012).

260. Coric, V. *et al.* A phase II study of the gamma-secretase inhibitor avagacestat (BMS-708163) in predementia Alzheimer's disease. *Alzheimer's Dement.* **9,** P283 (2013).

261. Mangialasche, F., Solomon, A., Winblad, B., Mecocci, P. & Kivipelto, M. Alzheimer's disease: clinical trials and drug development. *Lancet Neurol.* **9,** 702–16 (2010).

262. Hopkins, C. R. ACS chemical neuroscience molecule spotlight on ELND006: another γ-secretase inhibitor fails in the clinic. *ACS Chem. Neurosci.* **2,** 279–80 (2011).

263. Galasko, D. R. *et al.* Safety, tolerability, pharmacokinetics, and Abeta levels after short-term administration of R-flurbiprofen in healthy elderly individuals. *Alzheimer Dis. Assoc. Disord.* **21,** 292–9 (2007)

264. Imbimbo, B. P. *et al.* Pharmacokinetics and pharmacodynamics of CHF5074 after short-term administration in healthy subjects. *Alzheimer Dis. Assoc. Disord.* **27,** 278–86 (2013)

265. Ross, J. *et al.* CHF5074 reduces biomarkers of neuroinflammation in patients with mild cognitive impairment: a 12-week, double-blind, placebo-controlled study. *Curr. Alzheimer Res.* **10,** 742–53 (2013).

266. Aisen, P. S. *et al.* A Phase II study targeting amyloid-beta with 3APS in mild-to-moderate Alzheimer disease. *Neurology* **67,** 1757–63 (2006).

267. Regland, B. *et al.* Treatment of Alzheimer's disease with clioquinol. *Dement. Geriatr. Cogn. Disord.* **12,** 408–14 (2011)

268. Lannfelt, L. *et al.* Safety, efficacy, and biomarker findings of PBT2 in targeting Abeta as a modifying therapy for Alzheimer's disease: a phase IIa, double-blind, randomised, placebo-controlled trial. *Lancet. Neurol.* **7,** 779–86 (2008).

269. Salloway, S. *et al.* A phase 2 randomized trial of ELND005, scyllo-inositol, in mild to moderate Alzheimer disease. *Neurology* **77,** 1253–1262 (2011).

270. Black, R. *et al.* Safety, pharmacokinetics and pharmacodynamics of PQ912, the first glutaminyl cyclase (QC) inhibitor to treat Alzheimer's disease, in healthy elderly. *Alzheimer's Dement.* **9,** P280 (2013).

271. Winblad, B. *et al.* Safety, tolerability, and antibody response of active Aβ immunotherapy with CAD106 in patients with Alzheimer's disease: randomised, double-blind, placebo-controlled, first-in-human study. *Lancet. Neurol.* **11,** 597–604 (2012).

272. Blennow, K. *et al.* Effect of immunotherapy with bapineuzumab on cerebrospinal fluid biomarker levels in patients with mild to moderate Alzheimer disease. *Arch. Neurol.* **69,** 1002–10 (2012).

273. Salloway, S. *et al.* Two phase 3 trials of bapineuzumab in mild-to-moderate Alzheimer's disease. *N. Engl. J. Med.* **370,** 322–33 (2014).

274. Doody, R. S. *et al.* Phase 3 trials of solanezumab for mild-to-moderate Alzheimer's disease. *N. Engl. J. Med.* **370,** 311–21 (2014).

275. Siemers, E. R. *et al.* Safety and changes in plasma and cerebrospinal fluid amyloid beta after a single administration of an amyloid beta monoclonal antibody in subjects with Alzheimer disease. *Clin. Neuropharmacol.* **33,** 67–73 (2010)

276. Landen, J. W. *et al.* Safety and Pharmacology of a Single Intravenous Dose of Ponezumab in Subjects With Mild-to-Moderate Alzheimer Disease. *Clin. Neuropharmacol.* **36,** 14–23 (2013).

277. Dodel, R. C. *et al.* Intravenous immunoglobulins containing antibodies against beta-amyloid for the treatment of Alzheimer's disease. *J. Neurol. Neurosurg. Psychiatry* **75,** 1472–4 (2004).

278. Relkin, N., Bettger, L., Tsakanikas, D. & Ravdin, L. Three-year follow-up on the IVIg for Alzheimer's phase II study. *Alzheimer's Dement.* **8,** P589 (2012).

279. Robshaw, A. *et al.* Characterization of beta-amyloid 1-40 across species following treatment with beta-secretase inhibitors. *Alzheimer's Dement.* **9,** P502 (2013).

280. Roberds, S. L. *et al.* BACE knockout mice are healthy despite lacking the primary beta-secretase activity in brain: implications for Alzheimer's disease therapeutics. *Hum. Mol. Genet.* **10,** 1317–1324 (2001).

281. Bjerke, M. *et al.* Confounding factors influencing amyloid Beta concentration in cerebrospinal fluid. *Int. J. Alzheimers. Dis.* **2010,** (2010).

282. Slemmon, J. R. *et al.* Measurement of Aß1-42 in cerebrospinal fluid is influenced by matrix effects. *J. Neurochem.* **120,** 325–333 (2012).

283. Pannee, J. *et al.* A selected reaction monitoring (SRM)-based method for absolute quantification of Aβ38, Aβ40, and Aβ42 in cerebrospinal fluid of Alzheimer's disease patients and healthy controls. *J. Alzheimer's Dis.* **33,** 1021–1032 (2013).

284. Van Broeck, B. *et al.* Impact of frequent CSF sampling on Aβ levels: systematic approach to reveal influencing factors. *Submitt. Manuscr.*

285. Life Technologies. at <https://www.lifetechnologies.com>

286. Struyfs, H. *et al.* Diagnostic Accuracy of Cerebrospinal Fluid Amyloid-β Isoforms for Early and Differential Dementia Diagnosis. *J. Alzheimers. Dis.* (2015).

287. Van Broeck, B. *et al.* Simultaneous evaluation of Abeta37/38/40/42 levels after treatment with secretase inhibitors and modulators using a novel immunoassay. *Neurodegener. Dis.* **11,** (2013).

288. El Mouedden, M., Vandermeeren, M., Meert, T. & Mercken, M. Development of a specific ELISA for the quantitative study of amino-terminally truncated beta-amyloid peptides. *J. Neurosci. Methods* **145,** 97–105 (2005).

289. Mercken, M. *et al.* Specific ELISA systems for the detection of endogenous human and rodent ABETA40 and ABETA42. *Neurobiology of Aging* **21,** 41 (2000).

290. Lu, Y. *et al.* Cerebrospinal fluid amyloid-β (Aβ) as an effect biomarker for brain Aβ lowering verified by quantitative preclinical analyses. *J. Pharmacol. Exp. Ther.* **342,** 366–75 (2012).

291. Yang, H. C. *et al.* Biochemical and kinetic characterization of BACE1: Investigation into the putative species-specificity for β- and β′-cleavage sites by human and murine BACE1. *J. Neurochem.* **91,** 1249–1259 (2004).

292. Li, T. *et al.* γ-Secretase modulators do not induce Aβ-rebound and accumulation of β-C-terminal fragment. *J. Neurochem.* **121,** 277–286 (2012).

293. Hopkins, C. ACS Chemical Neuroscience Molecule Spotlight on Begacestat (GSI- 953). *ACS Chem. Neurosci.* **3,** 3–4 (2012)

294. Crump, C. J. *et al.* Piperidine acetic acid based gamma-secretase modulators directly bind to presenilin-1. *ACS Chem. Neurosci.* **2,** 705–710 (2011).

295. Gijsen, H. J. M. & Mercken, M. Gamma-secretase modulators: Can we combine potency with safety? *Int. J. Alzheimers. Dis.* (2012).

296. Hashimoto, T. *et al.* E2012: A novel gamma-secretase modulator-pharmacology part. *Alzheimer's & Dementia* **6,** S242 (2010).

297. Ranaldi, S. *et al.* N-truncated Aβ peptides in complex fluids unraveled by new specific immunoassays. *Neurobiol. Aging* **34,** 523–539 (2013).

298. Menting, K. W. & Claassen, J. A. H. R. β-secretase inhibitor; a promising novel therapeutic drug in Alzheimer's Disease. *Front. Aging Neurosci.* **6,** 1–20 (2014).

299. Alzforum. LY2886721. at <http://www.alzforum.org/therapeutics/ly2886721>

300. Jeppsson, F. *et al.* Discovery of AZD3839, a potent and selective BACE1 inhibitor clinical candidate for the treatment of alzheimer disease. *J. Biol. Chem.* **287,** 41245–41257 (2012).

301. Wagner, S. L. *et al.* Soluble gamma-secretase modulators selectively inhibit the production of the 42-amino acid amyloid beta peptide variant and augment the production of multiple carboxy-truncated amyloid ?? species. *Biochemistry* **53,** 702–713 (2014).

302. Kounnas, M. Z. *et al.* Modulation of beta-Secretase Reduces beta-Amyloid Deposition in a Transgenic Mouse Model of Alzheimer's Disease. *Neuron* **67,** 769–780 (2010).

303. Abraham, J.-D. *et al.* Cerebrospinal Aβ11-x and 17-x levels as indicators of mild cognitive impairment and patients' stratification in Alzheimer's disease. *Transl. Psychiatry* **3,** e281 (2013).

304. Bien, J. *et al.* The metalloprotease meprin β generates amino terminal-truncated amyloid β peptide species. *J. Biol. Chem.* **287,** 33304–33313 (2012).

305. Kummer, M. P. & Heneka, M. T. Truncated and modified amyloid-beta species. *Alzheimers. Res. Ther.* **6,** 28 (2014).

306. Drew, S. C., Masters, C. L. & Barnham, K. J. Alanine-2 carbonyl is an oxygen ligand in Cu2+ coordination of Alzheimer's disease amyloid-ß peptide - Relevance to N-terminally truncated forms. *J. Am. Chem. Soc.* **131,** 8760–8761 (2009).

307. Takeda, K., Araki, W., Akiyama, H. & Tabira, T. Amino-truncated amyloid beta-peptide (Abeta5-40/42) produced from caspase-cleaved amyloid precursor protein is deposited in Alzheimer's disease brain. *FASEB J.* **18,** 1755–1757 (2004).

308. Sevalle, J. *et al.* Aminopeptidase A contributes to the N-terminal truncation of amyloid β-peptide. *J. Neurochem.* **109,** 248–256 (2009).

309. Ditto, N. T., Kline, T. R., Alfinito, P. D. & Slemmon, J. R. Enrichment and analysis of Alzheimer's Aß1-42 peptide in human plasma and whole blood. *J. Neurosci. Methods* **182,** 260–265 (2009).

310. Hansson, O. *et al.* Prediction of Alzheimer's disease using the CSF Abeta42/Abeta40 ratio in patients with mild cognitive impairment. *Dement. Geriatr. Cogn. Disord.* **23,** 316–320 (2007).

311. Shoji, M. *et al.* Combination assay of CSF Tau, Aß1-40 and Aß1-42(43) as a biochemical marker of Alzheimer's disease. *J. Neurol. Sci.* **158,** 134–140 (1998).

312. Lewczuk, P. *et al.* Neurochemical diagnosis of Alzheimer's dementia by CSF Aß42, Aß42/Aß40 ratio and total tau. *Neurobiol. Aging* **25,** 273–281 (2004).

313. Graff-Radford, N. R. *et al.* Association of low plasma Abeta42/Abeta40 ratios with increased imminent risk for mild cognitive impairment and Alzheimer disease. *Arch. Neurol.* **64,** 354–362 (2007).

314. Wiltfang, J. *et al.* Amyloid β peptide ratio 42/40 but not Aβ42 correlates with phospho-Tau in patients with low- and high-CSF Aβ40 load. *J. Neurochem.* **101,** 1053–1059 (2007).

315. Welge, V. *et al.* Combined CSF tau, p-tau181 and amyloid-ß 38/40/42 for diagnosing Alzheimer's disease. *J. Neural Transm.* **116,** 203–212 (2009).

316. Sheridan, C. Pivotal trials for β-secretase inhibitors in Alzheimer's. *Nat. Biotechnol.* **33,** 115–116 (2015).

317. Vassar, R. BACE1 inhibitor drugs in clinical trials for Alzheimer's disease. *Alzheimers. Res. Ther.* **6,** (2014).

318. Miller, M., Evans, H. & De Lahunta, A. *Miller's Guide to the Dissection of the Dog*. (1974).